# Health Effects of PM Particles Emitted from Heavy-Duty Vehicles – A Comparison Between Different Biodiesel Fuels

Contract #12197


**Prepared for:**

**Brian Choe**
**South Coast Air Quality Management District**
21865 Copley Drive
Diamond Bar, CA. 91765

**February 2015**

**Submitted by:**

Drs. Georgios Karavalakis and Thomas D. Durbin, and Mr. Nicholas Gysel
University of California
CE-CERT
Riverside, CA 92521
951-781-5799
951-781-5790 (fax)

## Disclaimer

The statements and conclusions in this report are those of the contractor and not necessarily those of the South Coast Air Quality Management District or other participating organizations and their employees. The mention of commercial products, their source, or their use in connection with material reported herein is not to be construed as actual or implied endorsement of such products.

## Acknowledgments

This report was prepared at the University of California, Riverside, and Bourns College of Engineering-Center for Environmental Research and Technology (CE-CERT). The primary contributors to this report include Drs. Georgios Karavalakis, Thomas D. Durbin, and Mr. Nicholas Gysel. The authors thank the following organizations and individuals for their valuable contributions to this project. We acknowledge Don Pacocha, Edward O'Neil, and Joe Valdez of CE-CERT for their assistance in carrying out the experimental program.

Also, we would like to thank Professor Constantinos Sioutas and Dr. Payam Pakbin at the University of Southern California (USC) for their assistance and technical guidance in collecting PM samples using their high volume sampler during the test campaign. We acknowledge Professor James Schauer and Mr. Martin M. Shafer at the University of Wisconsin Madison for performing detailed chemical speciation analysis in PM samples. Finally, we thank Professor Arthur K. Cho and Ms. Debra A. Schmitz at the University of California Los Angeles (UCLA) for conducting the chemical reactivity and cellular assays in the PM samples.

# Table of Contents

## List of Figures

**List of Tables**

## Acronyms and Abbreviations

AFME .....Animal fat methyl ester
CARB .....California Air Resources Board
CE-CERT .....College of Engineering-Center for Environmental Research and Technology (University of California, Riverside)
CFR .....Code of Federal Regulations
$CH_4$ .....methane
CO .....carbon monoxide
$CO_2$ .....carbon dioxide
CPC .....condensation particle counter
CVS .....constant volume sampling
DOC .....diesel oxidation catalyst
DPF .....diesel particulate filter
DTT .....Dithiothreitol
ECM .....engine control module
EEPS .....engine exhaust particle sizer
EPA .....United States Environmental Protection Agency
FAME .....Fatty acid methyl esters
FID .....flame ionization detector
GMD .....geometric mean diameter
HO-1 .....Hemeoxygenase-1
MEL .....CE-CERT's Mobile Emissions Laboratory
MY .....model year
$NH_3$ .....Ammonia
NMHC .....non-methane hydrocarbons
$NO_x$ .....nitrogen oxides
PAHs .....polycyclic aromatic hydrocarbons
PM .....particulate matter
PN .....particle number
ROS .....reactive oxygen species
SCR .....selective catalytic reduction
SME .....Soy-methyl ester
TDL .....Tunable diode laser
THC .....total hydrocarbons
TNF-a .....tumor necrosis factor alpha
UCR .....University of California at Riverside
UDDS .....Urban dynamometer driving schedule
ULSD .....ultralow sulfur diesel
VOCs .....volatile organic compounds
WCO .....Waste cooking oil methyl ester
WSOC .....water-soluble organic carbon
40 CFR 1065 or 1065 .....Part 1065 of Title 40 of the Code of Federal Regulations

## Executive Summary

In recent years, governmental agencies around the world have implemented legislation that targets growing the use of renewable fuels in the transportation sector. In the U.S., the Energy Independence and Security Act of 2007 mandates the use of 36 billion gallons of biofuels in the transportation fuel pool by 2022. In California, the low carbon fuel standard (LCFS) was implemented in 2011 to promote the reduction of greenhouse gas emissions by targeting a reduction in the carbon intensity of transportation fuels by 10% by 2020. In addition, the implementation of more stringent standards for heavy-duty vehicles is a key strategy for the improvement of air quality in the South Coast Air Quality Management District (AQMD). These facts, coupled with the continuously growing concern over global warming and environmental degradation, have accentuated the public and scientific awareness and led to a substantial effort to develop alternative fuel sources and improve engine technologies.

The main goals of this study was to carry out chassis dynamometer testing of heavy-duty diesel trucks using different types of biodiesel fuel blends and a typical CARB ultra-low sulfur diesel while measuring: 1) regulated emissions; 2) unregulated emissions such as ammonia, carbonyl compounds, and volatile organic compounds (VOCs); 3) the physical properties of particulate matter (PM) emissions (e.g., PM mass, number, and size distributions); 4) the chemical properties of PM emissions (e.g., PAHs, WSOC, inorganic ions, organic compounds, and metals); and 5) the toxicological characteristics of PM emissions (e.g., redox activity, electrophilic properties, and pro-inflammatory properties). This study tested two heavy-duty diesel vehicles that were equipped with a 2002 model year Cummins ISX-450 engine without any emission control technology and a 2010 Cummins ISX-15 engine fitted with a diesel oxidation catalyst (DOC) followed by a diesel particle filter (DPF) and selective catalytic reduction (SCR), respectively.

The emission results for both vehicle/fuel combinations are summarized below:

- THC, NMHC, CO, and PM mass emissions for the uncontrolled Cummins ISX-450 engine showed reductions with the use of biodiesel blends compared to CARB ULSD. In most cases, the B50 blends resulted in statistically significant reductions for THC, NMHC, CO, and PM mass emissions relative to the reference fuel. These phenomena were as expected and can be explained by the higher oxygen content in the methyl ester moiety, which help reduce

rich combustion zones and promote more complete combustion and reduce the sooting tendency of biodiesel.

- For the heavily controlled Cummins ISX-15 engine, THC and NMHC emissions were practically below the detection limits, as these species were effectively fully oxidized in the DOC/DPF system. CO and PM mass emissions were also low for the DOC/DPF equipped engine, and did not show any strong fuel effects.
- $CO_2$ emissions showed some moderate decreases with the biodiesel blends relative to CARB ULSD, which is an indication that the engine efficiency wasn't influenced by the high biodiesel blend ratio.
- Overall, $NO_x$ emissions exhibited increases with biodiesel for both vehicles with the differences in $NO_x$ emissions relative to CARB ULSD being statistically significant for the newer Cummins ISX-15 engine. For the Cummins ISX-15 engine, $NO_x$ emissions showed some feedstock dependency with the unsaturated SME-50 producing higher $NO_x$ than CARB ULSD and the more saturated AFME-50 blend. Double bond structuring of the fatty acid chain (i.e., increased unsaturation of the biodiesel) tends to increase $NO_x$ emissions due to the formation of hydrocarbon radicals, which may cause higher adiabatic flame temperatures and thus formation of thermal $NO_x$.
- $NO_x$ emissions were found to be substantially lower for the SCR-fitted Cummins ISX-15 engine compared to the uncontrolled Cummins ISX-450 engine. The influence of temperature on the effectiveness of the SCR system in eliminating $NO_x$ was particularly noticeable, with $NO_x$ emissions being significantly higher at the beginning of the UDDS cycle when the SCR is cold and inactive (<250 °C) and lower when the SCR system was operating close or above 250 °C. This result points to the importance of the exhaust temperature for a vehicle with SCR aftertreatment, especially when operated under cold-starts and low load/slow speed driving conditions (the latter representing driving in urban settings).
- Particle number emissions did not show any strong trends between the test fuels for the uncontrolled engine, while for the Cummins ISX-15 engine particle number emissions were below the tunnel background levels.
- The uncontrolled Cummins ISX-450 engine showed bimodal particle size distributions with peaks at around 55 nm and 11 nm in diameter. As expected, the CARB ULSD produced more

accumulation mode particles compared to the B50 blends, while the more unsaturated SME-50 blend showed higher nucleation mode particle counts relative to CARB ULSD and the other biodiesel blends. For the newer Cummins ISX-15 engine, the particle size distributions were dominated by nucleation mode particles with peaks around 11 nm in diameter. This result suggests that most particles were in the ultrafine range compared to the uncontrolled engine, which is an important finding from a health effect perspective since epidemiological and toxicological studies have shown that inhalation and subsequent deposition of ultrafine particles into the lungs can induce adverse health effects. The CARB ULSD showed higher nucleation mode particles compared to biodiesel blends.

- Formaldehyde and acetaldehyde were the most abundant carbonyls in the exhaust with biodiesel generally showing lower formaldehyde and acetaldehyde emissions than CARB ULSD. For the newer Cummins ISX-15 engine, only formaldehyde was found above the tunnel background levels with the remaining low-molecular, aliphatic, aromatic, and heavier carbonyl compounds being effectively oxidized in the DOC/DPF system. Our data clearly demonstrated that the influence of vehicle technology greatly exceeds the influence of biodiesel source material for aldehyde emission rates.
- There were no significant differences between the fuels for 1,3-butadiene for any of the test vehicles, while for the uncontrolled Cummins ISX-450 engine benzene emissions decreased with the use of biodiesel relative to CARB ULSD. For the Cummins ISX-450 engine, all the mono-aromatic compounds showed reductions with the biodiesel blends relative to CARB ULSD, whereas no strong fuel trends were seen for the newer Cummins ISX-15 engine.
- $NH_3$ emissions were found to be significantly higher for the SCR-fitted Cummins ISX-15 engine compared to the uncontrolled vehicle. For the Cummins ISX-15 engine, the use of biodiesel blends showed increases in $NH_3$ emissions relative to CARB ULSD. The higher $NH_3$ emissions ($NH_3$ slip) for the biodiesel blends were probably due to a response of the dosing control system of the SCR to suppress the high engine-out $NO_x$ emissions.
- Polycyclic aromatic hydrocarbons (PAHs) were detected in higher concentrations for the uncontrolled engine than the Cummins ISX-15 engine. For the Cummins ISX-15 engine, most PAH compounds were practically undetectable as a result of their oxidation in the DOC/DPF

system, although some light molecular-weight PAHs were only seen for the newer engine, and did not show strong fuel trends.

- For the uncontrolled Cummins ISX-450 engine, the use of biodiesel resulted in decreases in PAH emissions. Although the absence of emission aftertreatment control technology led to greater levels of higher molecular weight PAH species, which are known as highly toxic, carcinogenic and/or mutagenic to humans, the addition of biodiesel decreased their emissions compared to CARB ULSD. However, some PAH increases were also observed to be higher with some biodiesel blends relative to CARB ULSD.
- Hopanes and steranes, which originate from lubricant oil combustion, were generally lower for the newer Cummins ISX-15 engine compared to the Cummins ISX-450 engine. This result indicates that hopanes and steranes were effectively trapped in the DOC/DPF system. Some fuel effects were also noted, with the biodiesel blends generally showing lower hopanes and steranes than CARB ULSD. Alkanes produced discordant results with both increases and decreases with the use of biodiesel blends.
- The uncontrolled Cummins ISX-450 engine emitted higher levels of inorganic ion species, with phosphate and sulfate emissions dominating the ions profile for both vehicles.
- The water soluble organic carbon (WSOC) was found to be lower for the biodiesel blends relative to CARB ULSD for the uncontrolled Cummins ISX-450 engine. For the Cummins ISX-15 engine, WSOC trended higher for the biodiesel blends, but at not statistically significant level due to the large measurement variability.
- Water-soluble metals were found to decrease with the use of biodiesel compared to CARB ULSD for both vehicles. The uncontrolled Cummins ISX-450 engine showed substantially higher water-soluble concentrations compared to the DPF-fitted Cummins ISX-15 engine. For both vehicles, the biodiesel resulted in decreases in redox-active metals and in carcinogenic metals relative to CARB ULSD.
- The oxidative potential, measured with the DTT assay, showed some dramatic reductions with the use of biodiesel blends relative to CARB ULSD for the uncontrolled Cummins ISX-450 engine. The redox activity measured with the macrophage ROS assay did not show any strong fuel trends for either test vehicle. The DTT assay confirmed that biodiesel exhaust was less potent than petroleum diesel. This observation was also supported by the vapor-

phase PM results where the redox activity of biodiesel blends was lower compared to CARB ULSD. For the Cummins ISX-15 engine, the macrophage ROS assay did not show any fuel effects, while the DTT values for the particle-phase components were well below the filter blank levels due to the very low PM mass adsorbed on the Teflon filters.

- To assess the inflammatory response of diesel and biodiesel blends for both vehicles, the expression of cytokine tumor necrosis alpha (TNF-α) by a mouse macrophage cell line (Raw 264.7) was used. The PM samples from the uncontrolled Cummins ISX-450 engine were capable of increasing TNF-α. The vapor-phase samples, on the other hand, showed high negative values that we hypothesize are real and important effects, which could reflect suppression of the TNF-α response. Overall, the results for TNF-α expression were not as clear, but the particle-phase appeared to be more active than the vapor-phase in increasing expression.
- To assess the protective response of diesel and biodiesel blends for both vehicles, the cellular hemeoxygenase-1 (HO-1) expression was determined. The notion of HO-1 as a protective response is based on its regulation. This protein is regulated by the antioxidant/antielectrophile response element (ARE), a transcription factor whose activation increases the expression of multiple protective proteins such as glutathione synthases (increase levels of glutathione, a protective chemical), phase II enzymes that metabolically inactivate toxins and HO-1, which is considered to be an antioxidant enzyme. HO-1 is used as a marker for this activation process because it is expressed in high concentration. An increase in HO-1 levels is thus interpreted to reflect activation of a protective or adaptive response. For the particle-phase samples, for the uncontrolled Cummins ISX-450 engine, only the WCO-50 blend showed increased the expression of HO-1 at greater levels than those exhibited by the CARB ULSD. The vapor-phase samples collected from the uncontrolled Cummins ISX-450 engine showed greater expression of HO-1 for the CARB ULSD than the biodiesel blends. The vapor-phase showed higher levels of HO-1 compared to the particle-phase with the order CARB ULSD>AFME-50>SME-50>WCO-50. We theorized that increased HO-1 expression indicates a protective or adaptive response to components of the test samples.

- The DTT redox activity of the emitted PM was found to correlate well with the WSOC, the redox-active transition metals, alkanes, hopanes and steranes, but not with PAHs. Our results indicate that these species are likely to be involved in the oxidation stress mechanism by the generation of ROS.

In summary, the data from this study confirm that heavy-duty diesel vehicles are exhibiting higher NOx emissions when operating with biodiesel blends than CARB ULSD. This result is important since biodiesel is becoming a more attractive alternative fuel in the U.S., and it also presents an obstacle to the AQMD plan for achieving clean air in the District in a timely manner. Results showed that NOx emissions depended on the biodiesel source material and temperature of the SCR technology. Other results showed that emissions of PM mass, THC, NMHC, CO, and selected toxics were all very low from the 2010-compliant engine, confirming the results of the CRC/HEI/EMA ACES project. Our findings showing that biodiesel is capable in reducing most toxic compounds, such as PAHs. The application of modern exhaust aftertreatment was able to trap and oxidize most carcinogenic compounds, thus, offsetting the beneficial role of biodiesel use. Overall, the biodiesel particle-phase samples had a lower prooxidant content compared to the CARB ULSD fuel samples, but the vapor-phase contained proportionally higher levels of prooxidants. The heavily controlled Cummins ISX-15 engine showed substantially lower inflammatory responses than the uncontrolled engine. This was particularly true for the AFME-50 and WCO-50 blends and their vapor-phase samples, which produced higher levels of prooxidants compared to their corresponding particle-phase samples.

Looking ahead, the results suggest that further testing is necessary utilizing modern technology heavy-duty vehicles on different types of biodiesel blends during cold-start driving cycles. Additional analysis should be performed in characterizing the nitrated derivatives of PAHs (nitro-PAHs), which are usually formed in the DPF/SCR system through PAH nitration reactions. A better evaluation of $NO_x$ emissions with the use of biodiesel and/or renewable diesel blends from 2010 compliant heavy-duty vehicles is also necessary in order to maintain AQMD's path to clean air, since diesel trucks are durable and can drive more than a million miles in their lifetime making them the single largest contributor of NOx emissions in California's ozone nonattainment areas including Los Angeles. A better evaluation of NOx emissions from these vehicles on alternative diesel fuels should be conducted during in-use testing representing a variety of engine conditions

associated with real-world driving conditions, which are not necessarily captured by the UDDS or other cycles developed for chassis dynamometer testing.

# 1 Introduction

## 1.1 Background

Diesel exhaust has been of concern of many decades due to its health effects and climate impact. The emission standards for diesel engines have become more and more stringent since the 1980's. Emissions from heavy-duty trucks and buses accounted for about one-third of $NO_x$ emissions and one-quarter of PM emissions from mobile sources when stringent emission standards were introduced by the U.S. EPA on December 21, 2000 and by CARB in October 2001. Recently, U.S. EPA implemented a new emission standard for PM of 0.01 g/bhp-hr for 2007 model year (MY) heavy-duty diesel engines and a new $NO_x$ emission standard of 0.2 g/bhp-hr for 2010 MY heavy-duty diesel engines. While there has been a tremendous improvement in diesel engine technologies, exhaust aftertreatment is generally required to meet these new stringent emission limits. Diesel particulate filters (DPFs) were developed to meet the 2007 PM standard and are now fitted in all new diesel vehicles in the U.S., Europe, and Japan. Diesel oxidation catalysts (DOCs) are often used as part of the DPF system, serving the role of oxidizing THC and CO emissions, burning fuel to actively regenerate filters, and generating nitrogen dioxide ($NO_2$) for passive DPF regeneration. For meeting 2010 $NO_x$ emission standard, selective catalytic reduction (SCR) is currently used for heavy-duty diesel engines, which converts $NO_x$ to elemental $N_2$ and $H_2O$ with an appropriate catalyst and reducing agent, such urea or ammonia ($NH_3$).

In addition to these advanced engine technologies, stringent diesel regulations, and aftertreatment controls to meet U.S. EPA requirements, there is a considerable interest in the use of biomass-derived fuels as means of reducing greenhouse gases (GHG) and other harmful emissions. Biodiesel, collectively known as fatty acid methyl esters (FAME), is a renewable transportation fuel consisting of long-chain alkyl esters, which contain two oxygen atoms per molecule. Biodiesel is generally produced by the transesterification process of vegetable oils, used cooking oils, and animal fats. Biodiesel has similar properties to middle distillate petroleum diesel, and is free of sulfur and aromatic compounds, non-toxic, and readily biodegradable. Regulations are a powerful driver for biofuels development. The European Union (EU) directive on renewable energy (2009/28/EC) stipulates that each member state has to ensure that 10% of the fuel for its transport sector is biofuel or renewable electricity by

2020. Furthermore, the EU fuel quality directive already allows for biodiesel levels in diesel of up to 7% (B7) by volume. In the U.S., the EPA Renewable Fuel Standard version 2 (EPA-RFS2) and the California Low Carbon Fuel Standard (CA-LCFS), a state-enacted policy to reduce GHG emissions from motor vehicles, are driving the U.S. biofuels market. The EPA-RFS2 requires that 36 billion gallons of renewable fuel are available in the U.S. market by 2022. Although over the next several years ethanol is expected to make up the majority of this requirement, biodiesel is expected to have the largest penetration into the diesel fuel market. For perspective, over 1 billion gallons of biodiesel were produced in the U.S. in 2011, and with an ever-increasing number of state mandates for biofuels, the use of biodiesel will become more common.

Biodiesel fuels have been widely studied for their effects on gaseous and PM emissions. The general consensus on biodiesel points to a reduction in PM, THC, and CO and an increase in $NO_x$ emissions [Durbin et al., 2000; Yang et al., 2007; Kousoulidou et al., 2010]. Increases in $NO_x$ emissions with biodiesel have been attributed to increased oxygen content compared to diesel fuels, higher bulk modulus of compressibility, cetane number, density, as well as the degree of unsaturation [Zhang and Boehman, 2007; Bittle et al., 2010]. McCormick et al. (2001) studied a group of 21 different biodiesel fuels during the FTP cycle on a 1991 MY engine. They found that the more saturated esters, which had higher cetane numbers and lower densities than the less saturated esters, emitted the lowest $NO_x$. Similar observations concerning the effect of unsaturation on $NO_x$ emissions have been reported by Knothe et al. (2006) on a heavy-duty diesel engine and by Fontaras et al. (2009) and Bakeas et al. (2011) on light-duty vehicles. Lammert et al. (2012) investigated six buses on a range of fuels, including CARB ultra-low sulfur diesel (ULSD), certification diesel, neat soy-based biodiesel, and B20 blends over the Manhattan, Orange County, and UDDS test cycles. They found that the buses without aftertreatment control showed little or no effect for B20 on $NO_x$ emissions compared to a certification diesel, but a statistically significant effect for B20 on $NO_x$ compared to CARB diesel. They also showed that SCR control eliminated any fuel effect on $NO_x$ emissions. Hajbabaei et al. (2012) conducted a comprehensive engine dynamometer study on two heavy-duty engines, with and without a DPF, focusing on $NO_x$ mitigation strategies from different types of biodiesel fuels. The authors found a consistent increase in $NO_x$ emissions with increasing biodiesel levels in a CARB ULSD, with soy biodiesel showing higher $NO_x$ emissions than a more saturated animal biodiesel. In an older study, Wang et al. (2000) tested six heavy-duty trucks on regular diesel

and a soy-based blend at 35% by volume and showed significant reductions in PM emissions. They also observed moderate reductions in THC and CO, while $NO_x$ emissions remained at the same levels for both fuels. Muncrief et al. (2008) tested a refuse truck equipped with exhaust gas recirculation (EGR)/DPF system on biodiesel blends during a low-load driving cycle. They found a large reduction in PM emissions with biodiesel relative to conventional ULSD.

Recent studies have shown increases in carbonyl emissions from on-road heavy-duty diesel engines with and without exhaust aftertreatment control operating on biodiesel blends [Turrio-Baldassarri et al., 2004; Lin et al., 2009]. Cahill and Okamoto (2012) measured two heavy-duty vehicles meeting different EPA emission standards on four fuels, including CARB ULSD, soy biodiesel, animal biodiesel, and renewable diesel. They found higher acrolein and crotonaldehyde emissions and lower aromatic aldehyde emissions with the biodiesels compared to the baseline diesel fuel. They also found that DOC/DPF configurations appeared to be very effective at lowering carbonyl emissions from the newer engine. Finally, Ratcliff et al. (2010) tested a heavy-duty truck fitted with a continuously regenerated DPF on ULSD, B20, and B100 soy-based biodiesel. They found that formaldehyde and acetaldehyde were the dominant aldehydes in the exhaust and that their emissions were higher with biodiesel compared to ULSD.

Aside from PM mass emissions, other information about particle emissions, such as particle number, PM composition, and health effects are also important. The majority of the studies focusing on the impact of biodiesel on ultrafine particles have been performed on light-duty vehicles [Fontaras et al., 2010a; Tzamkiozis et al., 2011]. Fontaras et al. (2009) found that total particle number increased with B50 and B100 fuels, whereas solid particle number progressively decreased. The authors attributed the increase in semivolatile PM to the lower volatility of biodiesel components. Likewise, Tinsdale et al. (2010) reported a 25% increase in the nucleation mode particle number over the New European Driving Cycle (NEDC) for a B30 blend compared to diesel fuel. On the other hand, Macor et al. (2011) found that the total particle number emissions decreased with biodiesel relative to diesel fuel between 10 and 20% over the NEDC and the Artemis driving cycles. Young et al. (2012) investigated various waste cooking oil biodiesel blends on a heavy-duty engine equipped with a DOC and DPF over the European Stationary Cycle (ESC). They showed the total particle number concentrations decreased with increasing biodiesel content. Westphal et al. (2013) performed testing on a

Euro 3 heavy-duty engine with neat jatropha and rapeseed methyl ester over the ESC. They found that particle number emissions were about 1 order of magnitude lower than those of regular diesel. Heikkila et al. (2009) investigated the effect of a rapeseed oil biodiesel, a regular diesel, and a synthetic diesel on nanoparticle emissions from a Euro 4 heavy-duty engine fitted with SCR control. They found that biodiesel produced substantially greater concentrations of nonvolatile nucleation mode particles with higher mean diameters than with the other fuels. They also found that the soot particle concentration and particle size were lowest with biodiesel.

With respect to health effects, biodiesel exhaust has been not been studied as extensively and is less understood compared to regular diesel. Several studies have shown that biodiesel is more mutagenic than regular ULSD. A recent CARB study on the effects of biodiesel and renewable diesel blends from heavy-duty vehicles showed that the CARB diesel and the biodiesel blends induce CYP1A1 production though compounds that bind to and activate the Ah-Receptor. The CARB diesel and biodiesel blends also induced inflammatory markers like COX-2 and IL-8 in macrophages, and MUC5AC in lung Clara cells. The effects of the biodiesel blends on inflammatory markers like COX-2 and IL-8 tended to be lower than for the CARB diesel for the 2000 MY Caterpillar vehicles. However, the authors found higher IL-8 in soy biodiesel and the blends than in CARB diesel for the 2007 MY MBE4000 engine vehicle [Durbin et al., 2011]. Ackland et al. (2007) has shown that exposure to 80% and 20% biodiesel blends increased formation of multinucleated cells by 16 and 52%, respectively. Studies by Brito et al. (2010) found that biodiesel shows equal and/or more toxic effects compared with diesel fuel. Yanamala et al. (2013) found that biomarkers of tissue damage and inflammation were significantly elevated in lungs of mice exposed to biodiesel PM, with biodiesel causing accumulation of oxidatively modified proteins and an increase in 4-hydroxynonenal. They also found that the up-regulation of inflammatory cytokine/chemokines/growth factors was higher in the lungs upon biodiesel exposure. Kooter et al. (2011) studied a number of different biodiesel blends on a Euro 3 heavy-duty truck engine over the European Transient Cycle (ETC). They showed that the redox activity, as measured by the DTT assay, was reduced for biodiesel blends and neat biodiesel compared to diesel fuel. On the other hand, Guarieiro et al. (2014) showed an increase in redox activity with increasing waste cooking oil biodiesel concentration. Similar findings were seen in a previous study conducted on a Euro 2 passenger car running on

B100 soy-based biodiesel and diesel fuel. The authors found that biodiesel had the most potent exhaust relative to diesel and to a Euro 3 compliant vehicle fitted with a DPF [Cheung et al., 2009]. Finally, Gerlofs-Nijland et al. (2013) tested two Euro 4 vehicles equipped with or without a DPF on regular diesel and B50 over a combination of urban and rural driving cycles. They showed that B50 decreased oxidative potential for urban driving, while rural driving showed no strong fuel effects.

### 1.2 Statement of Significance

The implementation of more stringent standards for heavy-duty highway engines was a key strategic element of the plan for improving air quality in the South Coast Air Quality Management District (SCAQMD). This study addresses the significant effects of hazardous air toxic (HAP) pollutants and PM emissions from heavy-duty diesel vehicles on health and the environment. Although certain air toxics and PM from heavy-duty diesel-powered vehicles are known to be responsible for a myriad of adverse health impacts, ranging from cancer to respiratory diseases, and environmental problems, and from global warming to photochemical smog, the combustion of biomass-derived fuels on heavy-duty vehicles and their effect on environment and public health is presently not well understood.

The objective of this program was to provide SCAQMD information for their strategic future research planning on the characterization of gaseous toxic pollutants and the physicochemical and toxicological properties of PM from heavy-duty vehicles fitted with and without exhaust aftertreatment and operating on different biodiesel blends. The State of California is emphasizing and implementing legislative requirements that promote the increased use of alternative fuels in California to reduce oil dependency, air pollution, and greenhouse gas emissions. The Low Carbon Fuel Standard is one of the most important pieces of legislation in this area, which mandates the reduction of the carbon intensity of fuels by 10% by 2020. Biodiesel and other renewable diesel fuels made from renewable feedstocks are alternative diesel fuels that have the potential to reduce greenhouse gas emissions, other pollutants, and can partially offset our use of petroleum-based fuels. In addition, heavy-duty diesel trucks constitute only a small fraction of the total fleet in California but have an important contribution to the emissions of fine and ultrafine particles. The outcomes of this study will provide important information about the potential impacts of mid-level biodiesel blends on

emissions and air quality during the near and medium term implementations of renewable fuel regulations. The results of this program will be helpful in assessing the health consequences of population exposure to heavy-duty diesel traffic sources in Southern California. Globalization and international trade have dramatically changed Southern California, which has increasingly become a distribution economy. The San Pedro Bay Ports are the largest port complex in the nation, receiving and moving nearly half of all imports in the U.S. The Inland Empire region has emerged as a wholesale and trade center for the massive Los Angeles-Long Beach port complex. Millions of cargo containers on diesel-powered trucks take freeway routes through southern California to the inland "rail ports" and large logistics centers from which they are distributed to the rest of the State and the country. Despite considerable improvements in air quality over the past two decades, the Los Angeles Basin continues to exhibit the most severe ozone and PM air quality episodes in the U.S. due to the continuing increase in population and traffic.

As part of this study, regulated emissions, gaseous air toxics, physicochemical, and toxicological properties of PM emissions were investigated from two heavy-duty trucks representing two technologies in the in-use fleet, including diesel vehicles with and without PM and $NO_x$ control technologies. This study emphasized the biodiesel source material impact on exhaust emissions and their potential toxicity. This study highlights the need of promulgating effective vehicular emission control strategies aiming at reducing environmental problems and public health risks.

### 1.3 Objectives

The main goal of this program is to provide scientific information on the regulated emissions, hazardous air toxics, and the physicochemical characteristics, as well as the toxicological properties of semivolatile and particle fractions of PM. For this study, emission measurements were collected from two different vehicles operating over the Urban Dynamometer Driving Schedule (UDDS). This was a collaborative study led by the College of Engineering - Center for Environmental Research and Technology (CE-CERT) at the University of California, Riverside with support from University of Southern California (USC), University of California, Los Angeles (UCLA), and University of Wisconsin Madison for chemical and toxicological analysis.

# 2 Driving Cycle, Vehicle, and Fuels

## 2.1 Test Cycle and Measurement Protocol

Testing was conducted over the EPA Urban Dynamometer Driving Schedule (UDDS) for each fuel for both vehicles. The UDDS was a basis for the development of the Federal Test Procedure (FTP) transient engine dynamometer cycle for heavy-duty engines. While not the FTP, values from the UDDS on a chassis dynamometer are often compared with the values from a "certification test" run on an engine dynamometer. The cycle has duration of 1060 seconds and covers a distance of 5.55 miles with an average speed of 18.8 miles/hour. A double UDDS (2X UDDS) test cycle was conducted for the newer truck equipped with the aftertreatment technologies to obtain sufficient PM mass for gravimetric analysis. A speed-time profile of the UDDS cycle is shown in Figure 2-1.

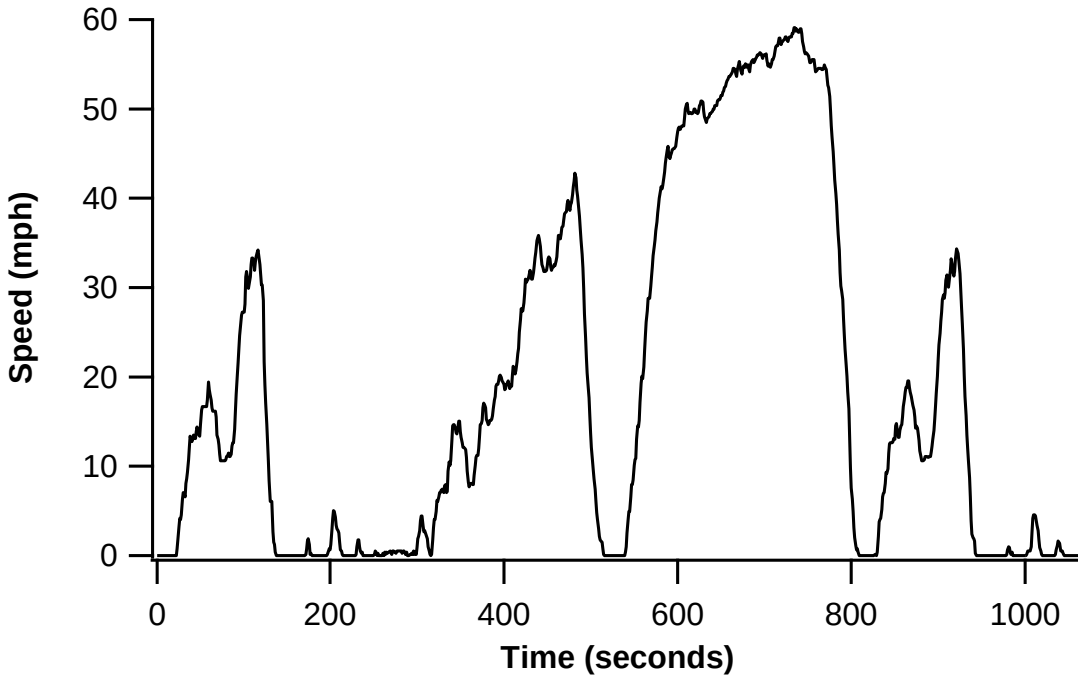


**Figure 2-1 Urban Dynamometer Driving Schedule (UDDS) speed-time profile**

The vehicles were preconditioned at the start of each test day by performing a power map to bring the vehicle up to its operational temperature. A preconditioning UDDS was then performed on each fuel prior to beginning testing on each fuel. The preconditioning cycle warmed up both the vehicle and dynamometer to the conditions of the test configuration, thus

reducing emissions variability between tests. This approach is commonly used for certification testing, fuel evaluations, and other repeatable test evaluations.

Between tests, there was a 'hot soak', where the engine was turned off for about 20 minutes. Soak time, or the time between tests, is an important factor that needs to be standardized to ensure test repeatability. Practically speaking, time is needed between each test to load new filter and sorption media, check instrument calibrations, and give the driver a break. For reference, EPA protocol certification tests use a 20 minute engine off soak period to return the engine to consistent baseline condition prior to the next test. As the EPA's recommended 20 minute interval proved sufficient to prepare all media and checks before subsequent tests, UCR used 20 minutes as the standard soak period for all cycles during this project. All tests were conducted as 'hot running' tests. The EPA UDDS test cycle was run on triplicate for each fuel.

## 2.2 Test Vehicles

Both vehicles selected by UCR were discussed with the AQMD project manager before any testing was initiated. Two vehicles were used in this study, including a vehicle with a 2010 MY Cummins ISX-15 engine and a vehicle with a 2002 MY Cummins ISX-450 engine. The vehicle with the Cummins ISX-450 engine was not equipped with aftertreatment technology. The vehicle with the Cummins ISX-15 engine was equipped with SCR for $NO_x$ removal, a DPF for PM removal, and a DOC for CO and THC removal. The main technical specifications of the engines are given in Table 2-1.

**Table 2-1 Technical specifications of the diesel engines**

| | | |
|---|---|---|
| Engine model | ISX-450 | ISX-15 |
| Oil system capacity | 52.9 L | 52.9 L |
| Displacement | 14.9 L | 14.9 L |
| Configuration | Inline, 6 Cylinders | Inline, 6 Cylinders |
| Peak torque | 2237 Nm/1200 rpm | 2237 Nm/1200 rpm |
| Horsepower | 336 kW/1700 rpm | 344 kW/1700 rpm |

| | | |
|---|---|---|
| Compression ratio | 19:1 | 18.9:1 |
| Bore and Stroke | 137mm & 169mm | 137mm & 169mm |

### 2.3 Test Fuels

A total of four fuels were utilized in this study. The reference fuel was a typical on-road CARB ULSD. Three fatty acid methyl esters that span the degree of unsaturation common in the marketplace were used as biodiesel blendstocks with the CARB ULSD. The biodiesels were blended at a 50% proportion by volume (B50). A methyl ester obtained from soybean oil (SME), a waste cooking oil methyl ester (WCO), and a methyl ester obtained from animal fat (AFME) were used. The soy-based biodiesel was selected because soybean oil is the dominant oil produced in the U.S., and the development of biodiesel in the U.S. has focused around this type of feedstock. Both the waste cooking oil and the animal fat feedstocks are considered to be low-cost and low environmental impact feedstocks, and are characterized as being $CO_2$ neutral. In addition, the animal fat biodiesel was selected since it is comprised of more saturated molecules and has less tendency to increase $NO_x$ emissions compared to other feedstocks. The soy-based biodiesel and the waste cooking oil biodiesel were procured by Imperial Western Products, CA, and the animal fat biodiesel was procured by Renewable Energy Group, TX. Both producers were BQ9000 accredited certified. The blends are labeled with the biodiesel type, followed by the percent concentration. For example, SME-50 denotes soy-based biodiesel blend at 50 volume percent. The basic physicochemical properties of the CARB ULSD and the three methyl esters are given in Table 2-2.

**Table 2-2 Properties of CARB ULSD and neat methyl esters**

| Properties | CARB ULSD | SME | AFME | WCO |
|---|---|---|---|---|
| Aromatics, % | 19.93 | | | |
| Olefins, % | 2.60 | | | |
| Saturates, % | 77.47 | | | |
| Heating value, cal/g | 10938 | 9522 | 9518 | 9486 |
| Density, g/mL (15 °C) | 0.84 | 0.88 | 0.87 | 0.88 |
| Cetane number | 53.13 | 49.23 | 61.10 | 54.57 |

# 3 Emissions Testing and Analysis

This section describes the measures performed by the mobile emissions laboratory (MEL) to ensure accuracy (trueness) and precision of the emissions data.

## 3.1 Emissions Measurement Laboratory

Emissions measurements were collected with UCR's Mobile Emissions Laboratory (MEL) using a heavy-duty chassis dynamometer. The dynamometer includes a 48" Electric AC Chassis Dynamometer with dual, direct connected, 300 horsepower motors attached to each roll set. The dynamometer applies appropriate loads to a vehicle to simulate factors such as the friction of the roadway and wind resistance, as would be experienced under typical in-use driving conditions. A driver accelerates and decelerates following a driving trace while on the dynamometer. UCR's Mobile Emission Lab (MEL) measures criteria pollutants, PM, and toxics with a CVS system, all meeting federal requirements [Cocker et al., 2004a,b]. The MEL was the second HDD lab in the United States to meet 40CFR Part 1065 specifications and successfully carried out cross laboratory comparisons of both gaseous and PM emissions with Southwest Research Institute in 2007 and 2009. Earlier cross correlation measurements were carried out with NREL in Denver in 2005, as well as with the ARB lab in Los Angeles. Results from UCR's MEL are recognized by the engine manufacturers and regulatory groups, including the U.S. EPA and CARB, and the data are often used to support regulation.

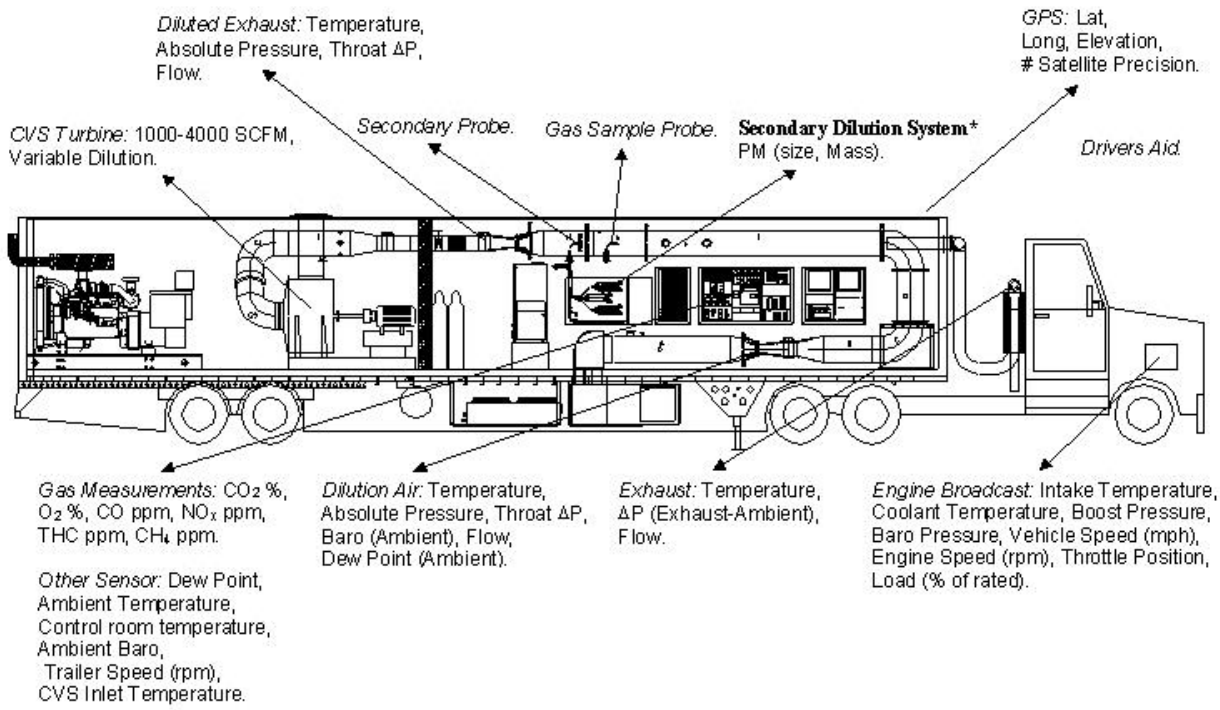


**Figure 3-1 UCR's Mobile Emissions Lab (MEL)**

Instruments within MEL continuously measure emissions of $NO_x$, CO, $CO_2$, NMHC, $CH_4$, and $PM_{2.5}$ with one-second resolution. A Dekati Mass Monitor (DMM) was used for real-time PM sampling. Total particle number was measured using a TSI 3776 ultrafine-Condensation Particle Counter (CPC). This is a butanol-based CPC that has the ability to count particles down to 2.5 nm. This instrument can sample about 300,000 particles per second, making the ultrafine CPC ideal for an accurate total particle number measurement. Integrated PM samples, such as PM mass and speciated PM, were collected on Teflo® and Quartz filters respectively.

Transient particle size distributions were obtained using an Engine Exhaust Particle Sizer (EEPS) spectrometer. The EEPS was used to obtain real-time second-by-second size distributions between 5.6 to 560 nm. Particles were sampled at a flow rate of 10 lpm, which is considered to be high enough to minimize diffusional losses. They were then charged with a corona charger and sized based on their electrical mobility in an electrical field. Concentrations were determined through the use of multiple electrometers.

Ammonia ($NH_3$) concentrations were continuously measured using a Unisearch Associates Inc. LasIR S Series Tunable Diode Laser (TDL) unit that is incorporated in MEL.

## 3.2 Laboratory Setup for the Off-line Analyses

This section provides information about the various analyses that were carried out in the UCR labs after the chassis test. Each of these test methods follows a Standard Operating Procedure created according to an EPA protocol guidance document.

### *3.2.1 Filter weighting for PM mass*

The mass concentrations of $PM_{2.5}$ were obtained by analysis of particulates collected on 47 mm diameter 2µm pore Teflo filters (Whatman brand). The filters were measured for net gains using a UMX2 ultra precision microbalance with buoyancy correction following the weighing procedure guidelines of the Code of Federal Regulations (CFR) (2). Before and after collection, the filters were conditioned for 24 hours in an environmentally controlled room (*Tdry* = 22 °C and *Tdew* = 9.5 °C or 45%RH at *Tdry* 22 °C) and weighed daily until two consecutive weight measurements were within 3 µg.

### *3.2.2 Carbonyl Compounds Analysis*

Samples for carbonyl analysis were collected onto 2,4-dinitrophenylhydrazine (DNPH) coated silica cartridges (Waters Corp., Milford, MA). A critical flow orifice controls the flow to 1.0 LPM through the cartridge and the sample time is adjusted to draw a known volume of exhaust sample through the DNPH cartridge so that the amount of carbonyls on the cartridge is at the mass level recommended by Waters. Sampled cartridges were extracted using 5 mL of acetonitrile and injected into an Agilent 1200 series high performance liquid chromatograph (HPLC) equipped with a variable wavelength detector. The column used was a 5 µm Deltabond AK resolution (200cm x 4.6mm ID) with upstream guard column. The HPLC sample injection and operating conditions were set up according to the specifications of the SAE 930142HP protocol. Samples from the dilution air were collected for background correction.

### *3.2.3 Volatile Toxic Compounds Analysis*

Samples for 1,3 butadiene, benzene, toluene, ethylbenzene, and xylenes were collected using Carbotrap adsorption tubes consisting of multi-beds, including a molecular sieve, activated charcoal, and carbotrap resin. An Agilent 6890 GC with a FID maintained at 300 °C was used to measure volatile organic compounds. A Gerstel TDS thermal adsorption unit was used for

sample injection. This unit ramps the temperature from 30 °C to 380 °C at a rate of 6 °C per minute to desorb the sample from the tubes. A 60 m x 0.32 mm HP-1 column was used. For these analyses, the GC column and operating conditions were set up according to the specifications of SAE 930142HP Method-2 for $C_4$-$C_{12}$ hydrocarbons. It should be noted that the amount of sample that is collected and injected into the GC using the Carbotrap absorption tubes is considerably greater than what can be achieved using Tedlar bag samples, since the absorption tubes are sampled over the duration of the test cycle, and hence allow for much large volume of sample to be injected into the GC. Thus, the detection limits with the thermal desorption tubes are improved by several orders of magnitude compared to levels achieved in earlier Auto/Oil programs. Samples from the dilution air were collected for background correction.

*3.2.4 PM Chemical Analysis*

PM samples were collected in pre-weighed Zefluor reinforced Teflon filters (Pallflex, 8 x 10 inch, Pall Corp., East Hills, NY) using a high volume sampler developed by USC (HI-Q Environmental Products Co., CA; flow rate = 450 l/min). The 8 x 10 inch filters were pre-weighed in a room with controlled relative humidity and temperature at USC. The speciated organic compounds, including polycyclic aromatic hydrocarbons (PAHs), hopanes and steranes, n-alkanes, and organic acids were quantified by gas chromatography-mass spectrometry (GC-MS). Samples were extracted in dichlomethane and methanol and were combined and reduced in volume to approximately 1 mL by rotary evaporation, followed by pure nitrogen evaporation. The underivatized samples were analyzed by auto injection into a GC-MSD system (GC model 5890, MSD model 5973, Agilent). A 30 m x0.25 mm DB-5MS capillary column (Agilent) was used with a split-less injection. Along with the samples, a set of authentic quantification standard solutions were also injected and used to determine response factors for the compounds of interest.

Inorganic ions, including nitrate, sulfate and ammonium, and other water soluble ions, such as chloride, sodium, and potassium, were analyzed by ion chromatography (IC) using a modified version of the NIOSH (National Institute for Occupational Safety and Health) Method 7903 and OSHA (Occupational Safety and Health Administration) Method 188.

Metals and trace elements concentrations (both total and water-soluble) were determined by Magnetic-Sector Inductively Coupled Plasma-Mass Spectroscopy (HR-ICP-MS). The details of the digestion analysis and method detection limits have been presented by Lough et al. (2005). Of particular interest were the concentrations of the following metals: Na, Mg, Al, K, Ca, Ti, V, Cr, Be, S, Mn, Fe, Co, Cu, Zn, Mo, Sr, Ba, Cd, Pt, Pb and Ni.

Water soluble organic carbon (WSOC) content was extracted from the 8 x 10 inch filters and subsequently analyzed by Shimadzu TOC-5000A liquid analyzer.

The oxidative activity of the collected particles was measured by two independent assays. This section describes the macrophage ROS (reactive oxygen species) assay measured on the PM collected onto the 8 x 10 inch filters. Sub-sections of the hi-volume PM samples were analyzed for ROS activity by macrophage assay. Samples were extracted with 15 mL of high purity water. Extractions were performed in 20 mL acid-leached, capped, polypropylene tubes, with continuous agitation for 16 hours at room temperature in the dark. Extracts were filtered through acid leached 0.22 µm polypropylene syringe filters. The ROS-activity of the PM extracts was measured by in vivo exposure to rat alveolar macrophage (NR8383, ATCC# CRL-2192) cells using 2',7'-dichlorofluorescin diacetate (DCFH-DA) as the fluorescent probe. DCFH-DA, a membrane permeable compound, is de-acetylated by cellular esterases generating 2',7'-dichlorofluorescein (DCH), which is highly fluorescent. The fluorescent is monitored using a plate reader method. Methodological procedures of this assay are described in Landreman et al. (2008). Sub-samples of the primary water extracts were further processed by chelation with the immobilized ligand iminodiacetate (Chelex chromatography) to remove the metal ions. For the Chelex treatment, mini-columns (1 mL polypropylene with Teflon frits) of chelex were prepared with 0.2 g of high purity water-slurried Na-Chelex. Columns were rinsed with high purity water and buffered with 0.1 M sodium acetate. PM extracts were processed through the columns, under gravity flow, in a solid phase extraction manifold, at a flow rate of ~1.0 mL/min. The Chelex-processed extract was collected and immediately assayed for ROS-activity and subsequent elemental analysis by magnetic sector ICP-MS. Control samples were processed through the Chelex columns to ensure that the treatment did not produce ROS active species or inhibit the activity of Zymosan (a β-1,3 polysaccharide of D-glycose). Zymosan was used as a

positive control as it is recognized by TLR-2 (Toll-like receptors) on macrophage cells, activating a strong immune-chemical and ROS response. ROS activity is therefore reported in terms of Zymosan units to facilitate the comparison of various data sets.

### *3.2.5 Chemical Reactivity and Cellular Assays*

Two chemical reactivity assays and two cellular assays were performed on both the vapor and particle fractions of PM samples for each vehicle/fuel combination. Particle and semivolatile fractions were collected using a filter based collection system containing a XAD resin bed below the 47 mm Teflo filters. The chemical reactivity assays assess the levels of prooxidants and electrophiles in the samples. For this study, the second assay that examined the prooxidant content in PM was the dithiothreitol (DTT) assay. This assay uses DTT as the electron source in a reaction catalyzed by prooxidants. The quantity of prooxidant is proportional to the rate of DTT consumption. The procedure has been applied to multiple samples of diesel exhaust particles and to ambient air particles and vapors [Biswas et al., 2009; Eiguren-Fernandez et al., 2010]. Prooxidants in this assay include redox active metals and organic compounds. The methodological details of this assay are provided by Cho et al. (2005). An additional assay was performed that detects electrophiles in PM samples using the active site of the thiol enzyme, glyceraldehyde-3-phosphate dehydrogenase (GAPDH), as the target nucleophile, and thus determines the extent of oxygen independent inactivation of the enzyme. Electrophile content was measured in terms of the mole equivalents of a standard electrophile (N-ethyl maleimide, NEM) present in the sample. The details of this assay can be found elsewhere [Shinyashiki 2009].

For the cellular assays, the PM samples were incubated with a mouse macrophage cell line (Raw 264.7) to assess their biological effects. Following exposure, levels of the inflammatory cytokine, tumor necrosis factor alpha (TNFα) released by cells into the incubation media were determined by enzyme linked immunosorbant assays (ELISA). To assess the protective or adaptive responses to the exhaust samples, the cell extract was assayed for levels of hemeoxygenase-1 (HO-1), a marker enzyme for the activation of the antioxidant/antielectophile response element (ARE). Activation of this DNA site results in the expression of multiple protective enzymes, including HO-1, catalase, glutathione synthases, and

glutathione transferases. These proteins are involved in the removal of cellular oxidants and foreign electrophiles.

# 4 Results and Discussion

The results for both vehicles as a function of different fuel types with the UDDS cycle are shown in the figures below. The error bars denote the standard deviation of the average for each fuel. Statistical comparisons between fuels for a given vehicle were made using a 2-tailed, 2-sample, equal variance *t*-test. For the purpose of this discussion, results are considered to be statistically significant for $p \leq 0.05$ and marginally statistically significant for $0.05<p \leq 0.1$.

## 4.1 CO Emissions

CO emissions depend mainly on the air-fuel equivalence ratio and are usually not significant during steady-state diesel engine operation and in modern diesel engines fitted with aftertreatment controls. CO emissions for the Cummins ISX-15 and Cummins ISX-450 are presented in Figure 4-1 and Figure 4-2, respectively. For the uncontrolled vehicle, there is a clear trend towards lower CO emissions with the B50 biodiesel blends compared to the baseline CARB ULSD fuel. Reductions in CO emissions were in the order of 19% ($p$=0.001), 21% ($p$=0.0002) and 22% ($p$=0.0006) for SME-50, AFME-50, and WCO-50, respectively, and were all found to be statistically significant. For the Cummins ISX-15 engine, there were no distinguishable trends between the biodiesel blends with the exception of AFME-50, which showed CO emissions reductions relative to CARB ULSD at a statistically significant level. CO emissions for the Cummins ISX-15 engines were found to be approximately an order of magnitude lower than those for the older vehicle. It appeared that the influence of exhaust aftertreatment, and in particular the presence of a DOC, played a major role in reducing CO emissions.

Our results showed lower CO emissions with biodiesel blends, particularly for the engine without aftertreatment, which is consistent with those reported in previous studies [Knothe et al., 2006; Nikanjam et al., 2011]. This can be attributed to both the higher oxygen content in the methyl ester molecule, as well as a lower carbon/hydrogen ratio in biodiesel compared to petroleum diesel. Higher oxygen content will lead to more complete combustion, and therefore lower CO emissions [Xue et al., 2011].

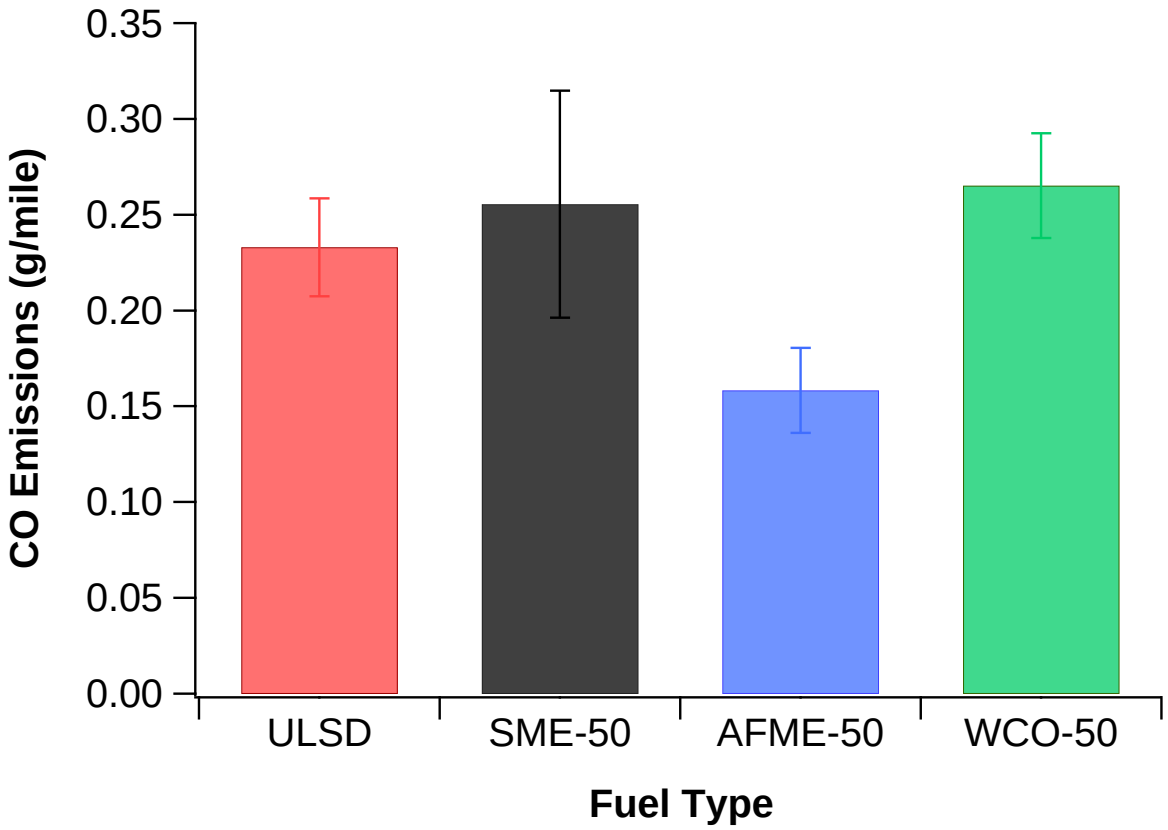


**Figure 4-1. CO emissions for the Cummins ISX-15 engine**

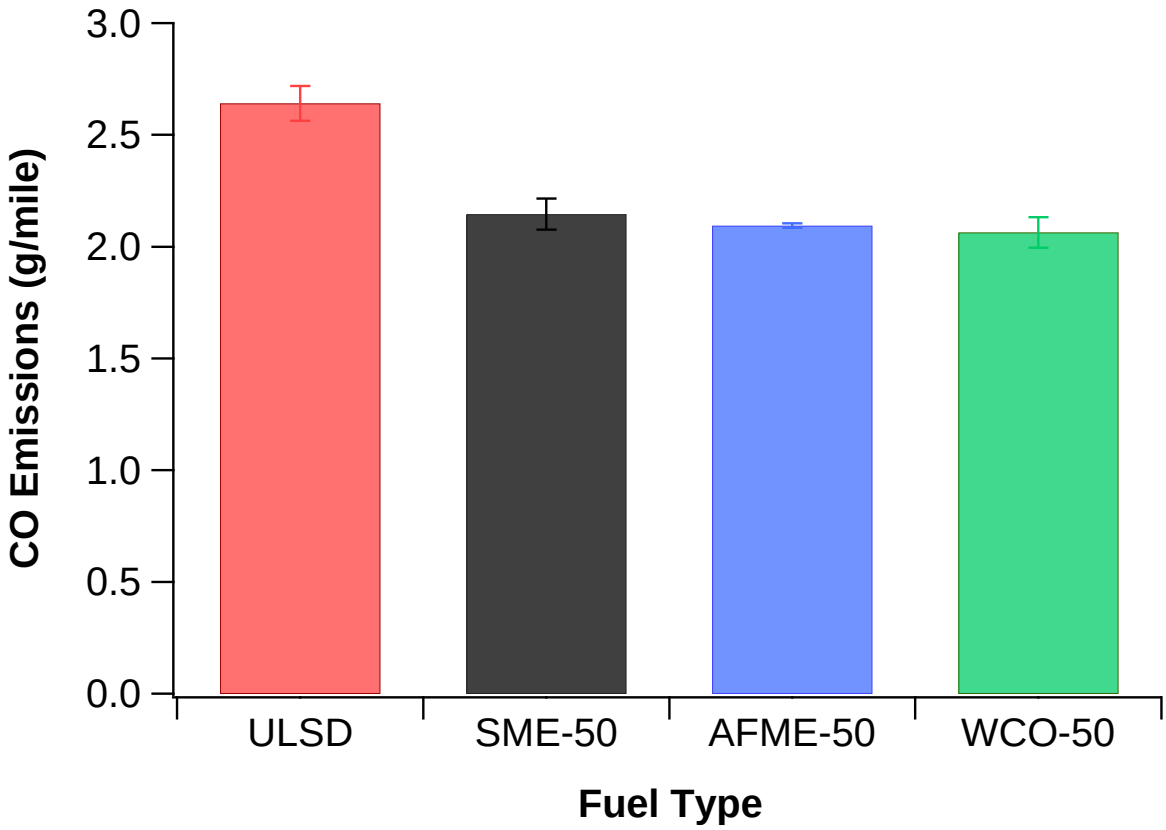


**Figure 4-2 CO emissions for the Cummins ISX-450 engine**

### 4.2 THC, NMHC, and $CH_4$ Emissions

Hydrocarbons form during the ignition delay period as the result of either very low air-fuel ratios or, mainly, under-mixing of fuel that cannot ignite or support a flame. Contrary to CO emissions that peak only during load increase or acceleration, turbocharged diesel engine THC emissions are noticed at the onset of deceleration or load decrease too, since in the latter cases, turbocharger lag effects lead to very high instantaneous air-fuel equivalence ratios [Giakoumis et al., 2012]. As shown in Figure 4-3, for the Cummins ISX-450 engine, THC emissions showed a declining trend with the B50 blends. The reductions relative to CARB ULSD were on the order of 53% ($p$=0.005), 31% ($p$=0.006), and 21% for SME-50, AFME-50, and WCO-50, respectively, with the differences in THC emissions for SME-50 and AFME-50 blends being statistically significant compared to CARB ULSD. The absence of aromatic compounds and the higher oxygen concentration of biodiesel, both promote more complete combustion and thus

reduce THC emissions. Moreover, the relatively higher cetane number of biodiesel contributes to a reduction of the ignition delay, where a significant amount of THC is formed. It should be noted that THC emissions for the newer Cummins ISX-15 engine are not presented here because were almost undetectable for all fuels, which was due to the presence of the DOC/DPF configuration.

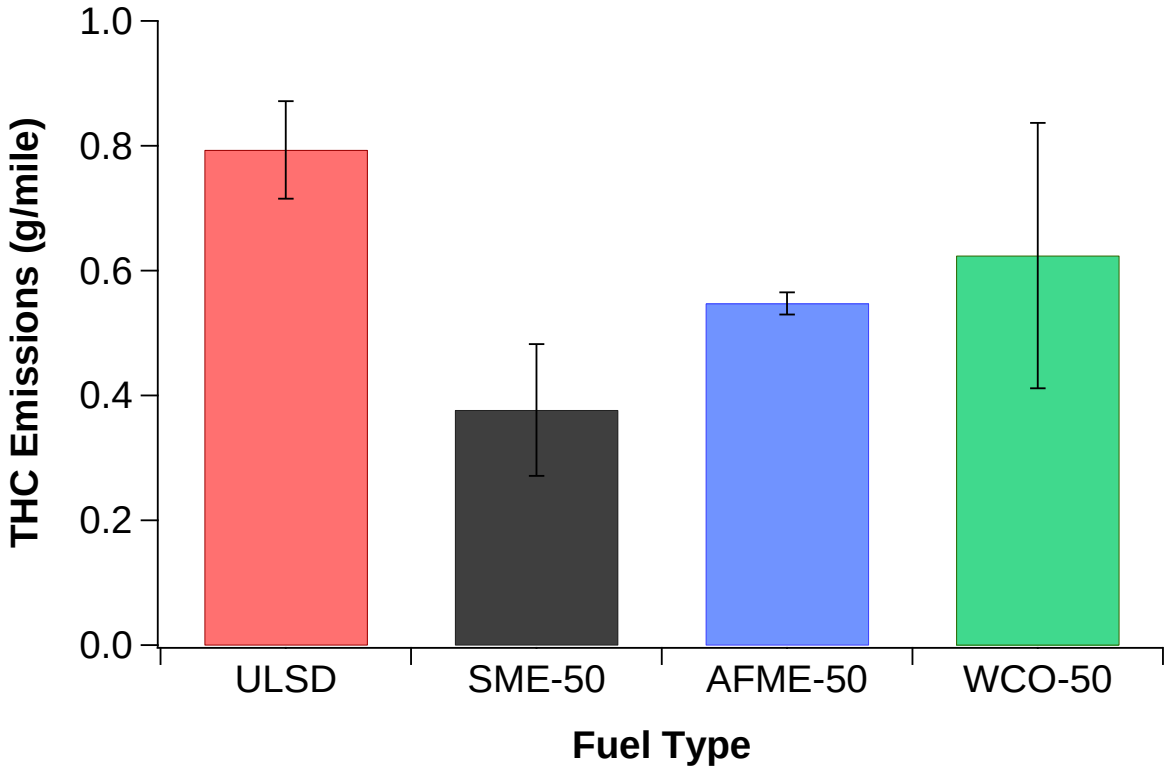


**Figure 4-3 THC emissions for the Cummins ISX-450 engine**

NMHC emissions followed similar patterns as with THC emissions, as shown in Figure 4-4. The addition of biodiesel, independent of its raw material, led to reductions in NMHC emissions compared to CARB ULSD, with SME-50 and AFME-50 showing statistically significant differences of 55% ($p$=0.005) and 31% ($p$=0.004), respectively. Analogous to THC emissions, for the Cummins ISX-15 engine the DOC/DPF configuration reduced NMHC emissions in the tailpipe to essentially undetectable levels.

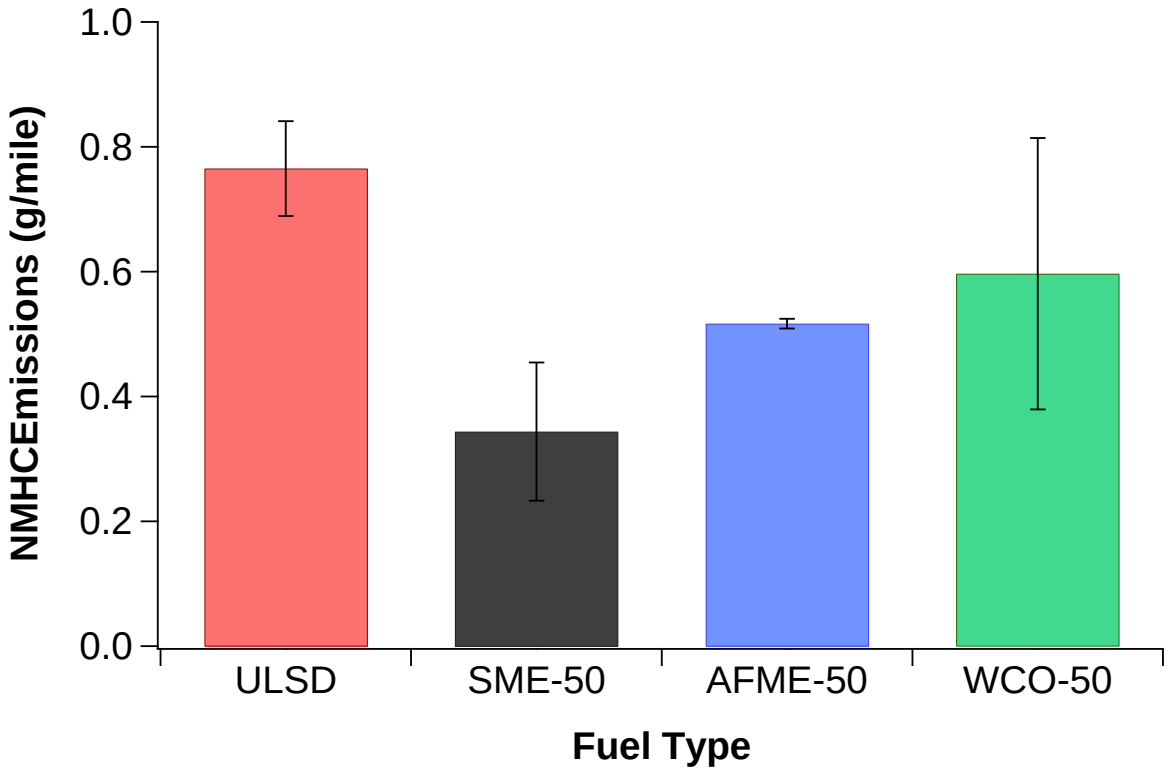


**Figure 4-4 NMHC emissions for the Cummins ISX-450 engine**

Emissions of $CH_4$ are presented in Figure 4-5 and Figure 4-6 for the Cummins ISX-15 and Cummins ISX-450 engine, respectively. $CH_4$ is an important greenhouse gas emitted by vehicles. Although $CH_4$ is not toxic and not relevant to ozone-forming processes, it is a potent greenhouse gas. Under the present test conditions, emissions of $CH_4$ for both vehicles were found in very low levels with the newer Cummins ISX-15 engine producing very low $CH_4$ concentrations due to the DOC/DPF configuration in the exhaust. The effect of biodiesel on $CH_4$ emissions wasn't particularly strong for either of the two test vehicles.

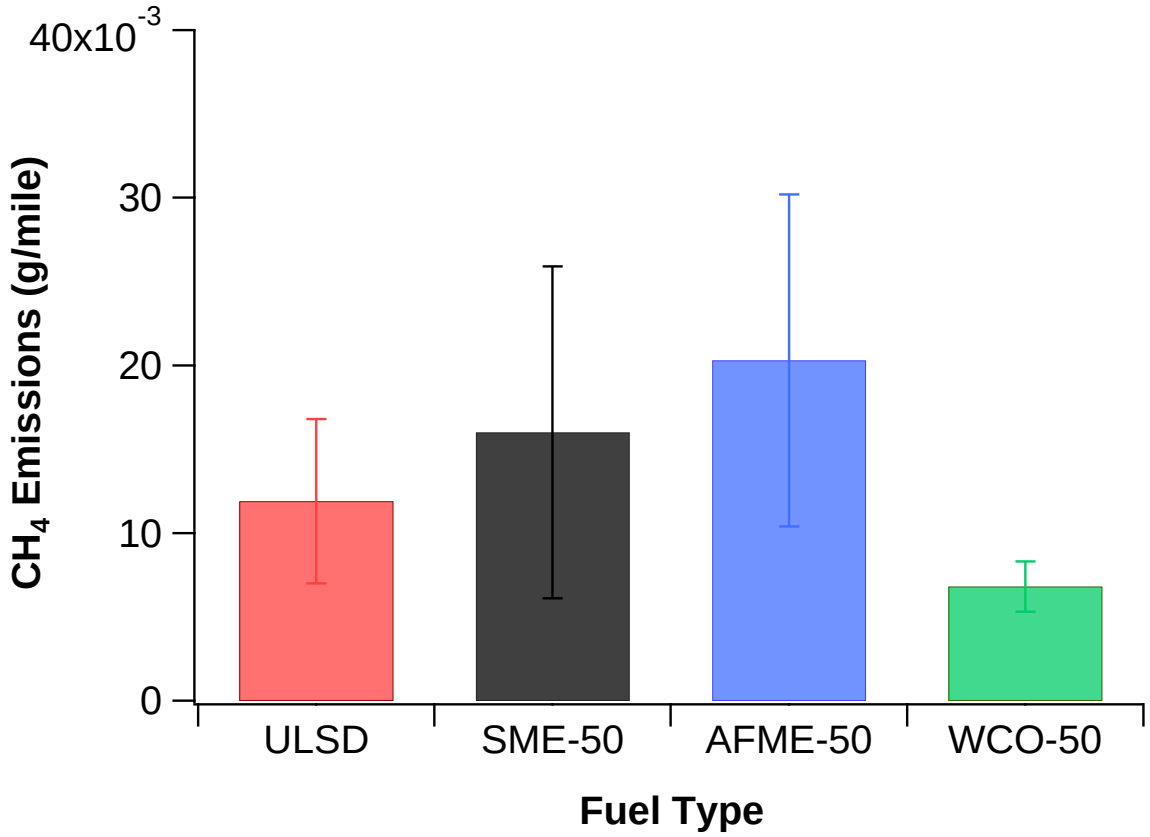


**Figure 4-5 $CH_4$ emissions for the Cummins ISX-15 engine**

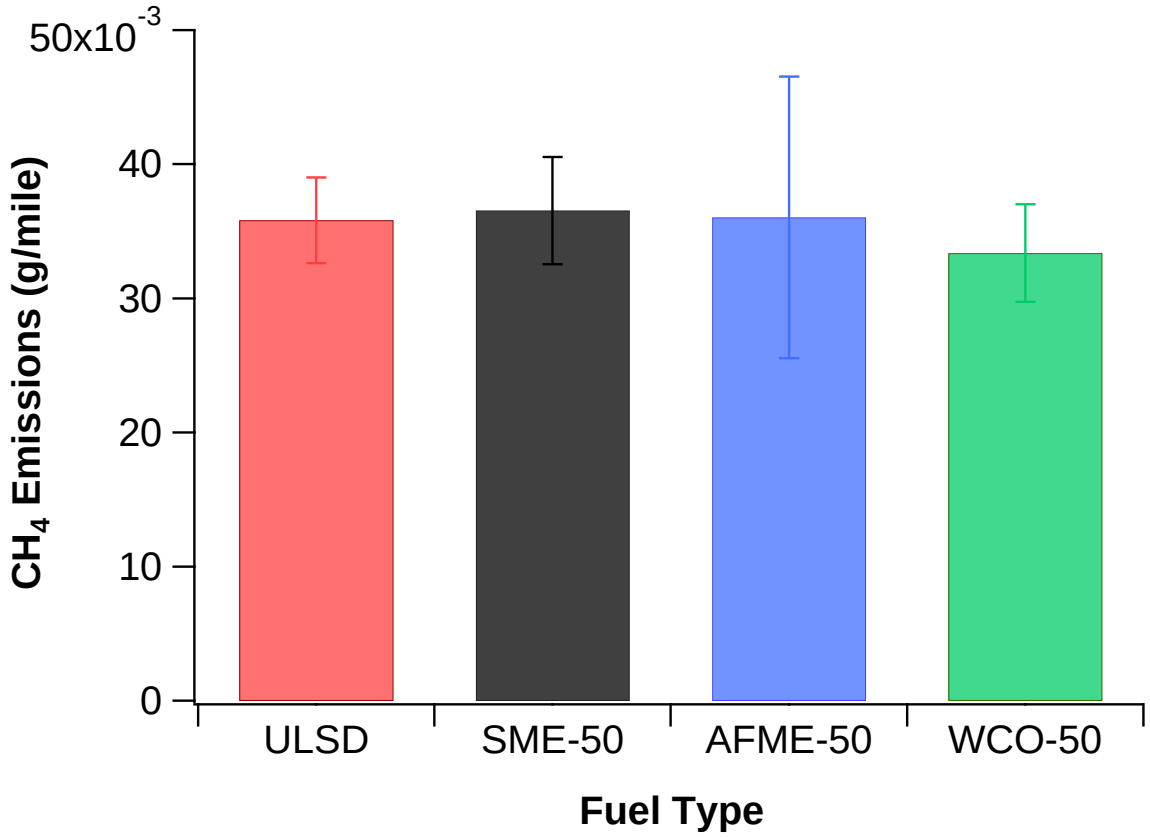


**Figure 4-6 $CH_4$ emissions for the Cummins ISX-450 engine**

### 4.3 $NO_x$ Emissions

Oxides of nitrogen ($NO_x$) are the toughest pollutant to control in a diesel engine. In diesel exhaust, $NO_x$ is predominantly composed of nitric oxide (NO), with lesser amounts of nitrogen dioxide ($NO_2$). The common mechanisms for NO formation in diesel combustion are: thermal (Zeldovich), prompt (Fenimore), and fuel-bound nitrogen. At high temperatures, $N_2$ and $O_2$ can react through a series of chemical steps represented by Reactions (1) through (3):

$O + N_2 \longleftrightarrow NO + N$ (1)

$N + O_2 \longleftrightarrow NO + O$ (2)

$N + OH \longleftrightarrow NO + H$ (3)

$NO_x$ formation occurs at temperatures above 1500 °C, and the rate of formation increases rapidly with increasing temperature. Under most diesel engine combustion conditions, thermal $NO_x$ is believed to be the predominant contributor to total $NO_x$.

The formation of prompt $NO_x$ involves intermediate hydrocarbon fragments from fuel combustion, particularly CH and $CH_2$, reacting with $N_2$ in the combustion chamber. The resulting C-N containing species then proceed through reaction pathways involving $O_2$ to produce $NO_x$. Prompt $NO_x$ is only prevalent under fuel rich conditions, where there is an abundance of hydrocarbon fragments to react with $N_2$. Due to this dependence on hydrocarbon fragments, prompt $NO_x$ is sensitive to fuel chemistry, whereas thermal $NO_x$ is largely insensitive to fuel chemistry [Hoekman and Robbins, 2012; Sun et al., 2010]. Cheng et al. (2006) for example mentioned that differences in the relative contribution of the prompt mechanism could be important when diagnosing differences in $NO_x$ emissions of biodiesel fuels. McCormick et al. (2001) found that changes in $NO_x$ emissions between biodiesel and diesel fuels were driven largely by pre-combustion chemistry of hydrocarbon free radicals. The thermal mechanism was unaffected by fuel chemistry, whereas the prompt mechanism was sensitive to radical concentrations within the reaction zone.

Fuel $NO_x$ is created when $N_2$ that is chemically bound in the fuel combines with excess oxygen during the combustion process. This type of $NO_x$ formation is only a problem with fuel containing chemically bound N. The main pathway for this type of $NO_x$ creation involves the creation of intermediate N containing species such as HCN, $NH_3$, NH, or CN. These molecules can be oxidized to form $NO_x$. However, since the natural N levels in biodiesel are extremely low, this formation process is generally negligible [Hoekman and Robbins, 2012].

$NO_x$ emissions as a function of fuel type are shown in Figure 4-7 and Figure 4-8 for the Cummins ISX-15 and Cummins ISX-450 engines, respectively. It is evident from the results that the newer Cummins ISX-15 produced significantly lower amounts of $NO_x$ compared to the Cummins ISX-450. This was a result of the SCR $NO_x$ aftertreatment, which reduced $NO_x$ emissions by 91%, 85.3%, 88.5%, and 84.2% for ULSD, SME-50, AFME-50, and WCO-50, respectively. For the Cummins ISX-15, SME-50 ($p$=0.0002) and WCO-50 ($p$=0.0084) biodiesel blends increased $NO_x$ emissions at a statistically significant level relative to CARB ULSD, while AFME-50 ($p$=0.065) produced a marginally statistically significant increase. These increases were 43% for SME-50, 101% for WCO-50, and 47% for AFME-50.

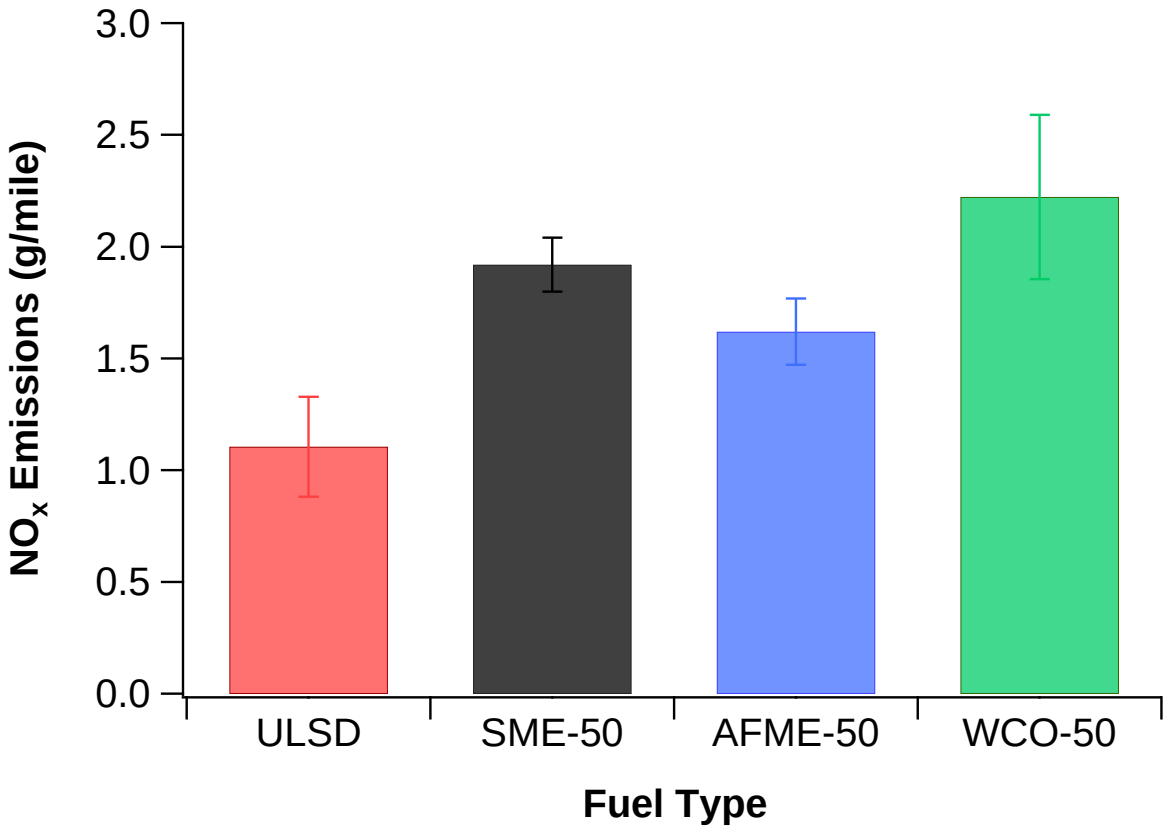


**Figure 4-7 $NO_x$ emissions for the Cummins ISX-15 engine**

For the Cummins ISX 450 engine, statistically significant increases in $NO_x$ emissions relative to CARB ULSD were seen with AME-50 ($p$=0.021) and WCO-50 ($p$=0.018). These increases were 8.4% and 7.9%, which were much smaller than the relative increases in $NO_x$ emissions from the Cummins ISX-15 engine equipped with SCR. On an absolute basis, however, the increases in $NO_x$ were higher than those seen for the Cummins ISX-15.

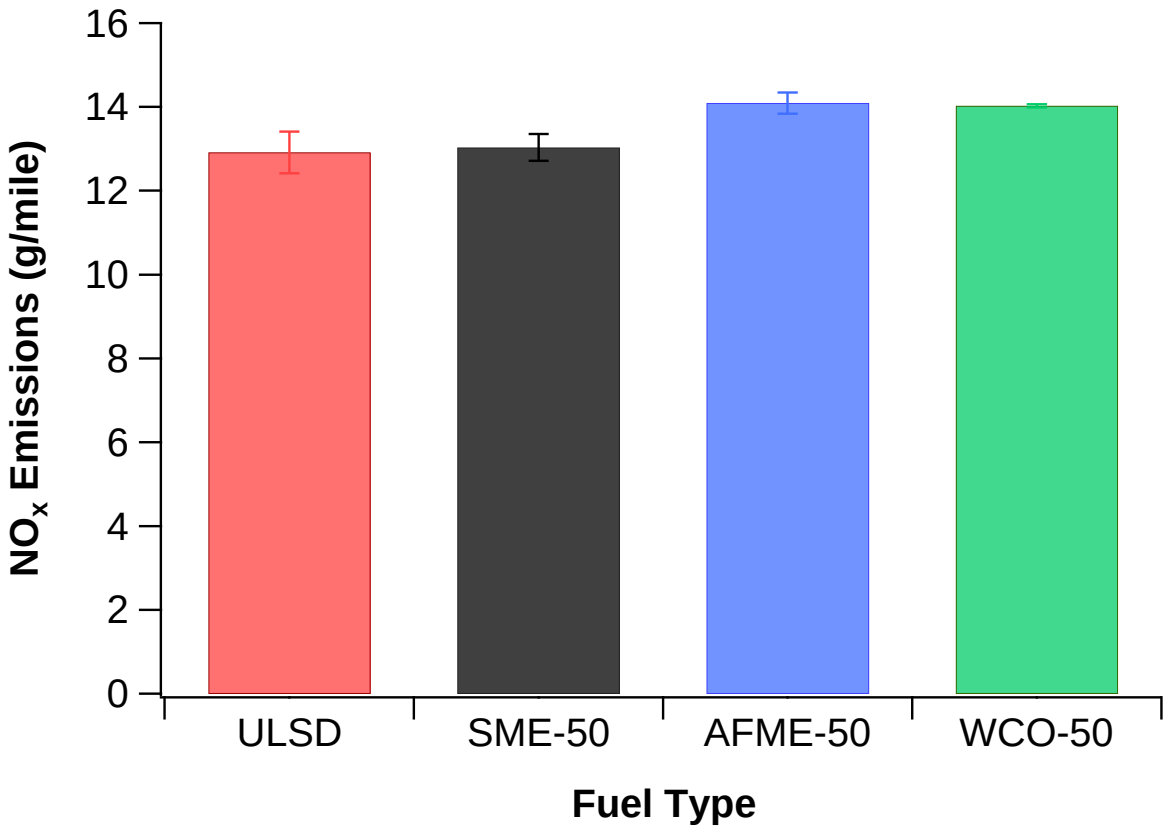


**Figure 4-8 $NO_x$ emissions for the Cummins ISX-450 engine**

Lammert et al. (2012) showed that the effect of SCR aftertreatment negates the effect of fuels on $NO_x$ emissions when they tested a 2011 Cummins ISL engine on B20 and B100. This is in contrast to the current study, which shows that there is a rather strong fuel effect with the B50 blends compared to CARB ULSD from the Cummins ISX-15 engine with SCR. Increases in $NO_x$ emissions with biodiesel from vehicles equipped with a SCR catalyst have been previously reported in other studies [Kawano et al., 2010]. The $NO_x$ increase with biodiesel for SCR-equipped engines is usually attributed by a reduction of exhaust temperature and a change of the $NO_2$/NO ratio in $NO_x$ emissions [Mizushima et al., 2010]. In general, the lower exhaust temperatures with biodiesel will lower the oxidation rates of NO to $NO_2$ from the DOC. It has been shown that a $NO_2/NO_x$ ratio below 0.5 significantly changes SCR reaction chemistry lowering the SCR removal efficiency of $NO_x$ [McWilliam and Zimmermann, 2010]. Walkowicz et al. (2009) found increases in $NO_x$ emissions of 7% with B20 and 26% with B99 compared to

ULSD for a heavy-duty diesel vehicle equipped with a 2004 Caterpillar 400 hp C13 engine. For the same vehicle equipped with a urea-based SCR system, $NO_x$ increases were very similar on a percentage basis, with B20 and B99 having 7% and 27%, respectively, higher $NO_x$ than ULSD. The SCR significantly reduced $NO_x$ emissions by 87.4%, 87.3%, and 87.3% with ULSD, B20, and B99, respectively, compared to the test conducted without the SCR.

Figure Figure 4-9 shows the profile of real-time $NO_x$ emissions of the test fuels for the Cummins ISX-15 engine in comparison with the SCR temperature. Interesting trends emerge from the data in Figure 4-9, showing that a relatively large portion of the $NO_x$ emissions for all test fuels were produced at the start of the UDDS when the SCR system temperature was <250 °C. The lowest $NO_x$ emissions for all fuels were found when the SCR system was at a temperature above 250 °C. This phenomenon can be explained by the fact that with the SCR system $NO_x$ is converted into $N_2$ by reaction with $NH_3$ over a catalyst. When operating temperatures are >250 °C, an aqueous solution of urea is injected into the exhaust upstream of the SCR catalyst. The heat converts the urea into $NH_3$, which is the reactant to convert $NO_x$ to nitrogen, and water. At temperatures <250 °C, urea is not injected so the full engine out $NO_x$ emissions are emitted. Under the present test conditions, it appeared that for a significant portion of the UDDS that the temperature was <250 °C, there was no urea injection, and thus no $NO_x$ control for the Cummins ISX-15 engine. It is interesting to note that the for the low-temperature period (<250 °C) the fuel effect was particularly strong, with WCO-50 blend showing higher $NO_x$ emissions relative to CARB ULSD, followed by SME-50 and AFME-50 blends. The WCO-50 blend systematically led to higher $NO_x$ emissions throughout the entire driving cycle and generally showed lower exhaust temperatures. In fact all biodiesel blends had lower exhaust temperatures, suggesting that our results for the SCR-fitted vehicle are in line with the studies conducted by Kawano et al. (2010) and Mizushima et al. (2010).

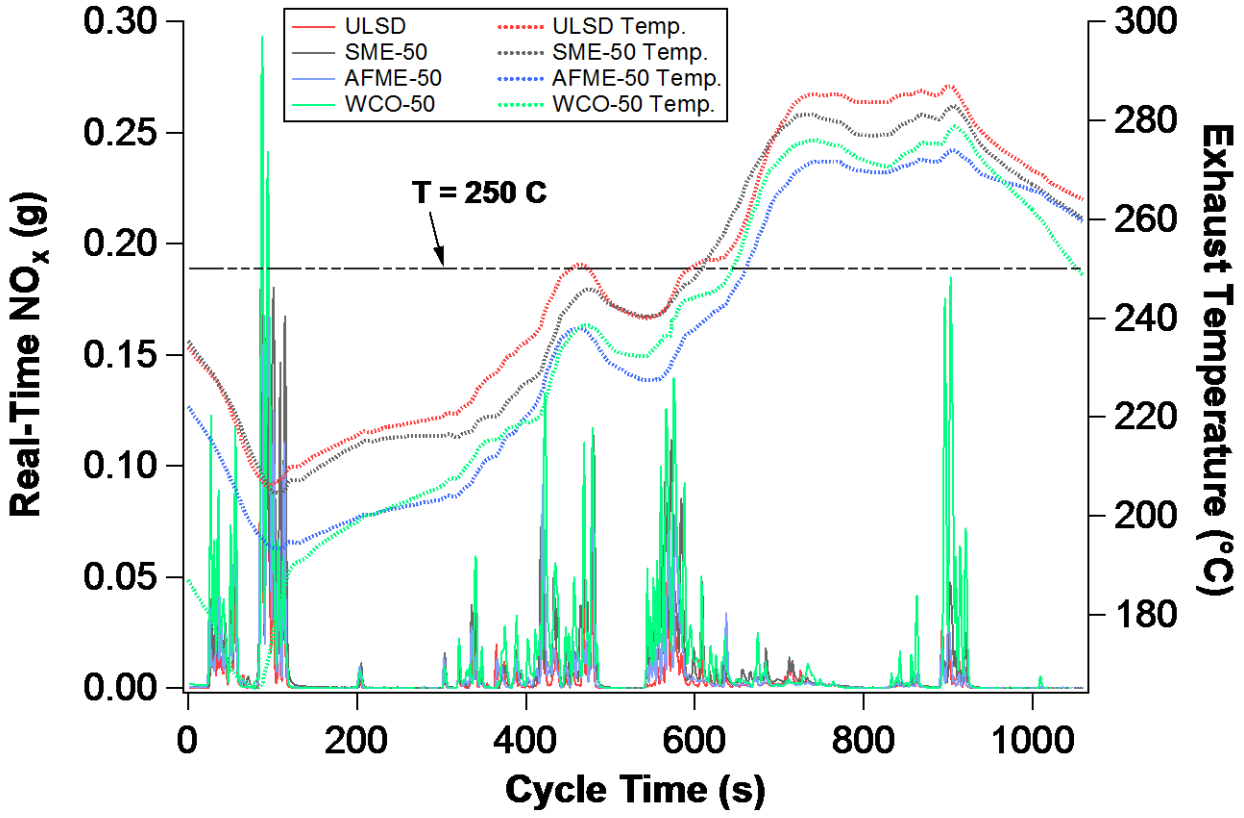


**Figure 4-9 Real-time $NO_x$ emissions as a function of SCR temperature**

The trend of increasing $NO_x$ emissions for biodiesel blends is consistent with a wide range of studies found in the literature. Comprehensive investigations conducted by Mueller et al. (2009) and Sun et al. (2010) confirmed that biodiesel promotes a combustion process that is shorter and more advanced than conventional diesel, which contributes to the formation of thermal $NO_x$. The higher $NO_x$ emissions with biodiesel for both vehicles could also be a consequence of the higher oxygen content in biodiesel, which enhances the formation of $NO_x$. The lower volatility of biodiesel compared to diesel fuel could also contribute to decreased fractions of premixed burn, as a result of fewer evaporated droplets during the ignition delay period [Giakoumis et al., 2012]. Another contributing factor for $NO_x$ emissions increase could be the engine control module (ECM), which may dictate a different injection strategy based on the lower volumetric energy content of biodiesel. Eckerle et al. (2008) suggested that a higher fuel flow is required with biodiesel compared to diesel fuel for an engine to achieve the same power. The ECM interprets this higher fuel flow as an indicator of higher torque, and therefore

makes adjustments to engine operating parameters that, under certain operating conditions, increase $NO_x$ emissions.

The trend of higher $NO_x$ emissions for the more highly unsaturated (i.e., having greater numbers of double bonds) biodiesel feedstocks is also consistent with previous studies [Hajbabaei et al., 2012; McCormick et al., 2011; Ban-Weiss et al., 2007]. More unsaturated methyl esters have lower cetane numbers and higher densities than saturated methyl esters. Double-bond structuring of methyl esters tends to decrease cetane number and lengthen ignition delay. The longer ignition delay can lead to greater premixed combustion, which can lead to greater $NO_x$ emissions. The greater number of double bonds for the more unsaturated methyl esters can also lead to higher adiabatic flame temperatures, although this argument has been criticized since it has been found that adiabatic flame temperatures do not usually vary with biodiesel feedstock, and measured peak temperatures show even less variation [Giakoumis et al., 2012].

### 4.4 $CO_2$ Emissions

Emissions of $CO_2$ are shown in Figure 4-10 and Figure 4-11 for the Cummins ISX-15 and Cummins ISX-450 engines, respectively. For the Cummins ISX-15 engine, the results did not show strong fuel trends in $CO_2$ emissions. For the uncontrolled Cummins ISX-450 engine, there was a slight decrease in $CO_2$ with SME-50 compared to CARB ULSD, while the AFME-50 and WCO-50 blends showed no statistically significant differences compared to the CARB ULSD. These results practically confirmed that during transient operation, the engine efficiency was effectively not impacted with the use of high concentration biodiesel blend ratios.

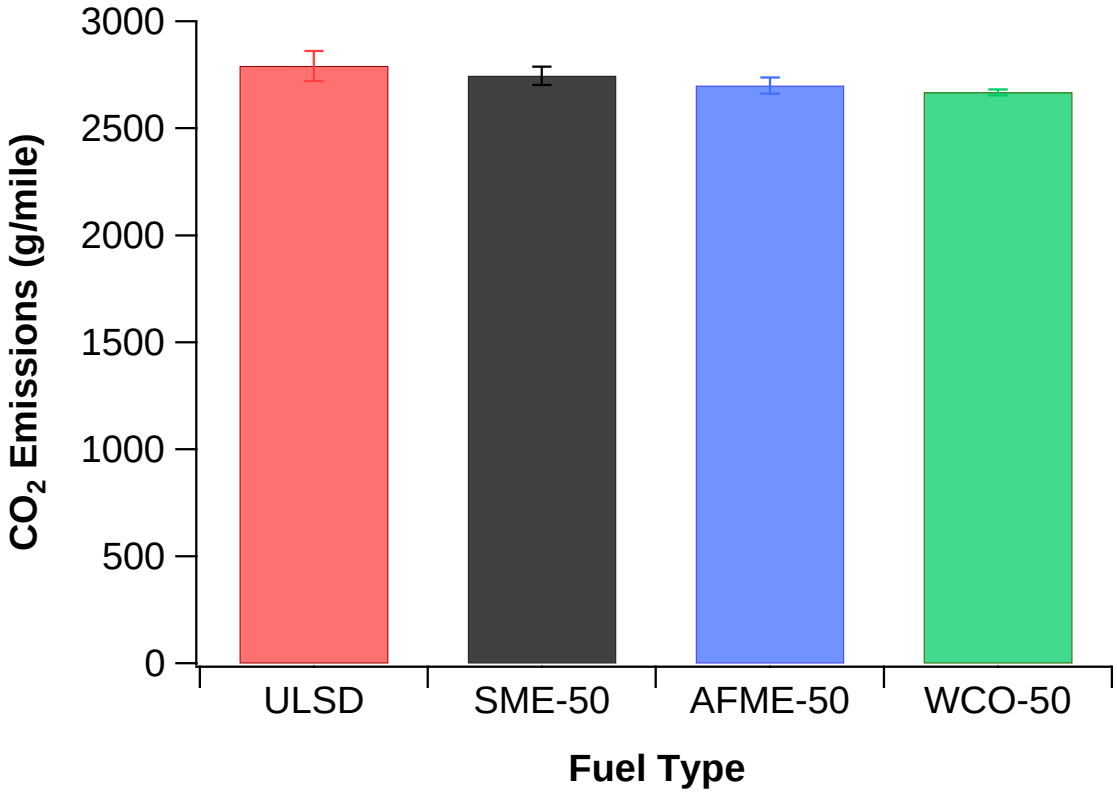


**Figure 4-10 $CO_2$ emissions for the Cummins ISX-15 engine**

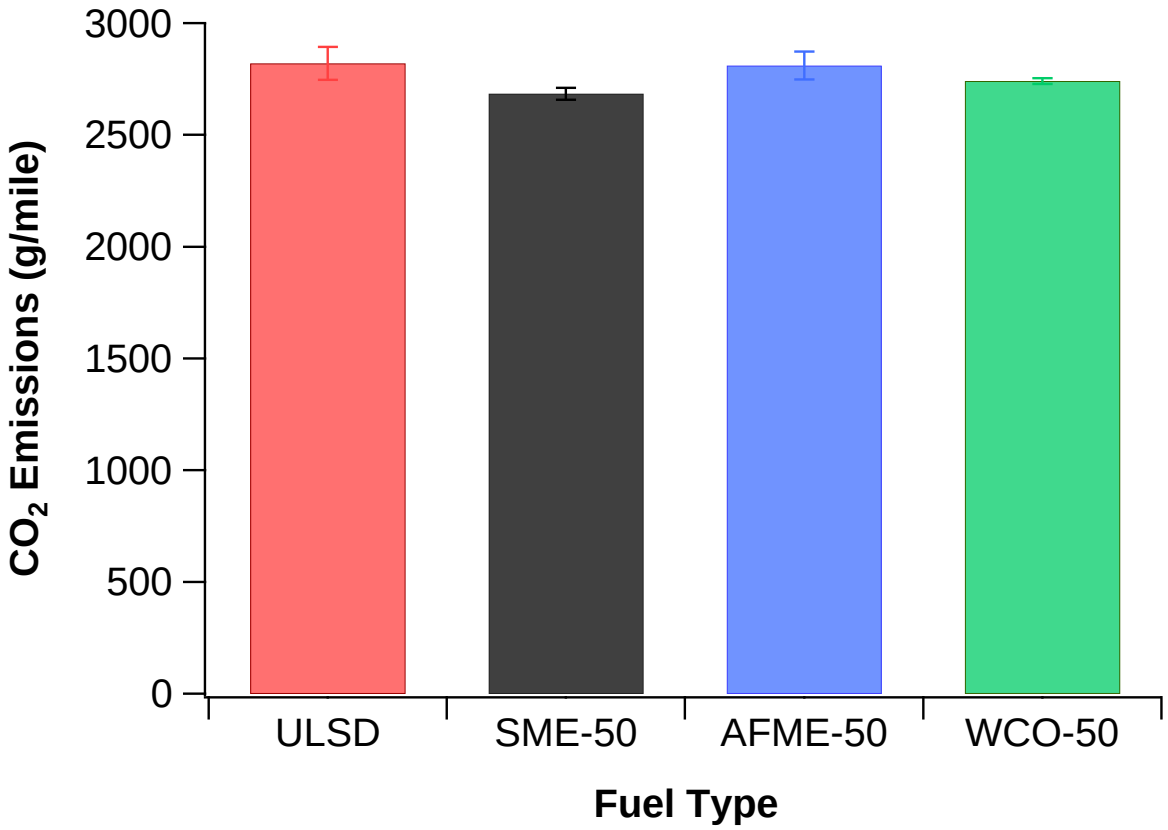


**Figure 4-11 $CO_2$ emissions for the Cummins ISX-450 engine**

### 4.5 PM Mass, Particle Number Emissions, and Particle Size Distributions

PM mass emissions are shown in Figure 4-12 and Figure 4-13 for the Cummins ISX-15 and Cummins ISX-450 engines, respectively. For the Cummins ISX-450 engine, the use of B50 blends, independent their source material resulted in dramatic PM mass reductions at a statistically significant level. These reductions were 67% ($p$=0.0002), 67% ($p$=0.001), and 74% ($p$=0.001) for SME-50, AFME-50, and WCO-50, respectively. For the Cummins ISX-15 engine, PM mass emissions were substantially lower than those of the older-technology Cummins ISX-450 engine and very low on an absolute basis. This observation indicates that the application of the DPF appeared to be very effective in reducing PM mass emissions. In general, DPF control system consists of four sections: 1) an inlet, 2) a DOC, 3) a DPF and 4) an outlet. Exhaust flows out of the engine and through a DOC before entering the DPF where PM is collected on the walls of the DPF. The collected carbon is oxidized to remove it from the DPF during the regeneration

process. When operating conditions maintain high exhaust temperatures, the DPF is self-regenerating. Otherwise, an active regeneration is required to remove a build-up of PM and pressure drop in the DPF by adding diesel fuel upstream of the DOC. The chemical reaction of the fuel over the DOC raises the exhaust gas temperature high enough to oxidize the carbon from the filter.

Fuel effects on PM mass emissions were literally absent for the Cummins ISX-15 engine, with some moderate decreases for some biodiesel blends relative to CARB ULSD, but not at a statistically significant level. For the Cummins ISX-15 engine, it was observed that biodiesel did not provide significant added benefits in PM reduction beyond those that were already being achieved with the DPF. On the other hand, the reductions in PM mass emissions for the Cummins ISX-450 engine could be attributed to the increased oxygen concentration in the biodiesel blend, which reduces locally fuel-rich regions and limits soot nucleation in the formation process [Lapuerta et al., 2008]. In addition to the oxygen content, the absence of aromatics, which act as soot precursors, could also contribute to the PM mass decrease with biodiesel [Szybist et al., 2007].

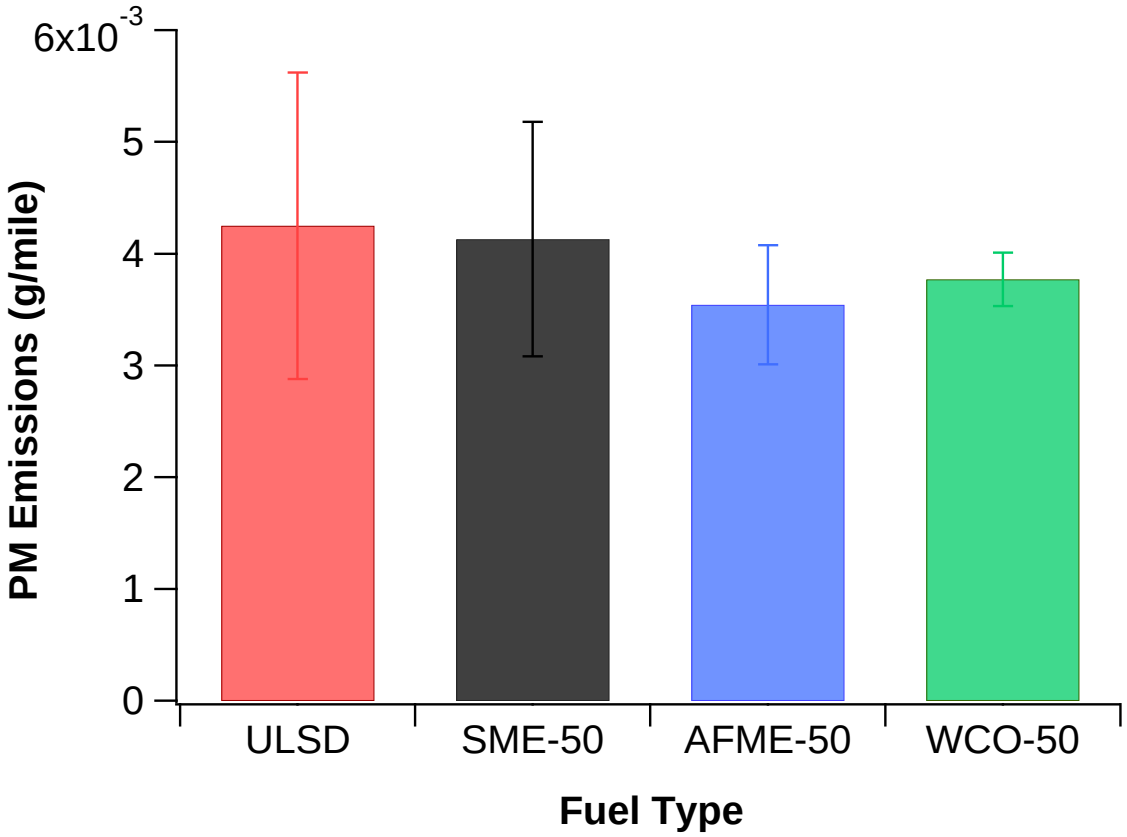


**Figure 4-12 PM mass emissions for the Cummins ISX-15 engine**

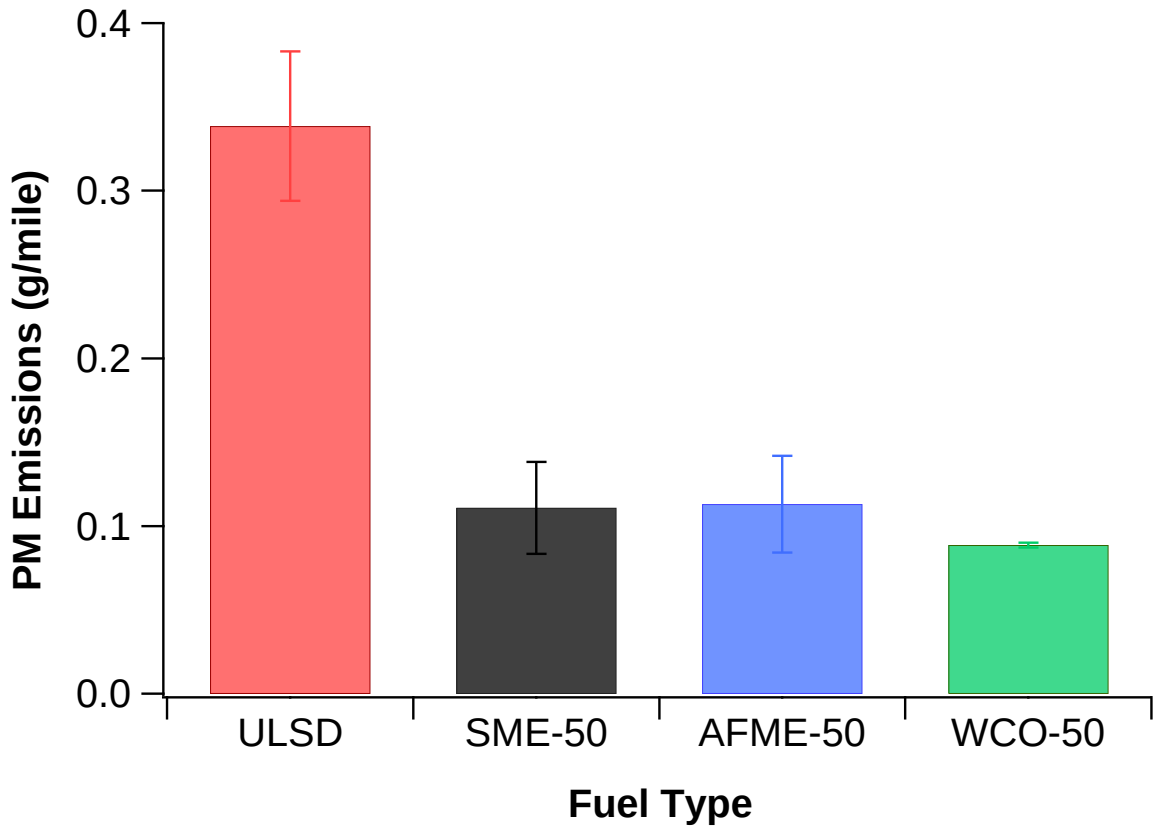


**Figure 4-13 PM mass emissions for the Cummins ISX-450 engine**

Figure 4-14 and Figure 4-15 display the total particle number emissions for the Cummins ISX-15 and Cummins ISX-450 engines, respectively. It is evident from the results that for the Cummins ISX-15 engine, total particle number counts were found to be significantly lower than those of the Cummins ISX-450 engine, suggesting that the DOC/DPF system effectively reduced particle emissions. It should be stressed that total particle number counts for the Cummins ISX-15 engine were actually below the tunnel background levels. For the Cummins ISX-450 engine, particle number emissions were about the same with all the test fuels, showing no strong trends as a function of biodiesel use.

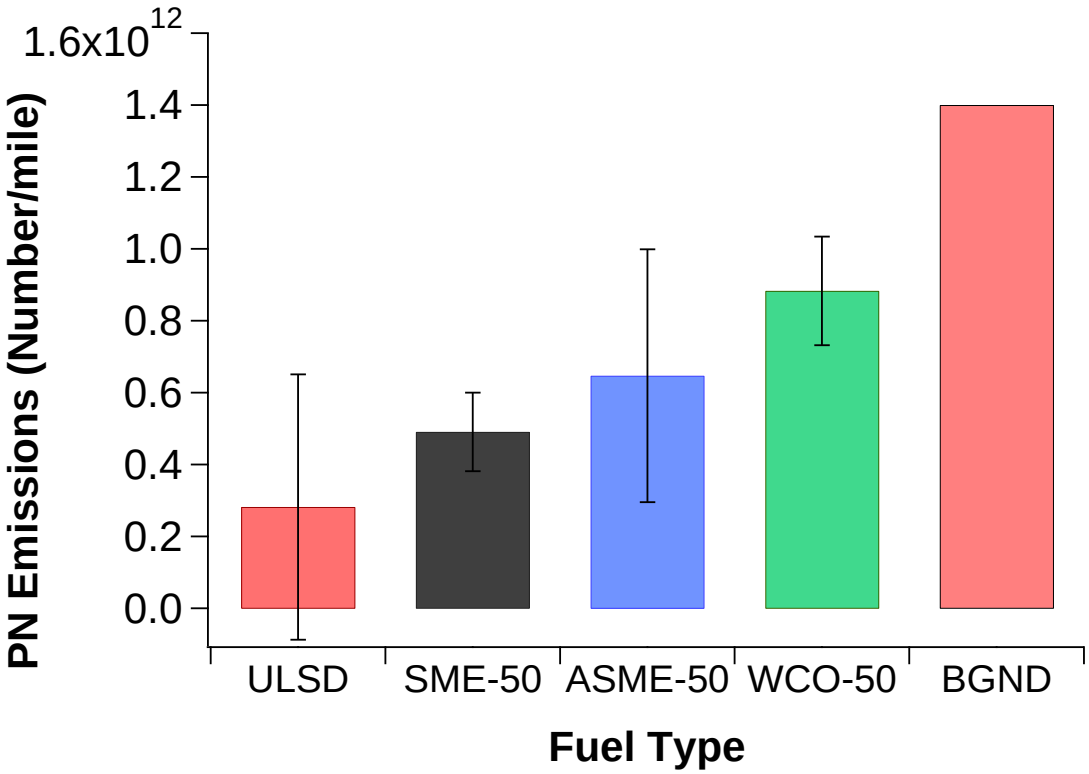


**Figure 4-14 Total particle number emissions for the Cummins ISX-15 engine**

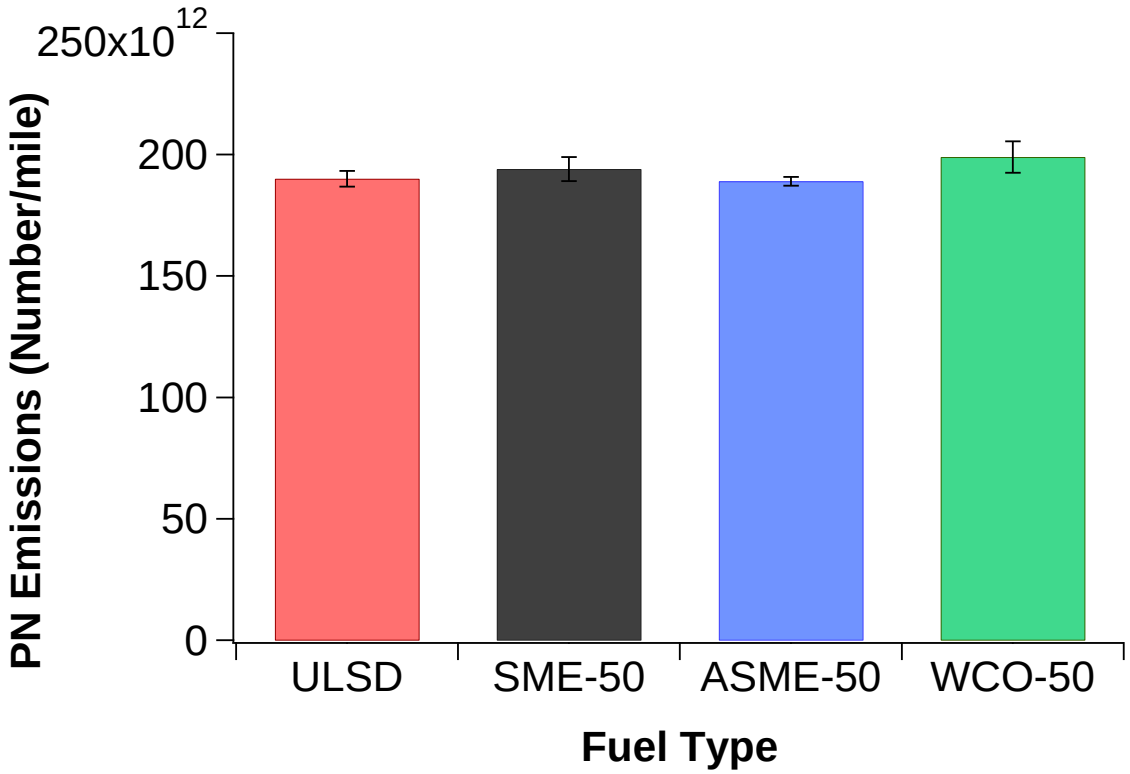


**Figure 4-15 Total particle number emissions for the Cummins ISX-450 engine**

Currently, diesel particulate matter legislation is primarily based on the emitted particle mass. However, particle size distributions are gaining increasing attention in terms of air quality, as it is believed that the toxicity increases as the particle size decreases [Oberdorster et al., 2005]. Ultrafine particles may be easily transported into cells and have higher surface area/volume ratios than larger particles. Transient particle size distributions for the Cummins ISX-15 and Cummins ISX-450 engines are shown in Figure 4-16 and Figure 4-17, respectively. For the Cummins ISX-15 engine, the particle size distributions for all test fuels exhibited a single lognormal mode characteristic of diesel engine PM. The particle size distributions were dominated by the nucleation mode with a peak at around 11 nm. The presence of nucleation mode particles and the significantly lower particle concentrations for the Cummins ISX-15 engine, suggests that the DOC/DPF configuration appeared to be very effective in trapping larger size particles. The CARB ULSD exhibited higher nucleation mode particle concentrations compared to the biodiesel blends, but not at a statistically significant level. The reductions in

nucleation mode particle concentrations with biodiesel could be due to the higher molecular oxygen content in biodiesel, which favored soot oxidation or the lack of aromatics [Surawski et al., 2011]. The findings derived from the Cummins ISX-15 engine are important because they are showing that most particles are in the ultrafine range compared to the uncontrolled engine, as shown below. We hypothesize that the ultrafine particles emitted from the DPF/SCR fitted engine consisted mainly of volatile material, such as sulfuric acid and ammonium sulfate coated with some organics, and were largely lacking of a solid soot core.

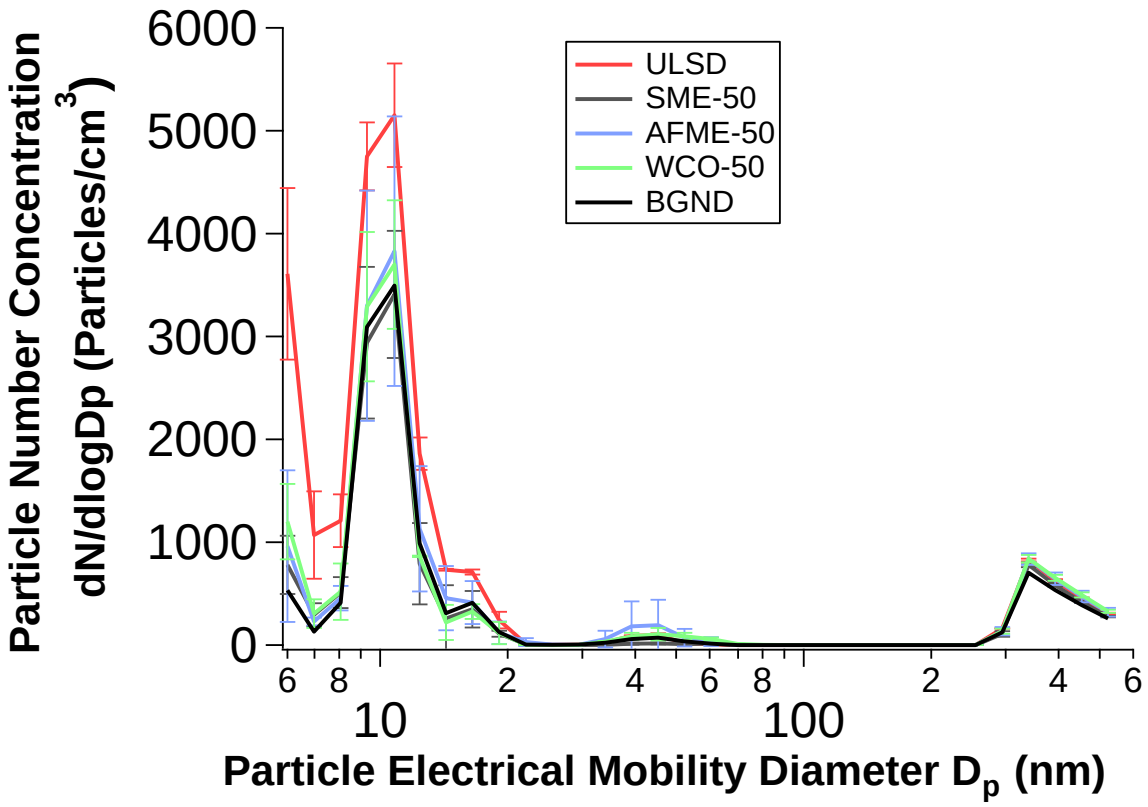


**Figure 4-16 Particle size distributions for the Cummins ISX-15 engine**

For the Cummins ISX-450 engine, particle size distributions exhibit a characteristic bimodal distribution for all fuels. All fuels showed nucleation mode particles with peaks at around 10 nm in diameter and accumulation mode particles with peaks ranged from 45 to 50 nm in diameter. It was observed that fuel type had varying effects on particle size distributions, with CARB ULSD producing more accumulation mode particles at larger mobility diameters compared to the biodiesel blends. This increase was found to be statistically significant. The lower accumulation

particle concentrations with biodiesel could be a consequence of the reduced aromatics content in the fuel blends. The general trend showing decreased geometric mean diameters (GMD) with the biodiesel blends, could also be due to a decrease of the percentage of carbon and an increase of oxygen, favoring the reduction of elemental carbon cores and decreasing the accumulation and agglomeration phenomena and hence the GMD. Another interesting feature is that the unsaturated SME-50 blend showed higher nucleation mode particle concentrations at a statistically significant level, followed by CARB ULSD, WCO-50, and AFME-50. Soy-based biodiesel, in particular, contains unsaturated fatty esters, which have been shown to increase nucleation mode particles, possibly because of the emission of organic species with high boiling points, which tend to be more condensable than hydrocarbon components. In addition, the double bonds in the ester molecules are likely to provide a direct path to the formation of carbonaceous soot via the formation of ethene and ethyne during the thermal decomposition of the molecule. Both of these species are known precursor molecules to carbonaceous soot [Schönborn et al., 2009; Mueller et al., 2003].

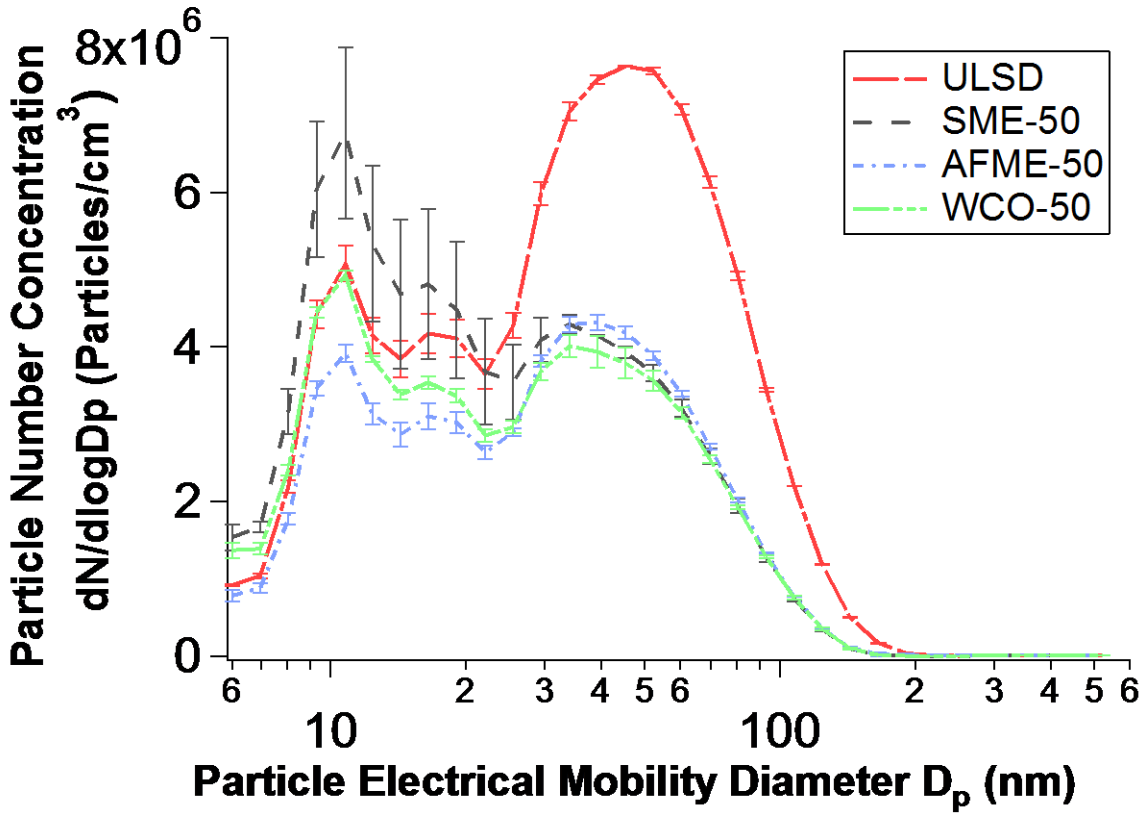


**Figure 4-17 Particle size distributions for the Cummins ISX-450 engine**

### 4.6 Carbonyl Emissions

Carbonyl compounds play an important role in atmospheric chemistry and urban air quality because they are precursors to free radicals, ozone, and peroxyacyl nitrates (PAN) [Grosjean et al., 2001]. Aldehydes such as formaldehyde, acetaldehyde, and acrolein are characterized as motor vehicle air toxics, and are known human carcinogens or irritants. Five carbonyl compounds (formaldehyde, acetaldenhyde, acrolein, propionaldehyde, and MEK) are listed as hazardous air pollutants (HAP) by U.S. Environmental Protection Agency. Some aldehydes, such as formaldehyde, acetaldehyde, acrolein, and some di-aldehydes also have high incremental reactivity for ozone formation, which may result in increased ground level ozone (a regulated air pollutant) and pose air quality problems for areas that are already in ozone non-attainment or on the borderline.

Carbonyl emissions are shown in Figure 4-18 and Figure 4-19 for the Cummins ISX-15 and Cummins ISX-450 engines, respectively. For a clearer presentation of the results, individual

carbonyl compounds for the uncontrolled Cummins ISX-450 engine were tunnel background subtracted. For the Cummins ISX-15 engine, on the other hand, tunnel backgrounds were not subtracted, but instead the tunnel blank levels are shown in Figure 4-18 for comparison. Overall, eleven carbonyl compounds were identified and quantified in the exhaust including formaldehyde, acetaldehyde, acrolein, propionaldehyde, butyraldehyde, benzaldehyde, valeraldehyde, tolualdehyde, and hexanaldehyde. Under the present test conditions, the Cummins ISX-450 engine produced substantially higher carbonyl emissions than the newer Cummins ISX-15 engine. The DOC/DPF configuration appeared to be very effective at fully oxidizing carbonyl emissions with unsaturated aldehydes and heavier saturated aliphatic aldehydes showing either very low concentrations in the exhaust or being below the detection limits. For both vehicles, low molecular-weight carbonyls, such as formaldehyde and acetaldehyde, were the dominant species in the exhaust. These results are comparable to previous studies, showing that formaldehyde and acetaldehyde are the most abundant carbonyls in biodiesel exhaust [Fontaras et al., 2010b; Martini et al., 2007; Ratcliff et al., 2010]. Heavier carbonyls were also present in the tailpipe exhaust, but in lesser amounts.

In general, the use of biodiesel blends resulted in systematic decreases in formaldehyde emissions for both vehicles. For the Cummins ISX-450 engine, the SME-50 fuel resulted in a statistically significant reduction in formaldehyde at 18% ($p=0.044$) and a marginally significant reduction with WCO-50 at 11% ($p=0.085$) relative to CARB ULSD, while no statistically significant differences were seen for acetaldehyde emissions. For the Cummins ISX-15 engine, although formaldehyde emissions trended lower for the biodiesel blends, these differences were not statistically significant. Interestingly, acetaldehyde emissions were found to be well below the background levels. Similar to acetaldehyde, most aldehyde species were below the background levels, with the exception of acrolein, butyraldehyde, and hexanaldehyde. The latter aldehydes were found at very low concentrations, however, and generally produced discordant results with both increases and decreases with the use of B50 blends. Although it has been reported that unsaturated aldehydes, such as acrolein, crotonaldehyde, and methacrolein, are the type of chemicals that are expected to increase in biodiesel due to the unsaturated sites in the fatty esters via the oxidation of hydrocarbons occurring at the α-carbon of the carbon-carbon double

bond [Cahill and Okamoto, 2012], this phenomenon was not observed in this study with these compounds being practically undetectable for the Cummins ISX-15 engine. Overall, the data clearly demonstrates that the influence of vehicle technology greatly exceeds the influence of biodiesel source material for aldehyde emission rates.

Previous studies have shown that carbonyl emissions from biodiesel exhaust are generally higher relative to petroleum diesel due to the oxygenated ester group in biodiesel [Correa and Arbilla, 2008; Karavalakis et al., 2010a]. Some studies have shown some decreases in carbonyl emissions with the use of biodiesel, however [Lin et al., 2009; Cahill and Okamoto, 2012]. Reductions in carbonyls with biodiesel could be attributed to the decomposition of esters via decarboxylation, which could decrease the probability of forming oxygenated combustion intermediates with respect to conventional diesel combustion [Lapuerta et al., 2008]. In addition, the reductions in aldehydes with biodiesel could be a consequence of the higher cetane number of the biodiesel blends, which can lead to reduced ignition delay and promote more complete combustion [He et al., 2009].

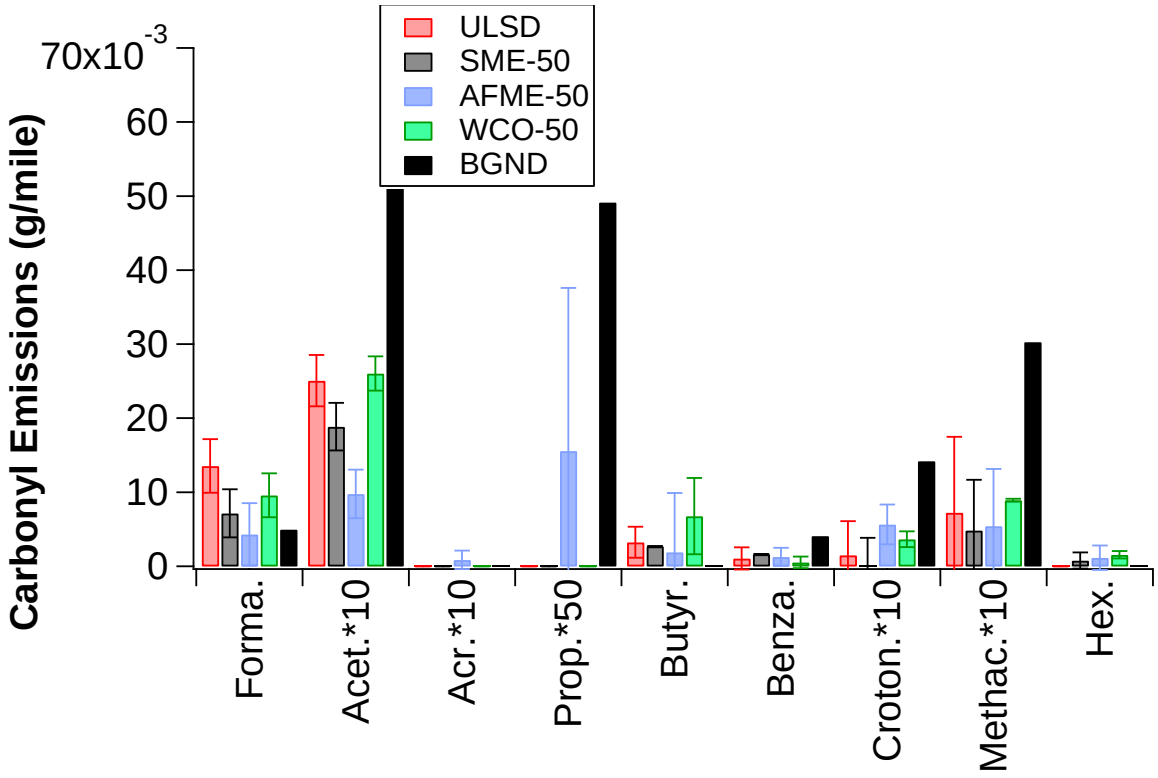


**Figure 4-18 Carbonyl emissions for the Cummins ISX-15 engine**

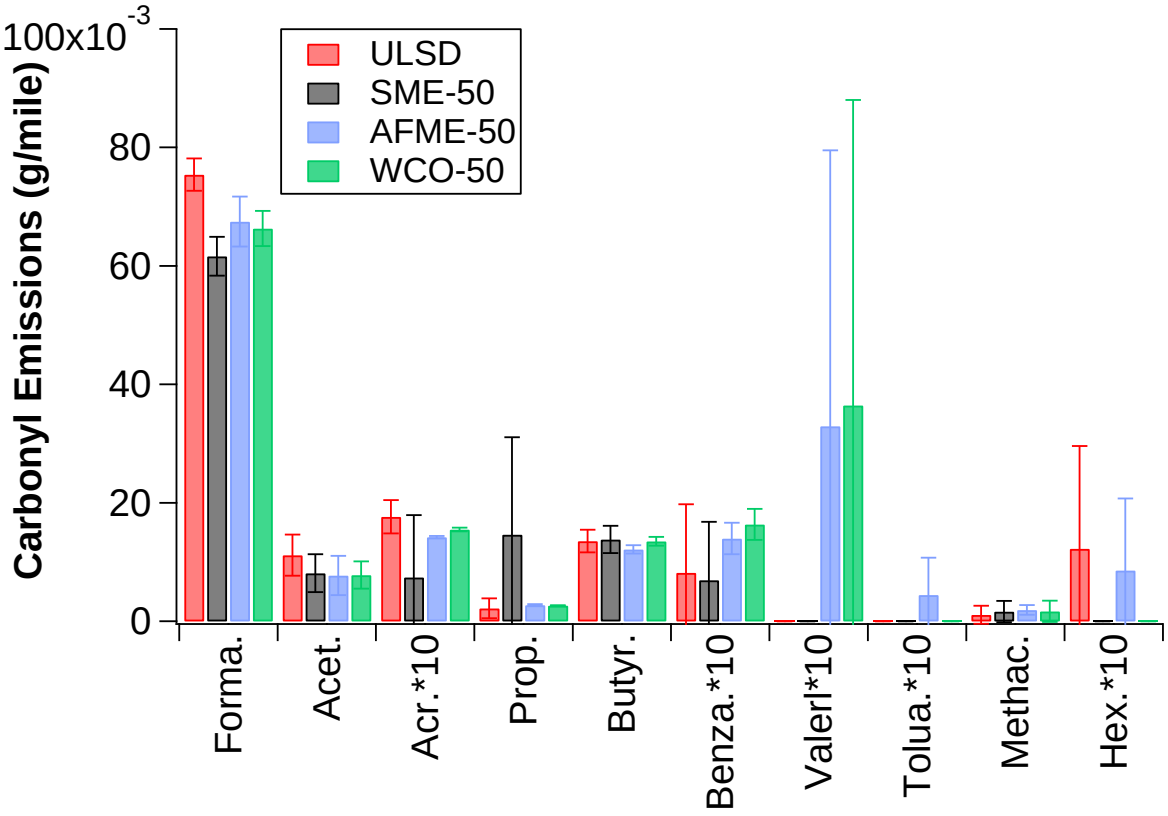


**Figure 4-19 Carbonyl emissions for the Cummins ISX-450 engine**

### 4.7 1,3-Butadiene and BTEX Emissions

Benzene, toluene, ethylbenzene, *m,p*-xylenes, and *o*-xylene, collectively known as BTEX compounds, and 1,3-butadiene are included in U.S. EPA's Hazardous Air Pollutants (HAP) List. The 1,3-butadiene species is an air toxic, which is recognized as a genotoxic carcinogen and classified as a group B2 carcinogen by U.S. EPA. BTEX compounds are most notably emitted from motor vehicles, and they yield the highest formation potentials for both ozone and peroxyacetyl nitrate (PAN). Figure 4-20 and Figure 4-21 show the emissions of 1,3-butadiene and BTEX species for the Cummins ISX-450 engine and the Cummins ISX-15 engine, respectively, as a function of fuel type. Overall, the Cummins ISX-15 engine produced significantly lower 1,3-butadiene and BTEX emissions than the uncontrolled Cummins ISX-450 engine. This observation suggests that these compounds were effectively oxidized in the DOC/DPF system.

For the Cummins ISX-450, 1,3-butadiene emissions did not show significant differences with the use of biodiesel blends, whereas for the Cummins ISX-15, a statistically significant decrease in

1,3-butadiene emissions was seen for WCO-50 blend relative to CARB ULSD at 60%, but not for the other biodiesel blends. Reductions in benzene emissions were seen for the biodiesel blends for the Cummins ISX-450 engine, but not for the Cummins ISX-15, where benzene emissions were about the same for all the test fuels. It appeared that the presence of exhaust aftertreatment negates the fuel effect with respect to benzene emissions. For the Cummins ISX-450, the reductions in benzene emissions for the SME-50 and AFME-50 blends relative to CARB ULSD were statistically significant. The lower benzene emissions with biodiesel could be due to the decrease in the aromatic and polyaromatic content in the fuel blend. Additionally, the oxygen enrichment with biodiesel may promote the oxidation of benzene, leading to a decrease of benzene emissions. Our results are in agreement with previous studies showing reductions in benzene emissions with biodiesel blends [Correa and Arbilla, 2006; Lapuerta et al., 2008].

For the toluene emissions, the influence of biodiesel use was more pronounced for the uncontrolled Cummins ISX-450 engine than the Cummins ISX-15 engine. For the Cummins ISX-450 engine, AFME-50 and WCO-50 blends showed marginally statistically significant reductions in toluene emissions compared to CARB ULSD, on the order of 56% ($p$=0.065) and 49% ($p$=0.085), respectively. The SME-50 blend trended lower for toluene emissions compared to CARB ULSD, however, only a single measurement was made for this fuel and no statistical comparison can be made. The reduction in aromatics content in the biodiesel blends is the dominating factor in the reduction of toluene emissions. For the Cummins ISX-15 engine, the large measurement variability in toluene emissions made comparisons between fuels difficult, although a marginally significant reduction of 30% ($p$=0.051) in toluene was seen for WCO-50 compared to CARB ULSD. For *m,p*-xylenes and *o*-xylene emissions, there was not a uniform trend between the two heavy-duty vehicles. For the Cummins ISX-450 engine, xylene emissions exhibited reductions with the use of biodiesel blends. Similar to toluene emissions, the reductions in xylene emissions with the use of biodiesel could be ascribed to the reduction of aromatics content in the fuel. Both increases and moderate differences in xylene emissions were observed with the biodiesel blends for the Cummins ISX-15 engine. The use of SME-50 showed a statistically significant increase in *m,p*-xylene emissions compared to CARB ULSD, with the other biodiesel blends showing moderate differences relative to CARB USLD.

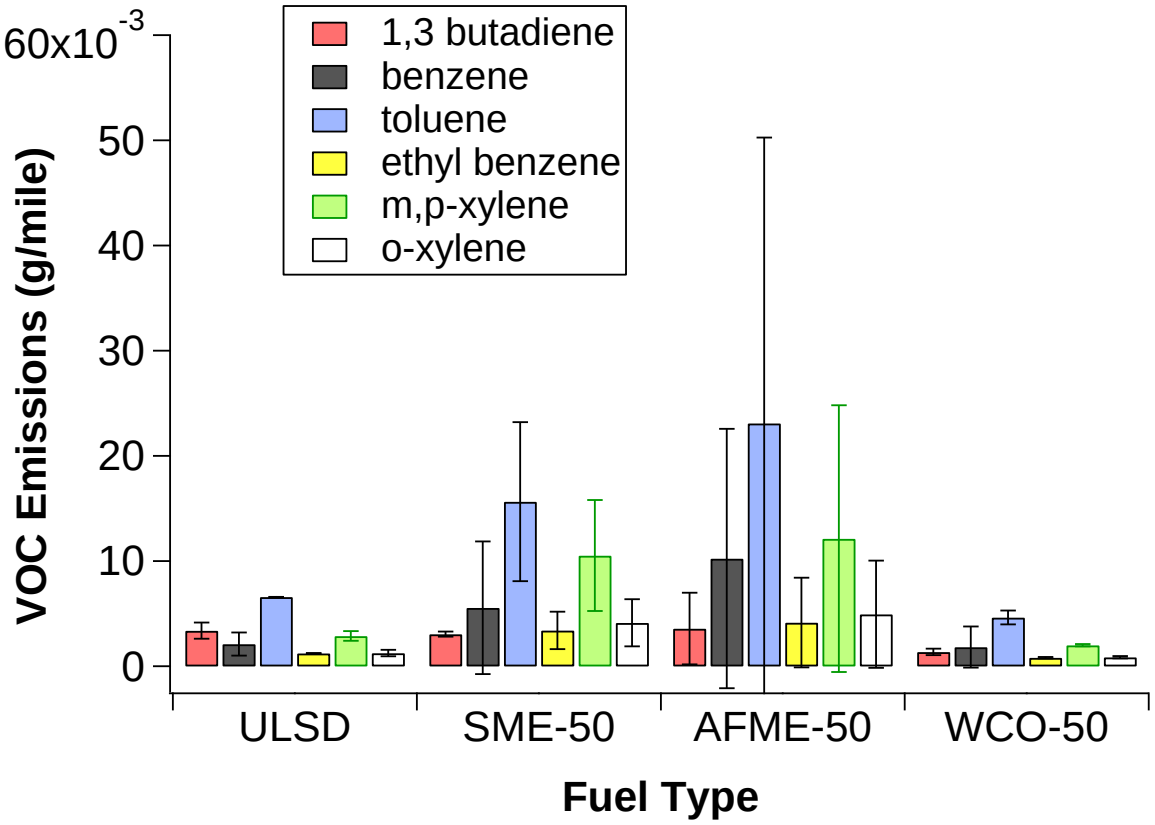


**Figure 4-20 Average VOC emissions for the Cummins ISX-15 engine**

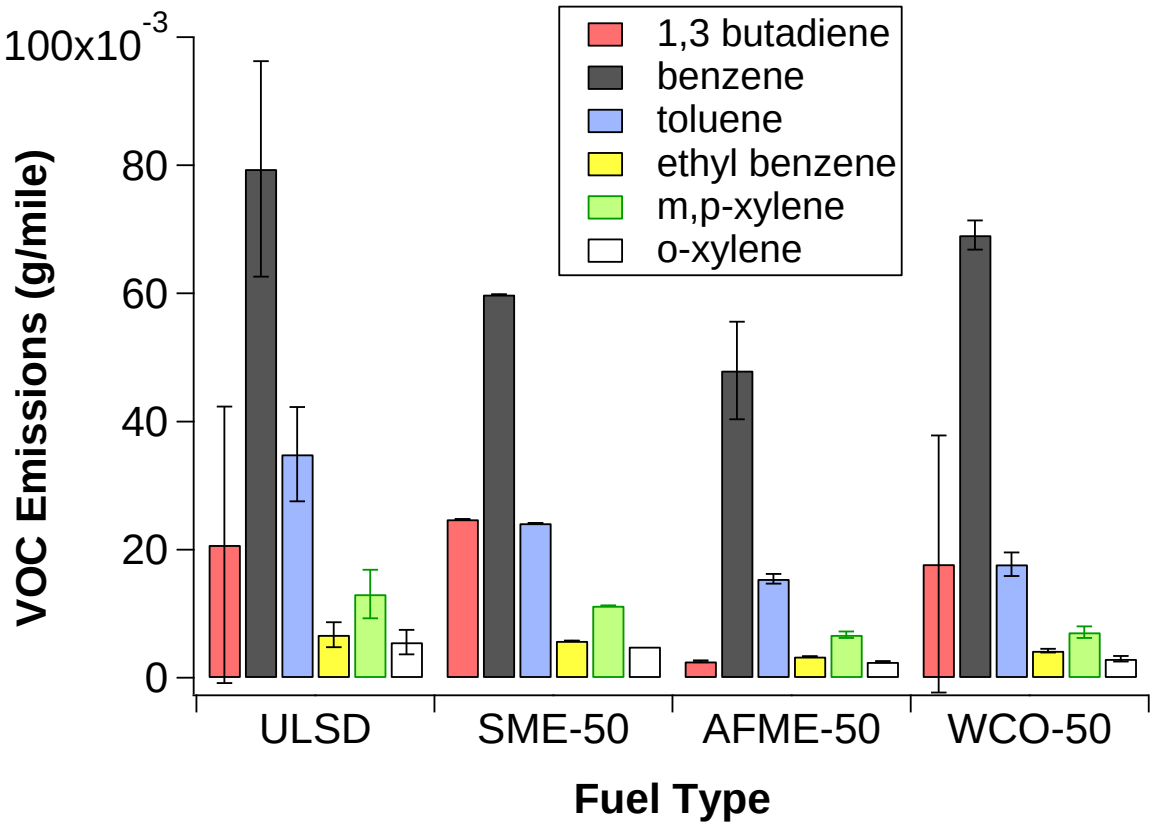


**Figure 4-21 Average VOC emissions for the Cummins ISX-450 engine**

### 4.8 Ammonia Emissions

Road traffic is a major source of reactive nitrogen compounds including $NH_3$, which is classified as a reactive toxic pollutant. While $NO_x$ emissions have been successfully lowered through fitting heavy-duty vehicles with catalytic converters, there are currently no limits for $NH_3$ emissions from heavy-duty diesel vehicles. Although not toxic to human health at ambient air concentrations, $NH_3$ is a toxic gas that contributes to secondary aerosols and can have an adverse impact on the local environment.

As shown in Figure 4-22, emissions of $NH_3$ were significantly higher for the SCR-equipped vehicle than the uncontrolled vehicle. The use of biodiesel blends produced increases in $NH_3$ emissions relative to CARB ULSD, which trended with the increases in $NO_x$ emissions for this vehicle. The differences in $NH_3$ emissions with the biodiesel blends were not statistically significant for the individual biodiesel blends, but when the biodiesel results are considered as a whole, a marginally statistically significant increase for the biodiesel blends was seen. It is

reasonable to assume that the high $NH_3$ emissions ($NH_3$ slip) for the biodiesel blends could be due to a response of the dosing control system for the SCR to the high engine-out $NO_x$ emissions. As previously discussed, owning to biodiesel's lower heating value the ECM may dictate a higher fuel flow rate that under certain operating conditions will result in $NO_x$ increases. It is, therefore, expected that the SCR system will inject more urea to be hydrolyzed into $NH_3$ to suppress $NO_x$ emissions. The functioning of the SCR is also dependent on driving conditions. For the current study, the highest $NH_3$ peaks were seen during the sharp acceleration periods of the UDDS test cycle (Figure 4-23), which is also where the highest $NO_x$ emission concentrations were seen.

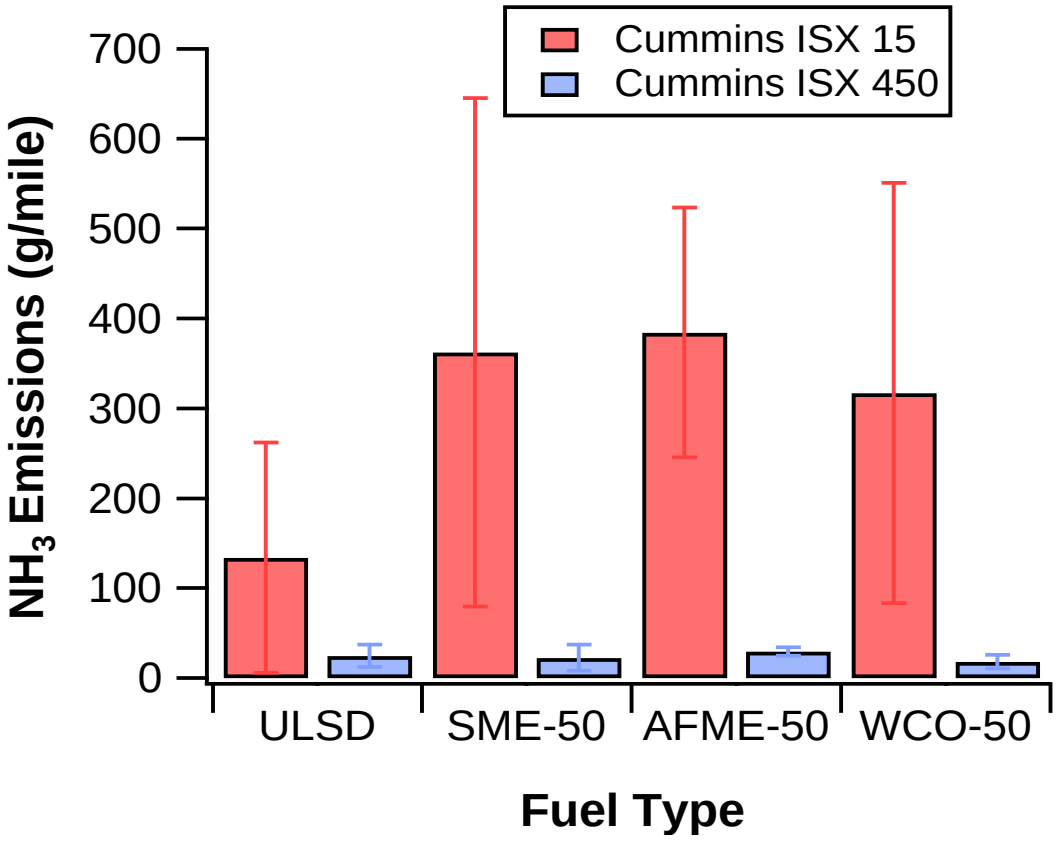


**Figure 4-22 Average $NH_3$ emissions for the Cummins ISX-15 and Cummins ISX-450 engines over the UDDS cycle**

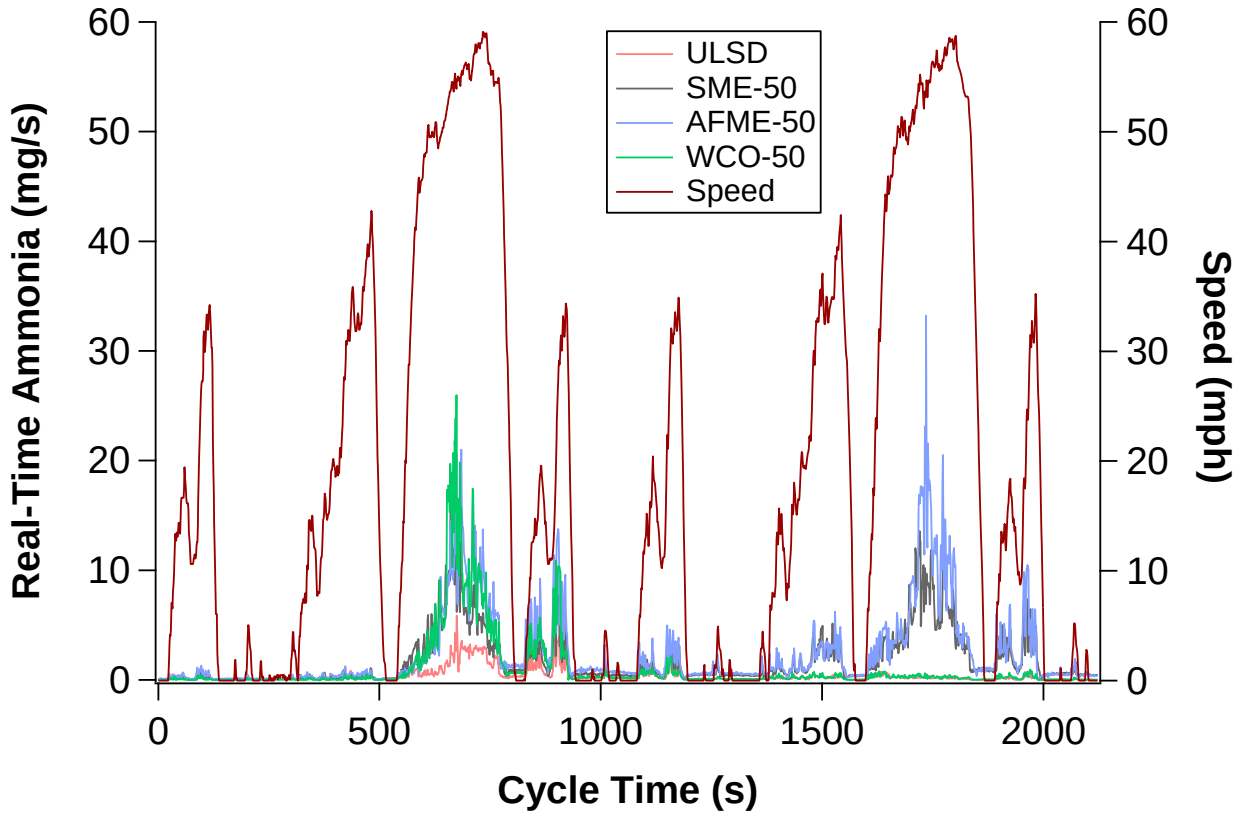


**Figure 4-23 Real-time $NH_3$ emissions for the CARB ULSD and the biodiesel blends from the Cummins ISX-15 engine over the UDDS cycle**

### 4.9 Polycyclic Aromatic Hydrocarbon (PAH) Emissions and Water-Soluble Organic Carbon

Polycyclic aromatic hydrocarbons (PAHs) are a class of complex organic molecules, which include carbon and hydrogen with a fused ring structure containing at least 2 benzene rings. PAH emissions mainly originate from fuel combustion (pyrosynthesis of aromatic compounds), unburned fuel (pyrolysis of fuel fragments), and unburned lubricating oil. PAH compounds are widely distributed in the atmosphere and they are well known for their mutagenic and carcinogenic properties. A total of 16 PAHs, ranging in size, from naphthalene (2-rings) to benzo[g,h,i]perylene and indeno[1,2,3-c,d]pyrene (6-rings) have been identified as priority pollutants by the U.S. EPA.

For this study, 26 particle-phase PAH compounds were identified and quantified in the exhaust for each vehicle/fuel combination over the UDDS cycle. As shown in Figure 4-24 for the heavily controlled Cummins ISX-15 engine, low molecular-weight PAHs with three to four rings were

the only compounds present in the tailpipe. Medium- and high molecular-weight PAHs were practically undetectable due to the presence of the DOC/DPF configuration, which retained these compounds more efficiently and facilitated their oxidation. While the B50 blends showed a trend towards higher PAH emissions relative to CARB ULSD, the differences in PAH emissions were not statistically significant and were characterized by large variability. It was assumed that the oxygen atoms in the methyl ester moiety together with the DOC/DPF system efficiently facilitated the oxidation of PAHs.

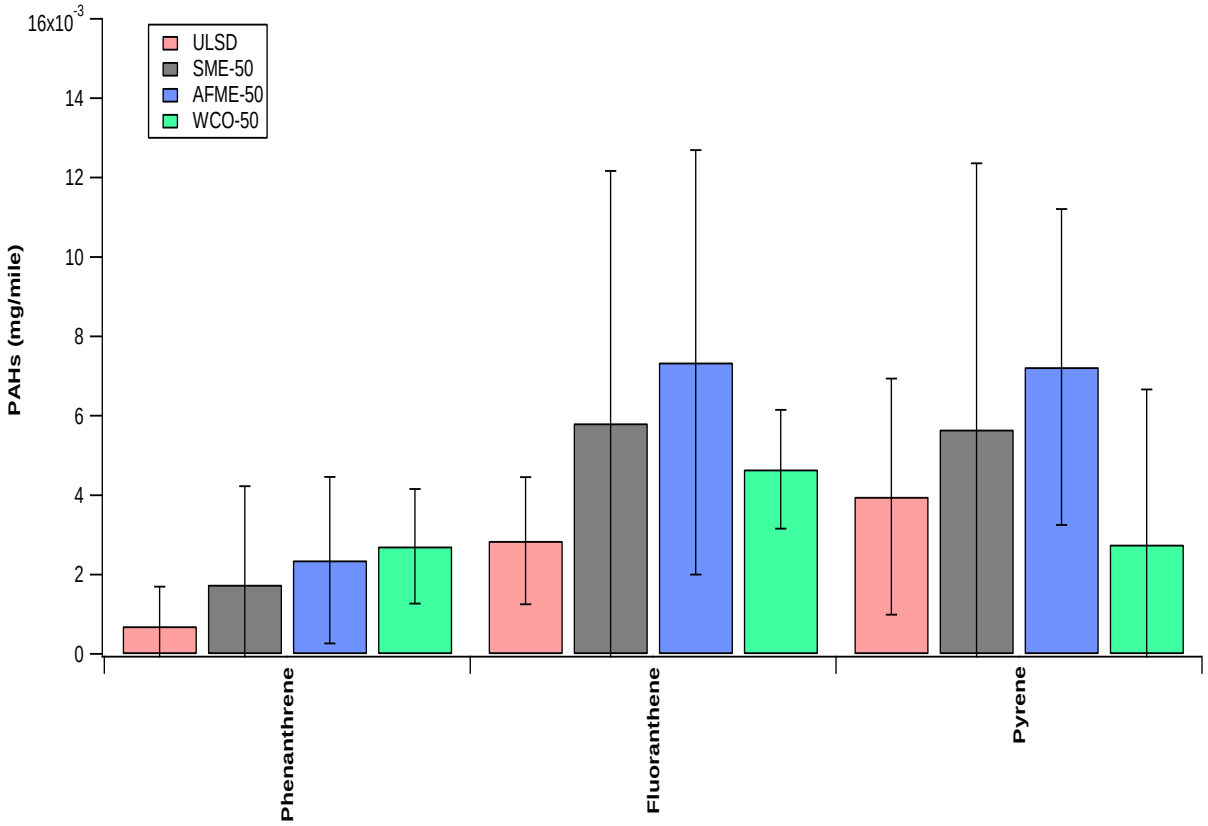


**Figure 4-24 PAH emissions for the Cummins ISX-15 engine**

For the uncontrolled Cummins ISX-450 engine, the PAH profile was dramatically different than the Cummins ISX-15 engine, showing significantly higher PAH emission levels and more PAH species detected in the exhaust (Figure 4-25). As expected, the lower and medium molecular-weight PAHs were the dominant compounds found in the exhaust for the uncontrolled vehicle. The higher levels of light PAHs suggest that these compounds were pyrolyzed from incomplete combustion of the fuel [Lea-Langton et al., 2008]. Previous vehicle and engine studies have also

reported the dominant profile of light PAHs in biodiesel exhaust [Martini et al., 2007; Karavalakis et al., 2010b; Karavalakis et al., 2011b; Macor et al., 2011]. Some heavier PAHs were also found in the exhaust, but in lesser amounts than those of light and medium molecular-weight PAHs. The formation of these species might be due to pyrosynthesis of lower molecular-weight aromatic compounds to larger PAHs and to the contribution of the lubricant oil [Lim McKenzie et al., 2007].

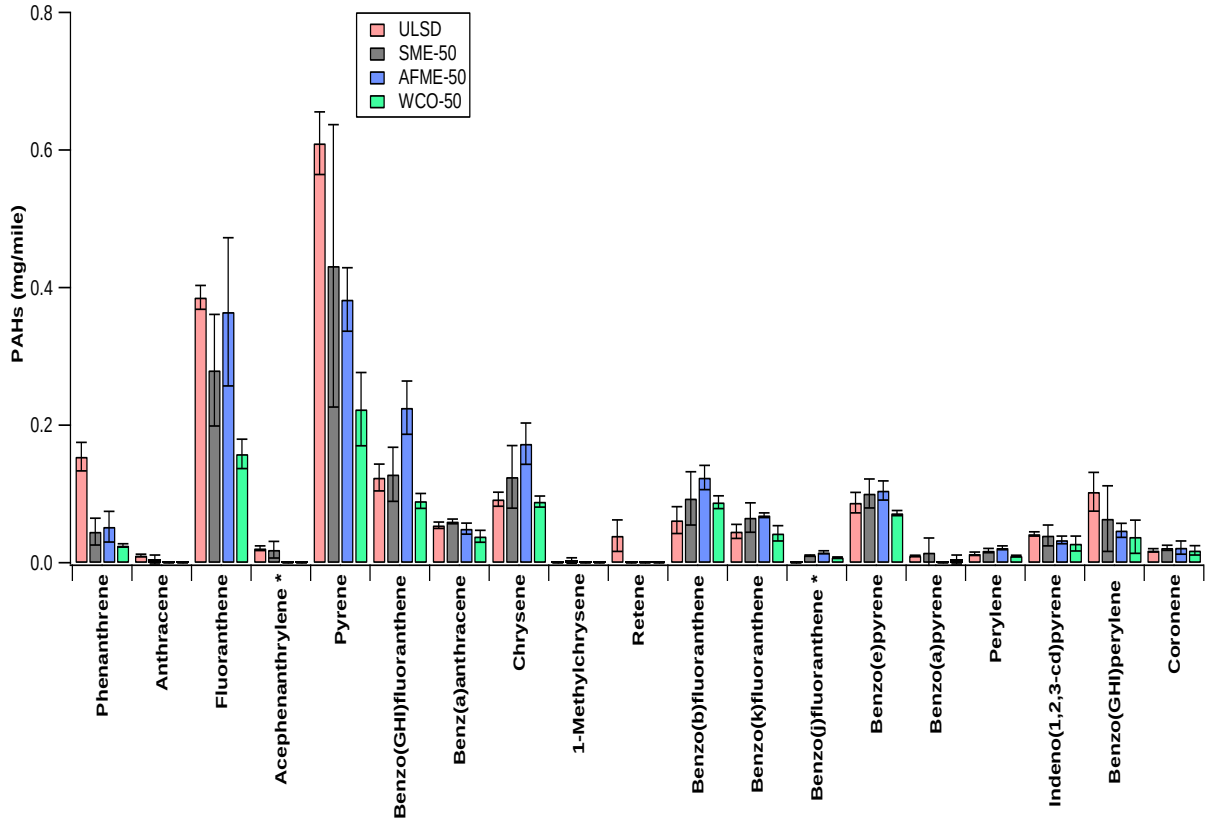


**Figure 4-25 PAH emissions for the Cummins ISX-450 engine**

Overall, the use of biodiesel blends resulted in some PAH emissions reductions compared to CARB ULSD. The reductions in PAH emissions with biodiesel could be a consequence of the absence of aromatics compounds in the biodiesel fuels and the presence of excess oxygen content in the fuel. More specifically, for the uncontrolled Cummins ISX-450 engine, most biodiesel blends led to statistically significant decreases relative to CARB ULSD in phenanthrene, fluoranthene, and pyrene emissions. The reduction of light PAHs with biodiesel is a desirable result since previous studies have shown that light molecular-weight PAHs are important in

terms of the potential to generate oxidative stress [Li et al., 2003]. On the other hand, benzo(b)fluoranthene, benzo(k)fluoranthene, and chrysene showed higher emissions for most biodiesel blends relative to CARB ULSD, with the AFME-50 blend showing statistically significant increases in these pollutants compared to the baseline fuel. It should be noted that the first two PAH compounds are probable carcinogens, while the latter is known for its carcinogenic and teratogenic properties. Other PAH compounds, which are considered as carcinogens or suspected carcinogens to humans, exhibited some decreases with the use of biodiesel blends including benzo(a)pyrene, benzo(a)anthracene, indeno(1,2,3-cd)pyrene, and benzo(ghi)perylene. It is also interesting to note that for some heavier PAHs, such as those of benzo(e)pyrene and perylene, the use of biodiesel showed some trends towards higher emissions relative to CARB ULSD but not at a statistically significant level.

Water soluble organic carbon (WSOC) may influence regional climate contributing to direct and indirect climate effect of aerosols. Figure 4-26 and Figure 4-27 show the WSOC emissions for the Cummins ISX-15 and Cummins ISX-450 engines, respectively. For the Cummins ISX-15 engine, WSOC emissions did not show any strong fuel effects with the WSOC measurements characterized by very large variability. It should be noted, however, that a trend towards higher WSOC emissions was seen for the biodiesel blends relative to CARB ULSD. Note that only a single measurement was available for the B50 WCO, hence there is no error bar associated with this data and statistically comparisons could not be made with the other fuels. The WSOC emission levels for the uncontrolled Cummins ISX-450 engine were higher than those of Cummins ISX-15 engine, indicating that the DOC/DPF configuration was effective in reducing organic species. Although the DPF captures mostly soot particles, it appeared that lowered the PM surface area available for condensation of semivolatile organic vapors, which likely lead to a decrease in WSOC concentrations in the exhaust. For the Cummins ISX-450 engine, WSOC emissions were lower for the biodiesel blends compared to CARB ULSD, with the AFME-50 showing a statistically significant reduction. Based on the PM mass results for the uncontrolled Cummins ISX-450 engine, the WSOC data indicates that all fuels showed water soluble organic emissions. This phenomenon was unexpected because the Cummins ISX-450 engine was not

fitted with aftertreatment control system to trap the semivolatile organic compounds and due to the expectation of more soot emissions as previously seen in Figure 4-17.

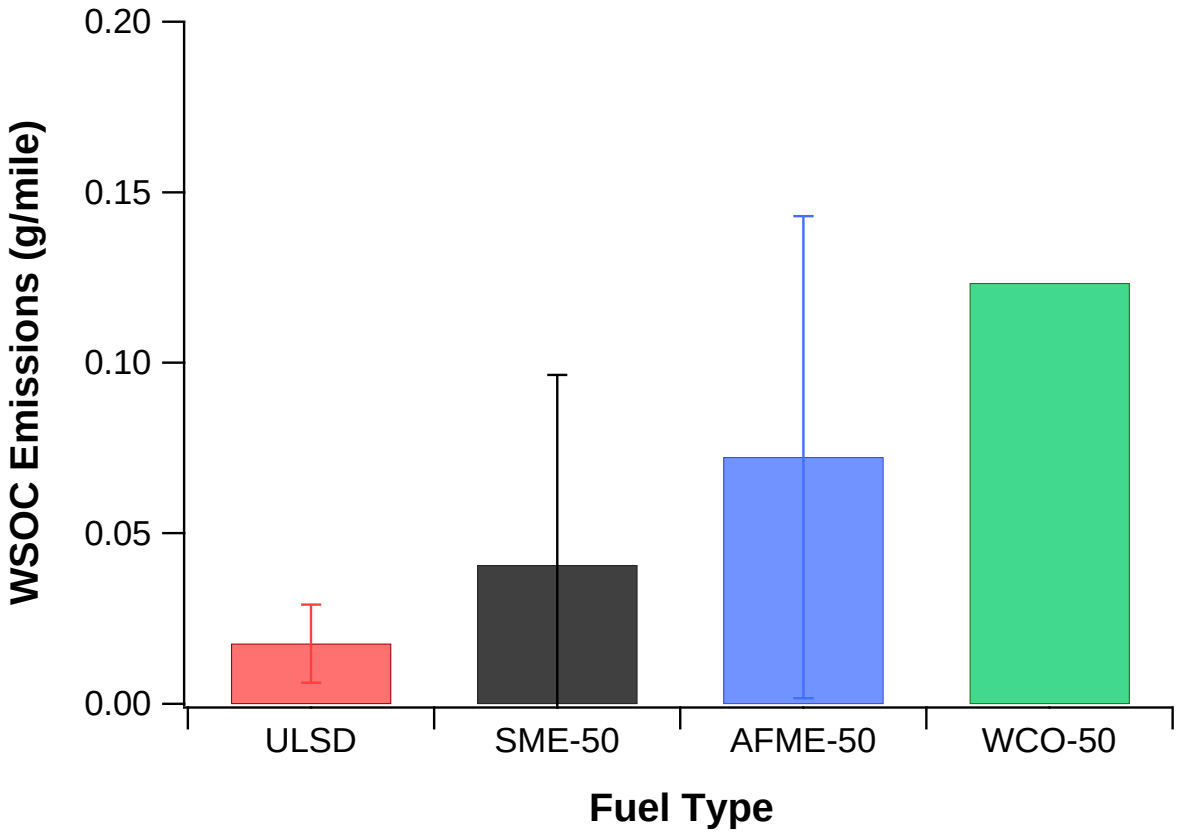


**Figure 4-26 WSOC emissions for the Cummins ISX-15 engine**

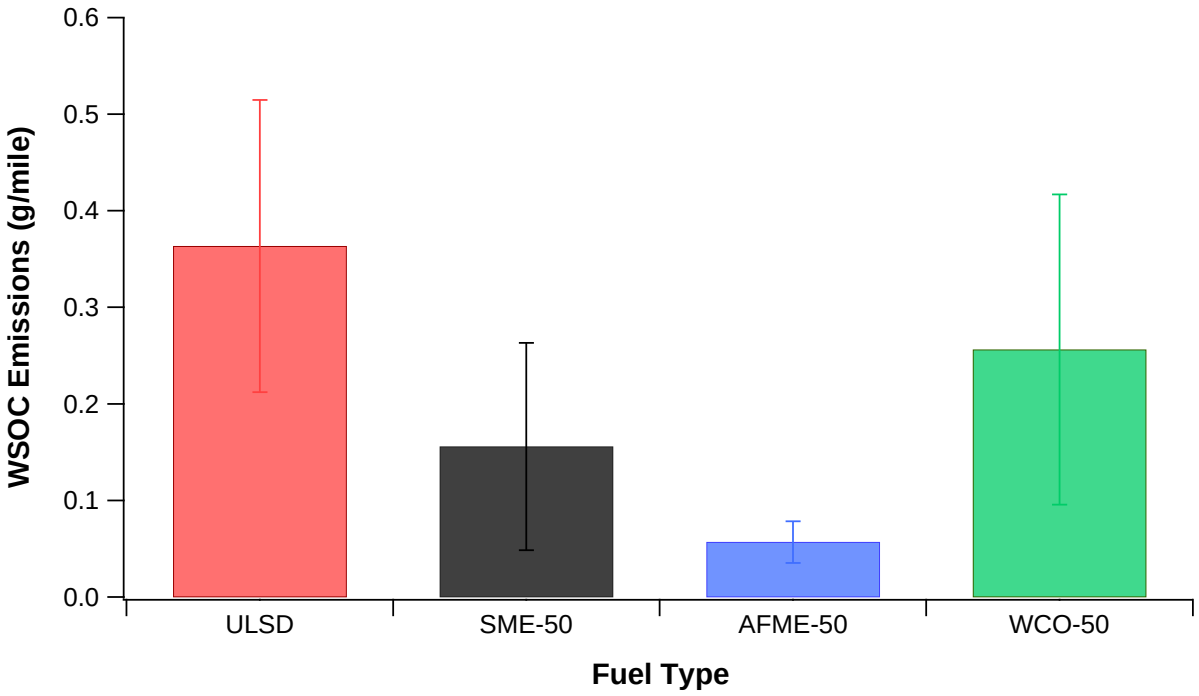


**Figure 4-27 WSOC emissions for the Cummins ISX-450 engine**

### 4.10 Hopanes, Steranes, and n-Alkanes

Hopanes and steranes are mainly lubricant oil components that are commonly used as organic tracers of diesel emissions in source apportionment of PM2.5, and which are virtually undetectable in the fuel. Figure 4-28 presents the hopane and sterane emissions for the Cummins ISX-15 engine over the UDDS cycle, whereas Figure 4-29 shows the hopane and sterane emissions for the uncontrolled Cummins ISX-450 engine. For the Cummins ISX-15 engine, hopane and sterane emissions were found to be at substantially lower concentrations than those of the uncontrolled Cummins ISX-450 engine. As might be expected, the very low concentrations of hopanes and steranes in our samples for the Cummins ISX-15 vehicles could be due to the newness of the diesel engine and also due to the presence of the DOC/DPF configuration, which proved to be effective in oxidizing these species. The fuel effect on a mass per mile basis wasn't particularly strong with the exception of the AFME-50 blend, which showed surprising high hopane and sterane emissions relative to the other fuels, but with large measurement variability, however. While hopane and sterane emissions are exclusively related

to the rate of lubricant oil consumption, it was possible that this type of feedstock contained some of these species, which were retained in the exhaust as unburned fuel fractions.

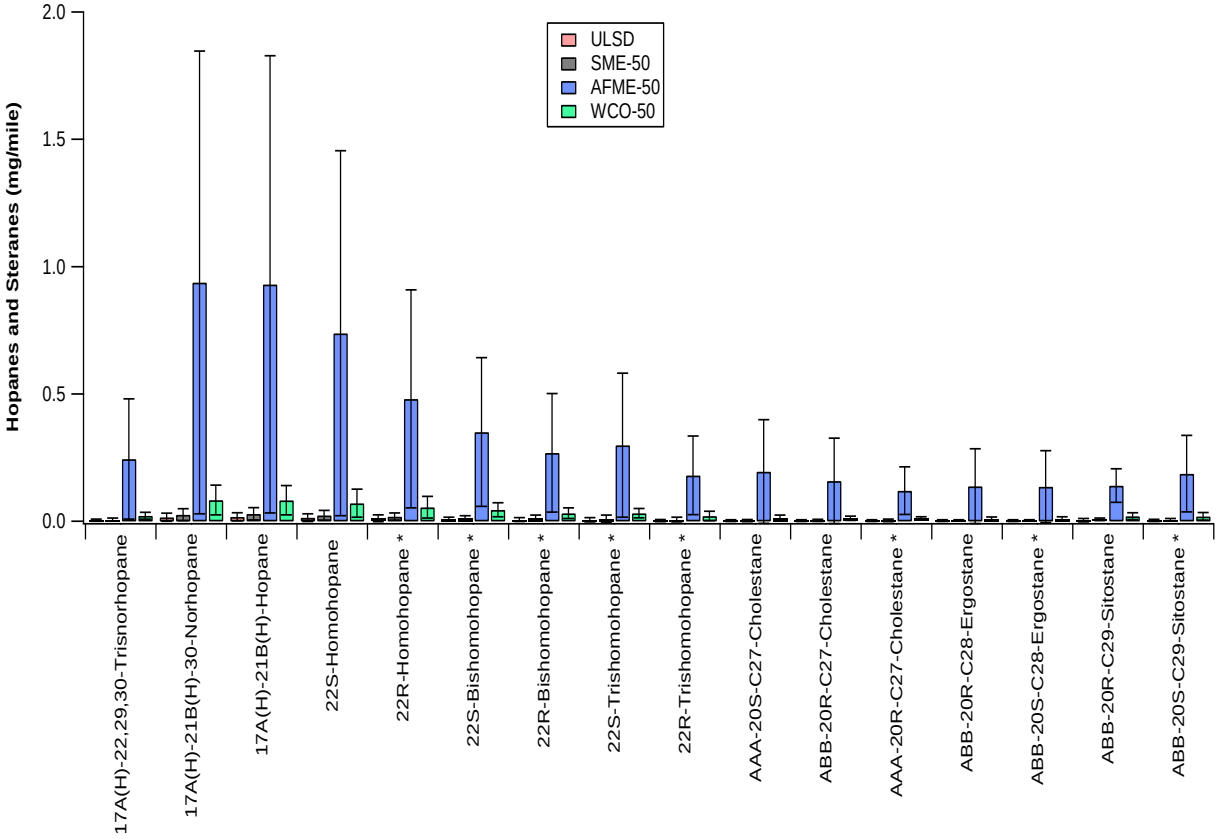


**Figure 4-28 Hopane and sterane emissions for the Cummins ISX-15 engine**

For the Cummins ISX-450 engine, the use of biodiesel blends resulted in some reductions in hopane and sterane emissions relative to CARB ULSD. Although the biodiesel blends did not show statistically significant differences in hopane and sterane emissions with CARB ULSD, they systematically trended lower somewhat following the PAH profile for this vehicle. It is likely that hopanes and steranes are precursors for the formation of some PAHs in petroleum diesel and biodiesel combustion reactions.

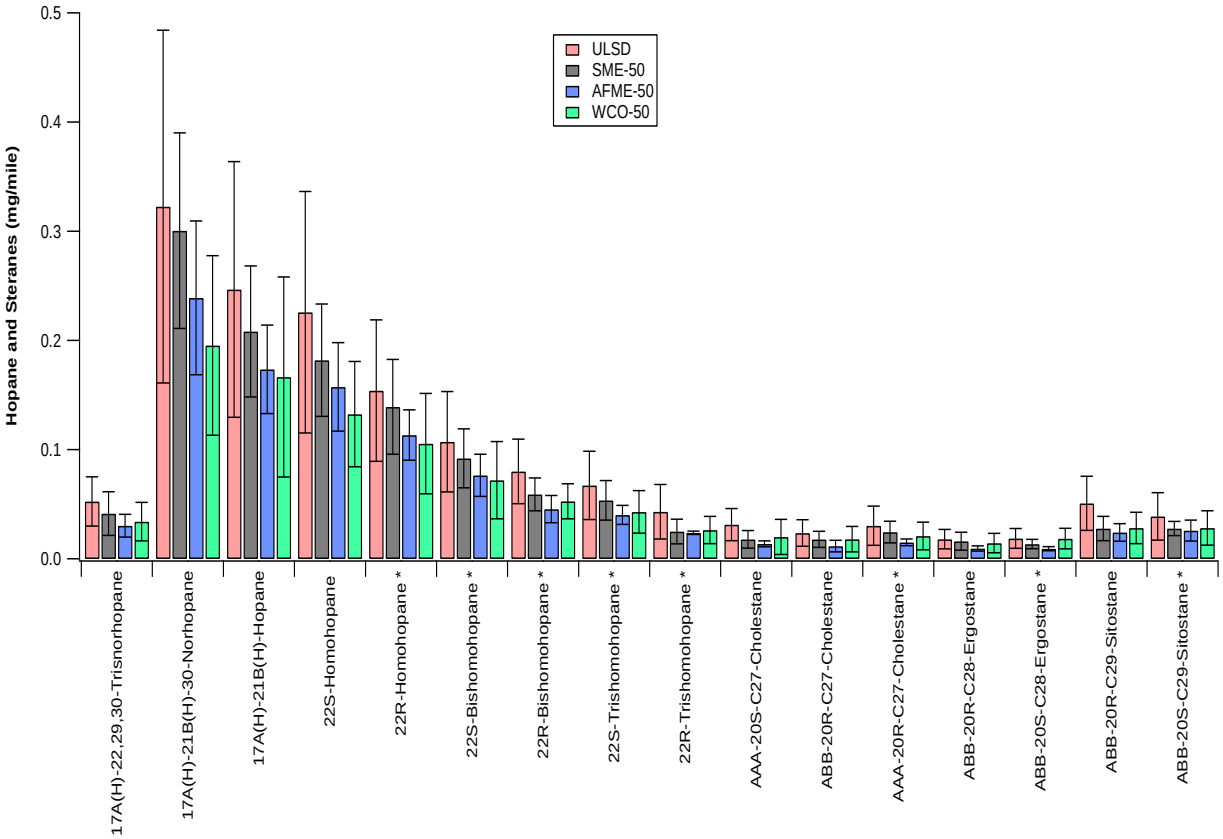


**Figure 4-29 Hopane and sterane emissions for the Cummins ISX-450 engine**

Alkane emissions are shown in Figure 4-30 and Figure 4-31 for the Cummins ISX-15 and Cummins ISX-450 engines, respectively. Alkanes are species that may originate from fuel combustion as well as lubricant oil. For both vehicles, the dominant alkane species ranged from nonadecane to pentacosane, which could be attributed to fuel combustion. Long-chain alkanes were also present (triacontane and higher), which is an indication of lubricant oil contribution. The uncontrolled Cummins ISX-450 engine emitted higher levels of alkanes, while the DOC/DPF-fitted Cummins ISX-15 engine had overall lower alkane emissions. Unlike the newer engine, the uncontrolled Cummins ISX-450 engine showed higher concentrations of long-chain alkanes, which could be due to a higher lubricant oil consumption rate or the merely the lack of a DOC/DPF to oxidize these species. For both vehicles, the use of biodiesel yielded discordant results in alkane emissions with both increases and decreases compared to CARB ULSD. For the Cummins ISX-15 engine, the AFME-50 blend showed very high alkane emissions relative to the other fuels and generally followed similar patterns to the hopane and sterane emissions. For

the Cummins ISX-450 engine, most biodiesel blends showed lower alkane emissions relative to CARB ULSD.

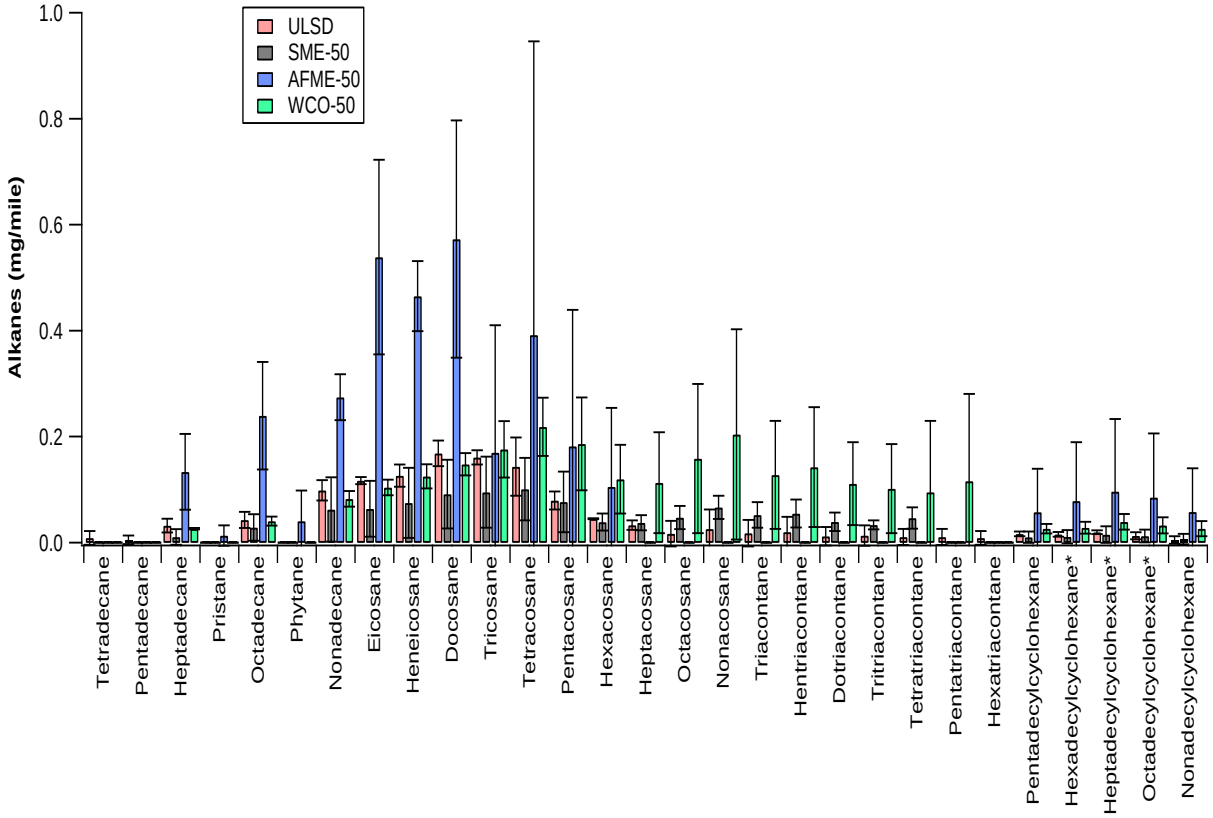


**Figure 4-30 Alkane emissions for the Cummins ISX-15 engine**

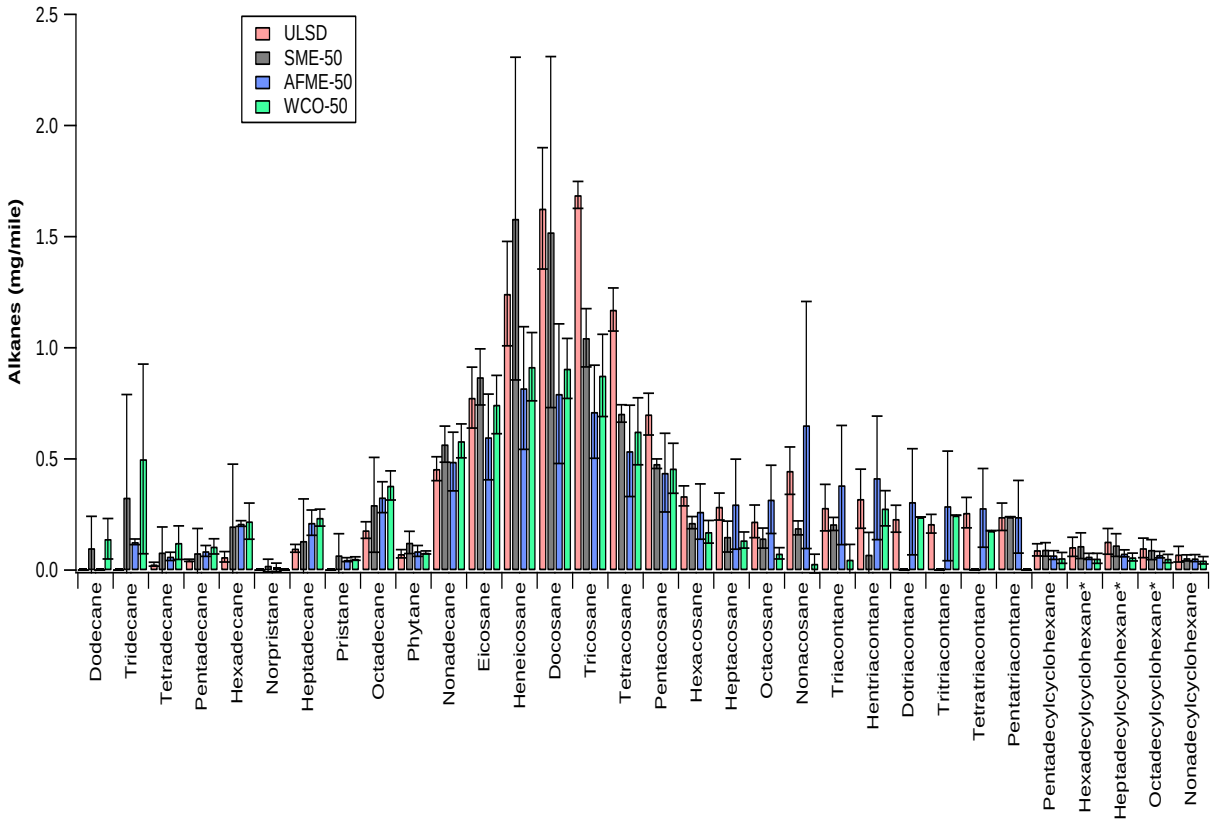


**Figure 4-31 Alkane emissions for the Cummins ISX-450 engine**

## 4.11 Inorganic Ions Emissions

Inorganic ion emissions yielded discordant results, as shown in Figure 4-32 and Figure 4-33 for the Cummins ISX-15 and Cummins ISX-450 engines, respectively. Overall, the inorganic ions were found to be in substantially lower concentrations for the Cummins ISX-15 engine than the uncontrolled Cummins ISX-15 engine. For the Cummins ISX-450 engine, the dominant inorganic ionic species were ammonium, nitrate, and sulfate. The nitrate emissions could be formed during combustion under high $NO_x$ conditions. The higher nitrate emissions for the biodiesel blends were as expected because of the general increase in $NO_x$ emissions for this vehicle with biodiesel compared to CARB ULSD. Sulfate emissions for the uncontrolled Cummins ISX-450 engine decreased with biodiesel blends compared to CARB ULSD. The latter result was expected due to the very low sulfur level in the biodiesel fuel. It was hypothesized that the sulfate emissions for the uncontrolled Cummins ISX-450 engine were largely originated from lubricant oil sulfur for the biodiesel fuels, with some fuel contribution for the CARB ULSD. For the

Cummins ISX-15 engine, the dominant inorganic ionic species were sulfate, nitrate, and chloride. There did not appear to be any Fuel effects were not particularly strong fuel effects for ions emissions for the Cummins ISX-15 engine, which was mainly due to the low measurement levels and the large measurement variability. Overall, the results reported here indicate that the presence of aftertreatment device together with the use of biodiesel fuels were effective in removing inorganic ions and changing their formation mechanism. More studies on heavy-duty vehicles running on biodiesel are necessary to assess the ions emissions, since they play a critical role in the formation of semivolatile nanoparticles by heterogeneous nucleation.

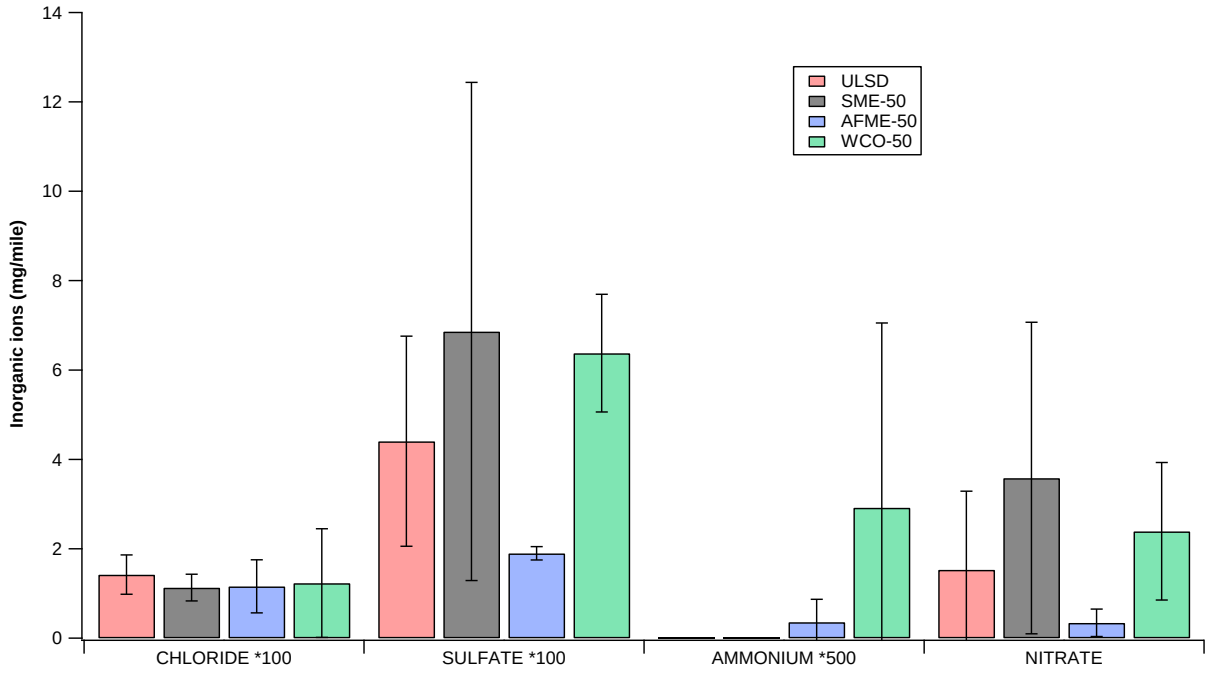


**Figure 4-32 Inorganic ions emissions for the Cummins ISX-15 engine**

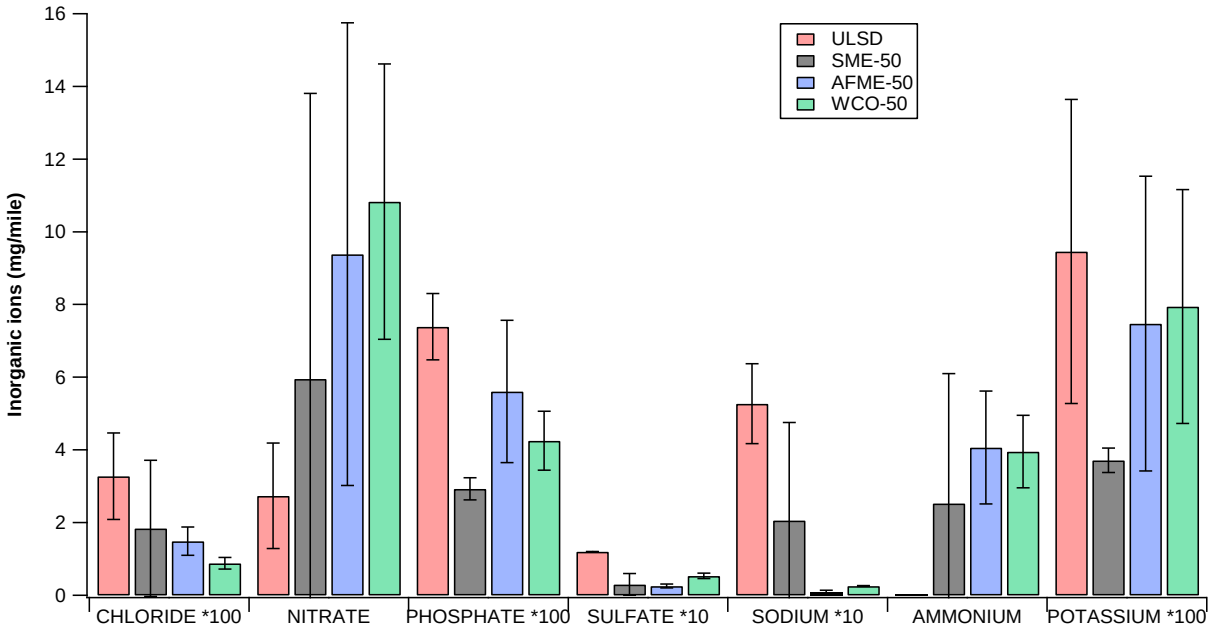


**Figure 4-33 Inorganic ions emissions for the Cummins ISX-450 engine**

## 4.12 Water-Soluble Metal Emissions

The metal content in most of the conventional on-road fuels is usually relatively low, whereas lubrication oils often contain much higher metal concentrations. Low level metal emissions from engine wear occur in all internal combustion engines [Agarwal et al., 2011]. Metal compounds collected in lubrication oil can be re-entrained into the cylinder and then oxidized during combustion. Metals are also thought to be very important in PM cellular toxicity. For this study, 49 metallic elements were identified and quantified in the exhausts of both vehicles including redox active transition metals (Mn, V, Ni, Cu, Fe, and Cr), divalent transition metals (Zn, Cd, and Co), heavy metals (Tl, Pb, U, Th, and W), alkaline earth metals (Sr, Mg, Ba, and Ca), platinum-group elements (Rh, Pt, and Pd), rare earth (Eu, Pr, Ce, Nd, La, Sm, Y, Dy, Ho, Yb, and Lu), semi-metals (As, and Sb), and higher valent/hydrolyzed metals (Ti, Sc, and Al). For a more illustrative interpretation, these metals are categorized into different groups based on their periodic properties. Figures 4-34 through 4-35 and Figures 4-36 through 4-37 present the distribution of water-soluble metals categorized into different groups based on their periodic table properties and redox active metals for the Cummins ISX-15 and the Cummins ISX-450

engines, respectively. Tables 4-1 and 4-2 list the water-soluble metals, expressed in mg/mile, for the Cummins ISX-15 and the Cummins ISX-450 engines, respectively.

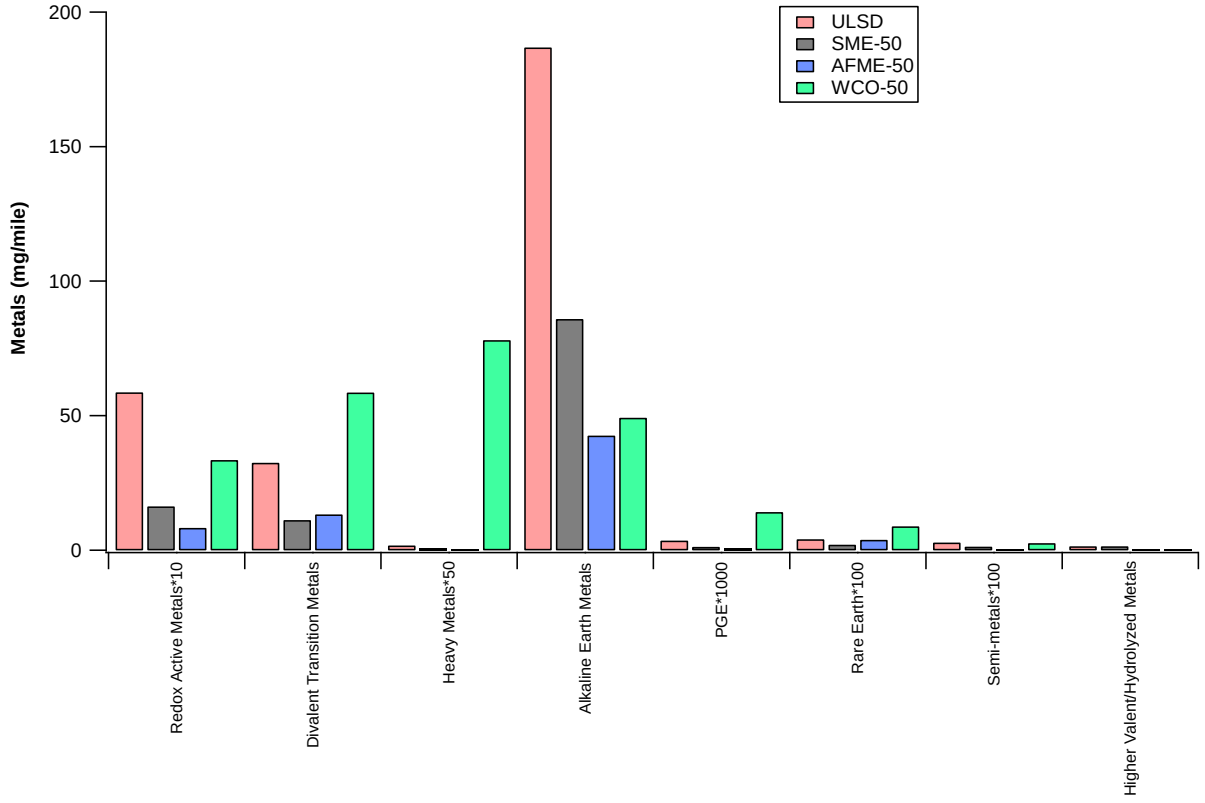


**Figure 4-34 Distribution of water-soluble metals, categorized into different groups based on their periodic properties, in the exhaust PM for the Cummins ISX-15 engine**

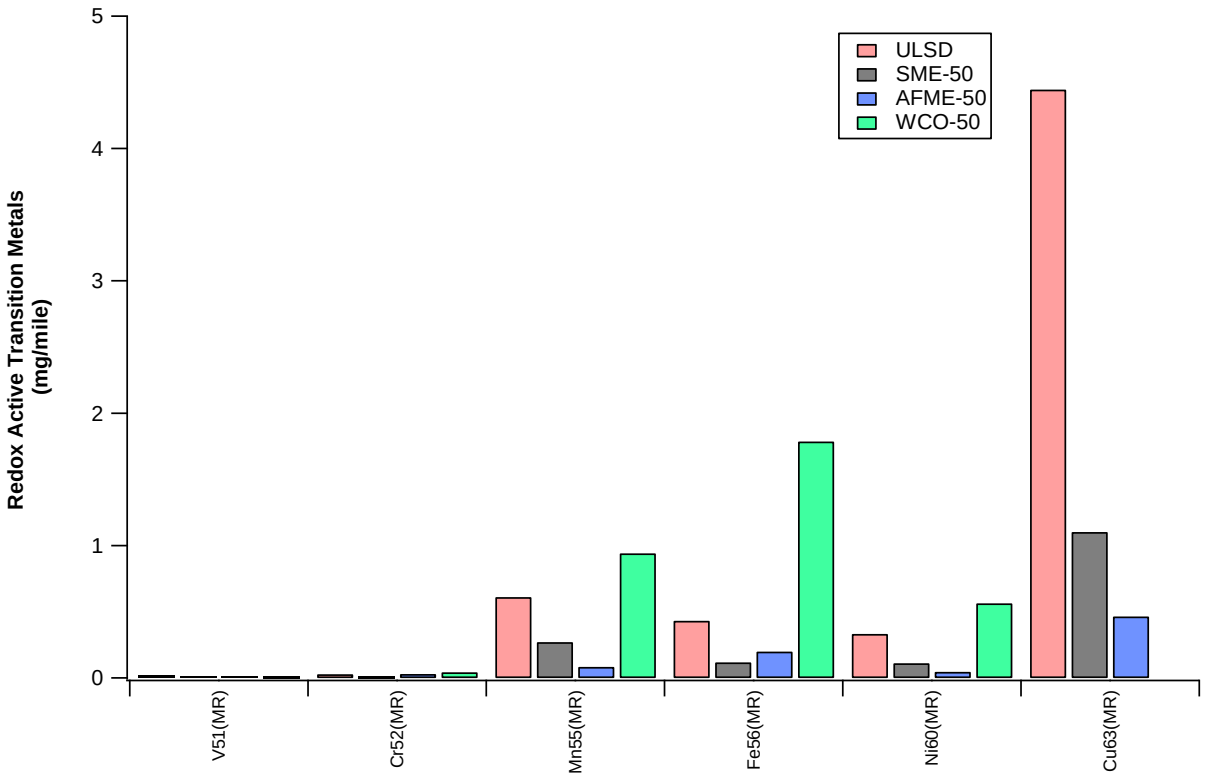


**Figure 4-35 Water-soluble content of major redox-active transition in the exhaust PM for the Cummins ISX-15 engine**

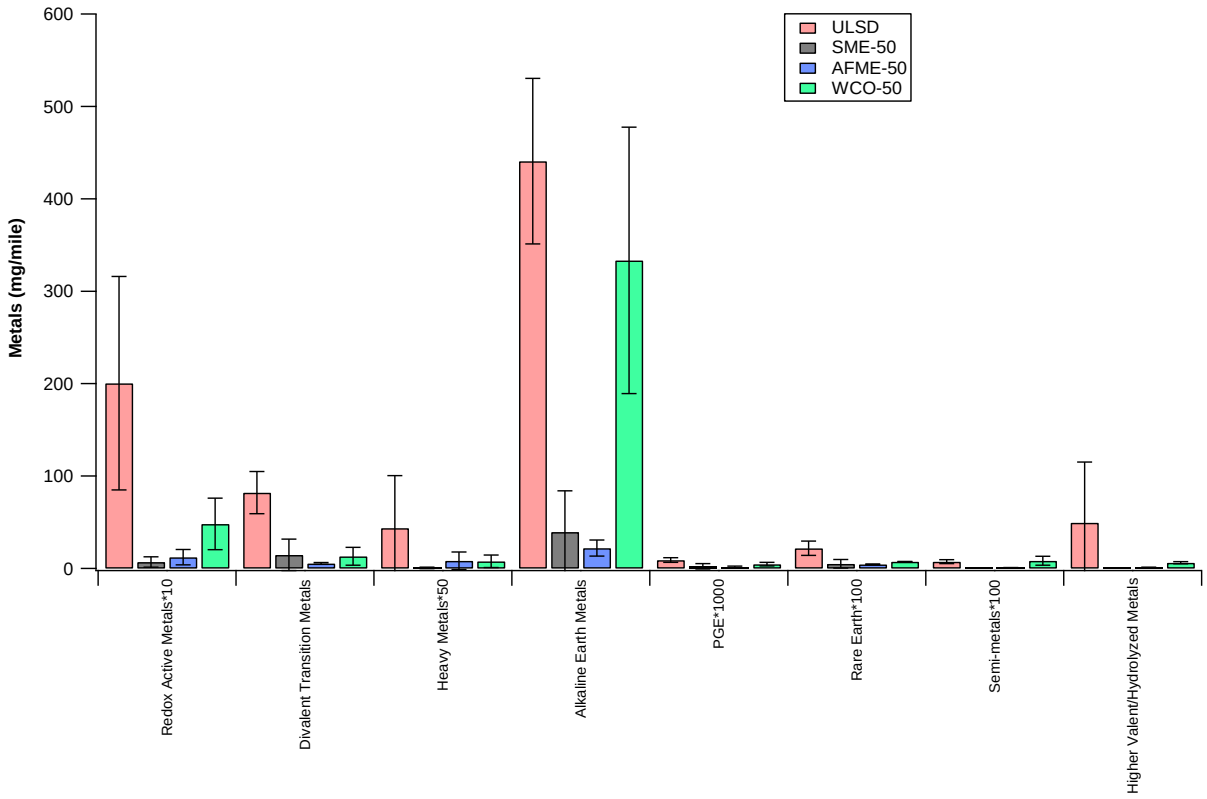


**Figure 4-36 Distribution of water-soluble metals, categorized into different groups based on their periodic properties, in the exhaust PM for the Cummins ISX-450 engine**

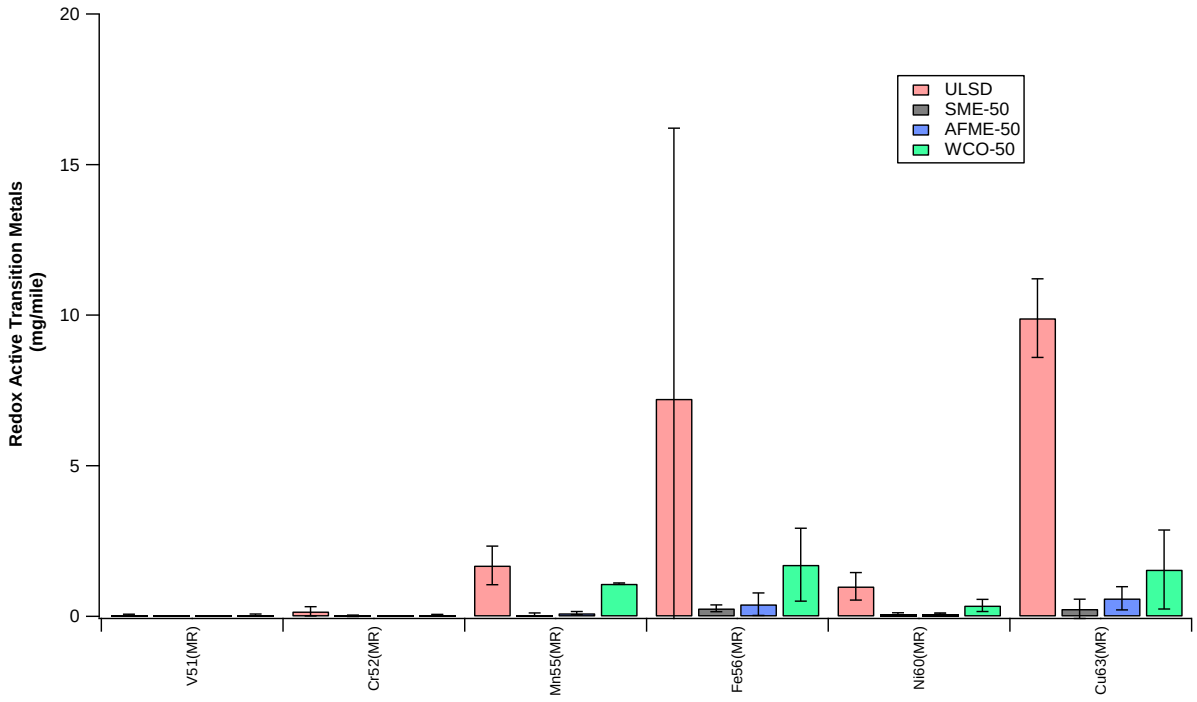


**Figure 4-37 Water-soluble content of major redox-active transition in the exhaust PM for the Cummins ISX-450 engine**

**Table 4-1 Water-soluble metals for the Cummins ISX-15 engine**

| | CARB ULSD | SME-50 | AFME-50 | WCO-50 |
|---|---|---|---|---|
| V51(MR) | 0.01913 | 0.01130 | 0.00384 | 0.01693 |
| Cr52(MR) | 0.02932 | 0.01643 | 0.03068 | 0.04474 |
| Mn55(MR) | 0.61170 | 0.27197 | 0.08543 | 0.94343 |
| Fe56(MR) | 0.43390 | 0.11916 | 0.20089 | 1.78718 |
| Ni60(MR) | 0.33310 | 0.11164 | 0.04786 | 0.56456 |
| Cu63(MR) | 4.44677 | 1.10373 | 0.46641 | n/a |
| Co59(MR) | 0.03417 | 0.01085 | 0.00246 | 0.03389 |
| Zn66(MR) | 32.52184 | 11.28471 | 13.40822 | 58.63857 |
| Cd111(LR) | 0.02493 | 0.00534 | 0.00079 | 0.02446 |
| Tl205(LR) | 0.00004 | 0.00006 | 0.00006 | 0.00093 |
| PbSum | 0.03051 | 0.01527 | 0.00235 | 1.54090 |
| Th232(LR) | 0.00007 | 0.00002 | 0.00008 | 0.00007 |
| U238(LR) | 0.00009 | 0.00005 | 0.00004 | 0.00070 |
| W184(LR) | 0.00493 | 0.00287 | 0.00045 | 0.02084 |
| Sr88(MR) | 0.72654 | 0.36325 | 0.25067 | 0.79567 |
| Mg25(MR) | 10.40272 | 4.38714 | 1.59773 | 11.40773 |
| Ca44(MR) | 148.82900 | 67.42782 | 14.96677 | n/a |
| Ba137(MR) | 26.95247 | 13.79532 | 25.85766 | 37.05280 |
| Pt195(LR) | 0.00003 | 0.00004 | 0.00004 | 0.00010 |
| Rh103(LR) | 0.00038 | 0.00013 | 0.00010 | 0.00220 |
| Pd105(LR) | 0.00325 | 0.00112 | 0.00091 | 0.01196 |
| Eu153(LR) | 0.03756 | 0.01830 | 0.03543 | 0.05014 |
| Ce140(LR) | 0.00042 | 0.00094 | 0.00025 | 0.00343 |
| Pr141(LR) | 0.00006 | 0.00005 | 0.00007 | 0.00035 |
| Nd146(LR) | 0.00106 | 0.00054 | 0.00087 | 0.00244 |
| La139(LR) | 0.00103 | 0.00057 | 0.00091 | 0.00408 |
| Sm147(LR) | 0.00029 | 0.00022 | 0.00028 | 0.00056 |
| Dy163(LR) | 0.00006 | 0.00003 | 0.00003 | 0.00027 |
| Y89(LR) | 0.00099 | 0.00056 | 0.00105 | 0.02793 |
| Ho165(LR) | 0.00001 | 0.00001 | 0.00001 | 0.00006 |
| Lu175(LR) | 0.00001 | 0.00000 | 0.00001 | 0.00004 |
| Yb173(LR) | 0.00002 | 0.00002 | 0.00003 | 0.00018 |
| Sb121(LR) | 0.01937 | 0.00999 | 0.00134 | 0.02019 |
| As75(HR) | 0.00948 | 0.00378 | 0.00260 | 0.00640 |
| Sc45(MR) | 0.00013 | 0.00008 | 0.00012 | 0.00012 |
| Ti49(MR) | 0.00464 | 0.00049 | 0.00290 | 0.00602 |
| Al27(MR) | 1.50249 | 1.54086 | 0.37010 | n/a |

**Table 4-2 Water-soluble metals for the Cummins ISX-450 engine**

| | CARB ULSD | SME-50 | AFME-50 | WCO-50 |
|---|---|---|---|---|
| V51(MR) | 0.051 | 0.015 | 0.003 | 0.050 |
| Cr52(MR) | 0.168 | 0.020 | 0.008 | 0.051 |
| Mn55(MR) | 1.690 | 0.065 | 0.106 | 1.085 |
| Fe56(MR) | 7.226 | 0.267 | 0.405 | 1.712 |
| Ni60(MR) | 0.998 | 0.077 | 0.097 | 0.363 |
| Cu63(MR) | 9.903 | 0.252 | 0.598 | 1.552 |
| Co59(MR) | 0.085 | 0.012 | 0.044 | 0.020 |
| Zn66(MR) | 81.838 | 14.628 | 13.178 | 5.448 |
| Cd111(LR) | 0.048 | 0.002 | 0.025 | 0.006 |
| Tl205(LR) | 0.001 | 0.000 | 0.001 | 0.002 |
| PbSum | 0.861 | 0.010 | 0.137 | 0.162 |
| Th232(LR) | 0.000 | 0.000 | 0.000 | 0.000 |
| U238(LR) | 0.001 | 0.000 | 0.000 | 0.000 |
| W184(LR) | 0.010 | 0.002 | 0.016 | 0.001 |
| Sr88(MR) | 1.681 | 0.231 | 1.080 | 0.058 |
| Mg25(MR) | 25.824 | 3.091 | 19.591 | 2.737 |
| Ca44(MR) | 336.799 | 14.478 | 311.158 | 18.987 |
| Ba137(MR | 76.511 | 21.712 | 1.577 | 0.196 |
| Pt195(LR) | 0.000 | 0.000 | 0.000 | 0.000 |
| Rh103(LR) | 0.001 | 0.000 | 0.000 | 0.000 |
| Pd105(LR) | 0.008 | 0.002 | 0.004 | 0.001 |
| Eu153(LR) | 0.109 | 0.029 | 0.002 | 0.000 |
| Ce140(LR) | 0.007 | 0.000 | 0.001 | 0.000 |
| Pr141(LR) | 0.001 | 0.000 | 0.000 | 0.000 |
| Nd146(LR) | 0.006 | 0.001 | 0.001 | 0.000 |
| La139(LR) | 0.007 | 0.001 | 0.001 | 0.000 |
| Sm147(LR) | 0.001 | 0.000 | 0.000 | 0.000 |
| Dy163(LR) | 0.001 | 0.000 | 0.000 | 0.000 |
| Y89(LR) | 0.088 | 0.018 | 0.068 | 0.043 |
| Ho165(LR) | 0.000 | 0.000 | 0.000 | 0.000 |
| Lu175(LR) | 0.000 | 0.000 | 0.000 | 0.000 |
| Yb173(LR) | 0.000 | 0.000 | 0.000 | 0.000 |
| Sb121(LR) | 0.048 | 0.002 | 0.049 | 0.004 |
| As75(HR) | 0.025 | 0.004 | 0.035 | 0.004 |
| Sc45(MR) | 0.001 | 0.000 | 0.000 | 0.000 |
| Ti49(MR) | 0.020 | 0.006 | 0.023 | 0.002 |
| Al27(MR) | 49.454 | 0.427 | 6.185 | 0.878 |

For both vehicles, the elemental matrix is composed largely of alkaline earth metals and divalent transition metals, followed by redox active transition metals. The first two metal categories, primarily originate from the lubricant oil and its additive package components. For the Cummins ISX-15 engine, the fraction of alkaline earth metals was significantly lower than that of the uncontrolled Cummins ISX-450 engine. In fact, the use of the DOC/DPF configuration reduced most metal fractions, suggesting a high removal efficiency of these elements in the DPF. In addition to the effect of the aftertreatment control technology, the use of biodiesel blends led to reductions in most metal fractions for both vehicles. It should be stressed that all biodiesel blends showed reductions in the fraction of redox-active metals for both vehicles. Looking at the individual distribution of redox-active metals, iron (Fe) showed decreases with most biodiesel blends relative to CARB ULSD for both engines with the exception of WCO-50 blend, which was systematically higher than the other biodiesel blends and higher than CARB ULSD for the Cummins ISX-15 engine. The Fe in the PM can be sourced from the fuel itself or engine wear. The emissions of nickel (Ni) were also found to be lower with biodiesel compared to CARB ULSD for both vehicles. Ni can be released through the engine exhaust due to wear and tear of the engine. Biodiesel's self-lubricity properties and smaller concentration of Ni in the fuel were the main reason for the lower Ni emissions [Agarwal et al., 2011]. In addition, the use of biodiesel resulted in reductions in As and Cd, which are class I carcinogenic metals classified by the International Agency for Research on Cancer (IARC) [Betha and Balasubramanian, 2013].

### 4.13 Macrophage ROS Assay

The pathway through which diesel exhaust induces airway inflammation has yet to be elucidated, but oxidative stress is thought to be an important underlying mechanism of action [Li et al., 2002a,b; Ayres et al., 2008]. Oxidative stress can be caused by ROS production overwhelming the antioxidant protection [Bowler and Crapo, 2002]. Oxidative stress can be viewed as a biological emergency that elicits a range of cellular responses [Li et al., 2002a,b]. The first and most sensitive responses are the induction of antioxidant and phase-2 drug-metabolizing enzymes, which are often regulated by the antioxidant response element (ARE) in the promoter of the corresponding genes of these enzymes [Takizawa et al., 1999]. It has been suggested that the failure of these antioxidant and detoxifying mechanisms to control the level

of oxidative stress will lead to more damaging responses in the next step. This next step may be the initiation of inflammation, and finally the activation of programmed cell death. For this study, the oxidative potential of diesel and biodiesel exhaust was measured using the macrophage ROS assay and the DTT assay.

The macrophage ROS assay is a fluorogenic cellular method to measure the generation of reactive oxygen species in alveolar macrophages on exposure to aqueous suspensions of PM. Due to the location of alveolar macrophages on the inner epithelial surface of the lung, this assay provides an excellent model of pulmonary inflammation in response to PM exposure. Figure 4-38 and Figure 4-39 show the results of macrophage ROS assay conducted on the water extracts of exhaust PM samples from the Cummins ISX-15 and Cummins ISX-450 engines, respectively. The results are expressed on a per mass of PM emitted basis (g ROS activity/mg of PM).

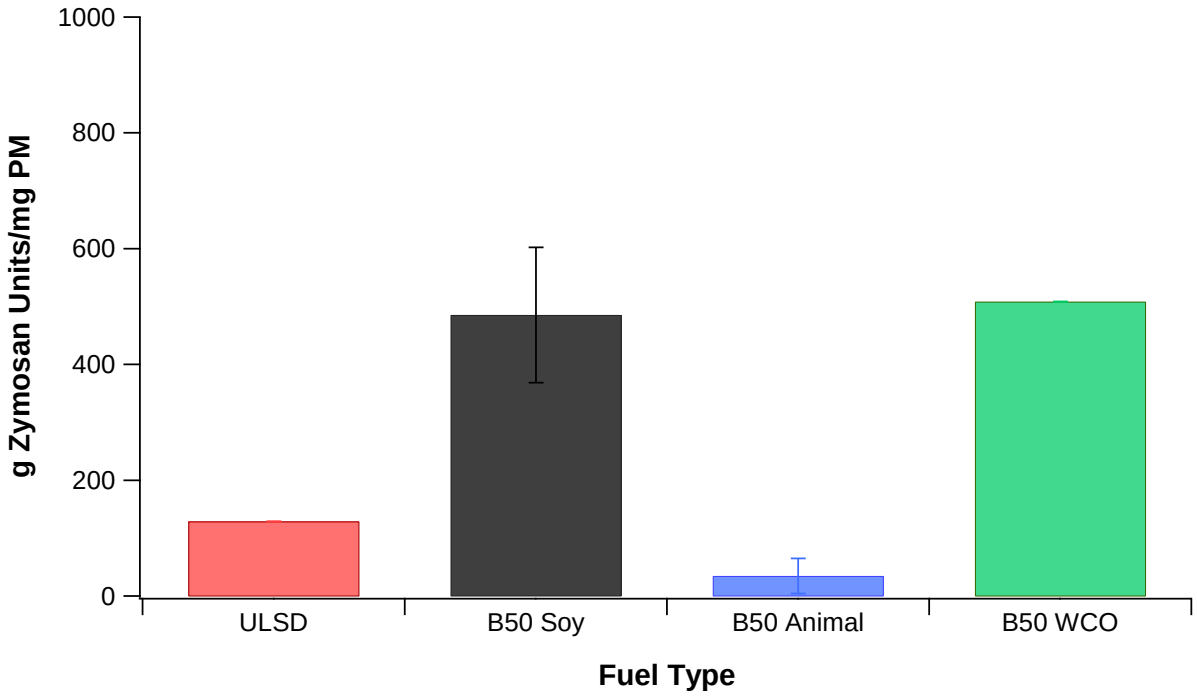


**Figure 4-38 Reactive Oxygen Species (ROS) activity of PM from the Cummins ISX-15 engine**

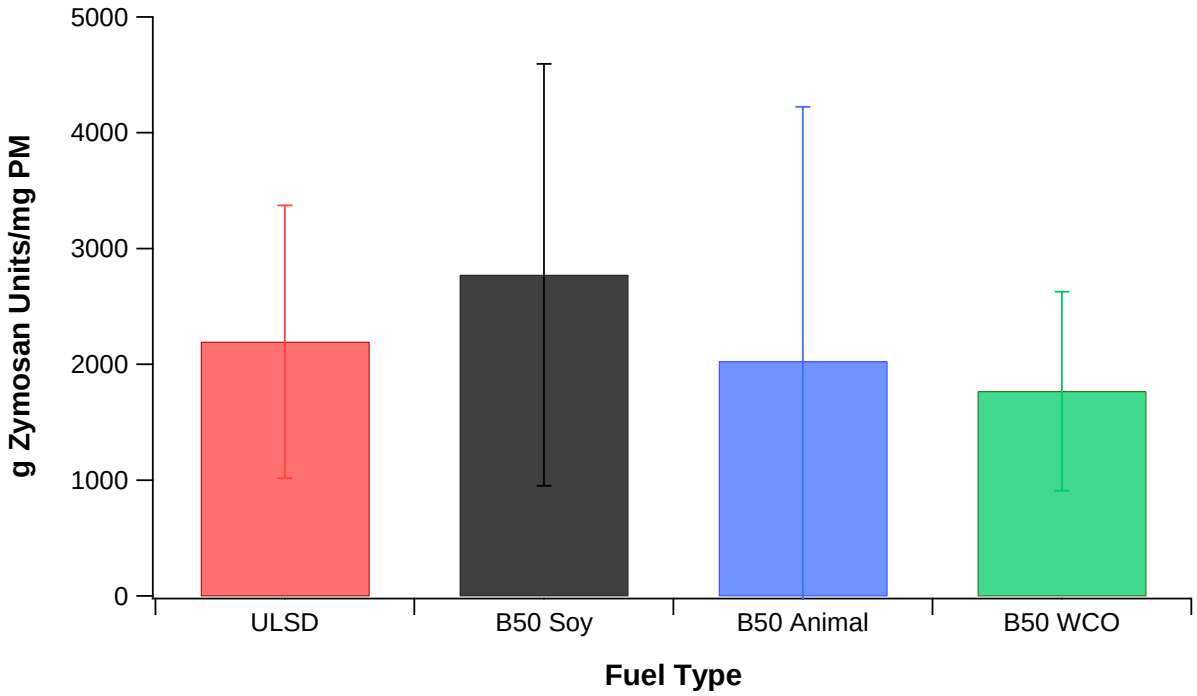


**Figure 4-39 Reactive Oxygen Species (ROS) activity of PM from the Cummins ISX-450 engine**

It is of particular note that, the heavily controlled Cummins ISX-15 engine significantly reduced the ROS activity of PM compared to the uncontrolled Cummins ISX-450 engine, even when the comparisons are made on a per mass basis. However, some increases in ROS activity of PM were seen for the SME-50 and WCO-50 blends relative to CARB ULSD for the Cummins ISX-15 engine. It should be noted that for the CARB ULSD and WCO-50 fuels, only a single measurement was included in data analysis due to large analytical uncertainties. For the Cummins ISX-450 engine, the results showed a fair amount of variability and the test fuels did not show any effect in ROS activity on a per mass basis.

### 4.14 Chemical Reactivity Assay (DTT)

Redox activity is believed to reflect the ability to generate ROS, which can induce a state of oxidative stress. Studies have shown that adverse health effects may derive from oxidative stress, initiated by the formation of ROS within damaged cells [O'Brien, 1991]. The redox activity, as measured by the prooxidant content determined from the DTT assay, is shown in Figures 4-40, 4-41, and 4-42, respectively, for the particle-phase components for the Cummins

ISX-450, the vapor-phase components for the Cummins ISX-450, and the vapor-phase components for the Cummins ISX-15. The results are expressed as DTT activity per mile. It should be mentioned that the DTT values for the particle-phase components of the DPF-fitted Cummins ISX-15 engine were found to be well below the filter blank levels due to the very low PM mass adsorbed on the Teflon filters.

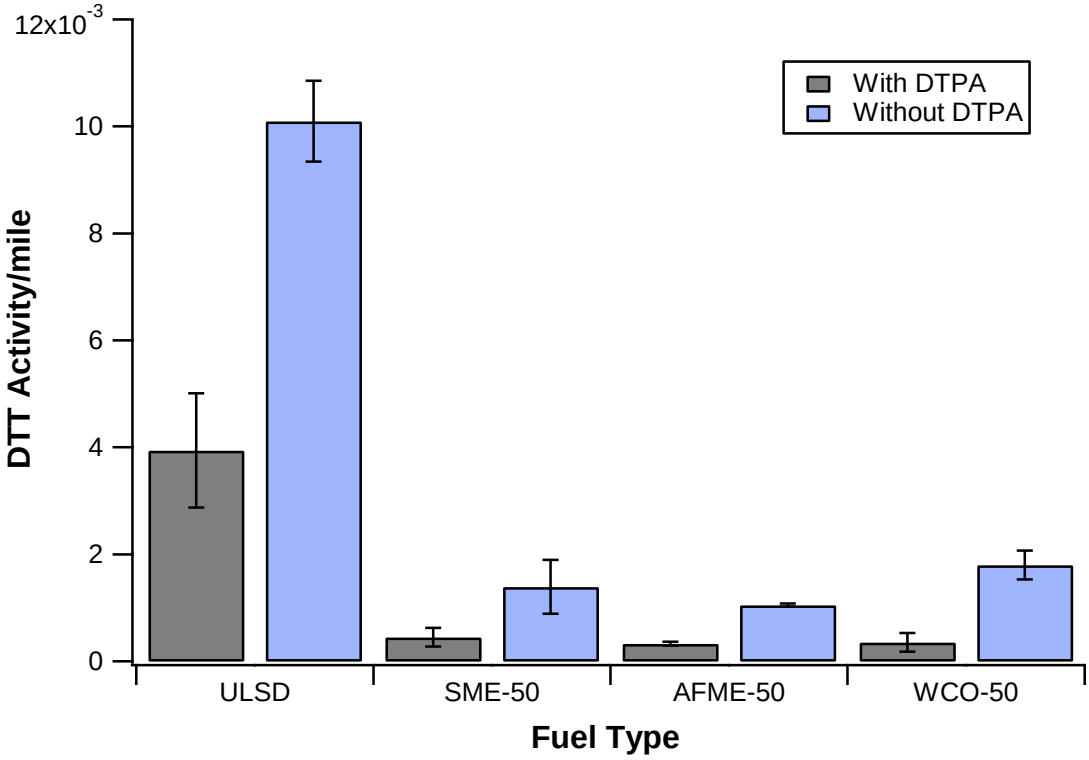


**Figure 4-40 Prooxidant content of the particle-phase components of PM for the Cummins ISX-450 engine**

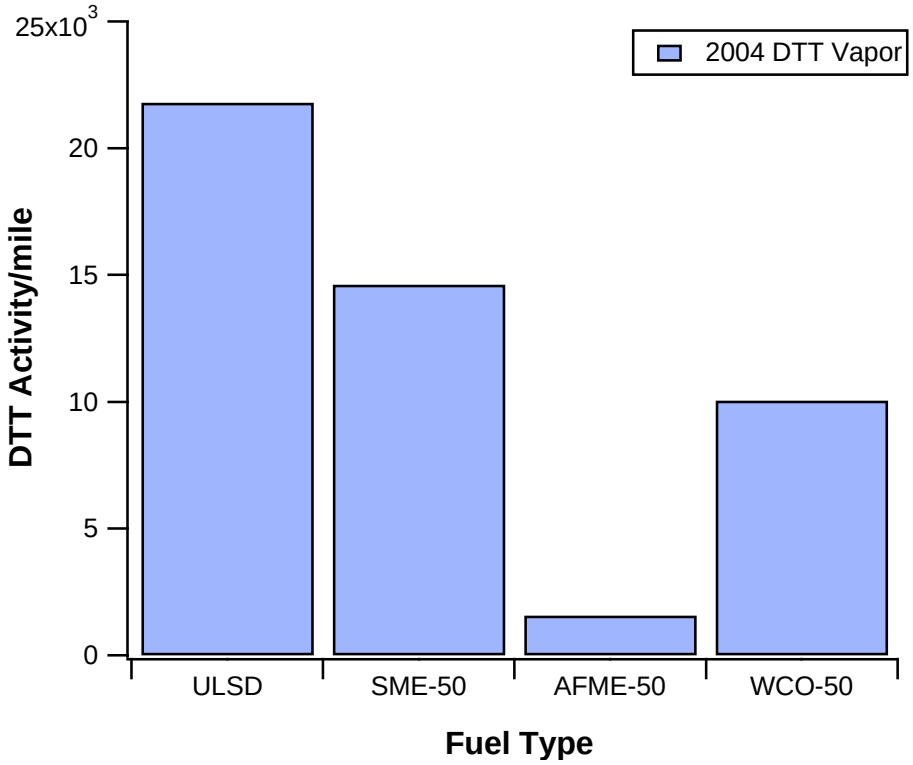


**Figure 4-41 Prooxidant content of the vapor-phase components of PM for the Cummins ISX-450 engine**

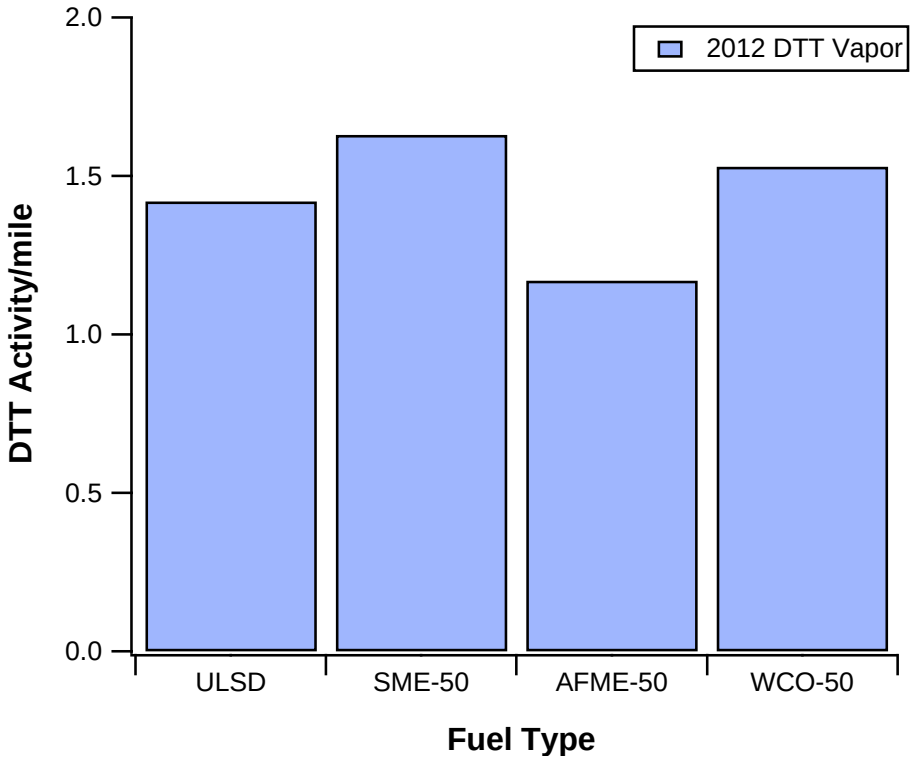


**Figure 4-42 Prooxidant content of the vapor-phase components of PM for the Cummins ISX-15 engine**

The results reported here show that the DTT consumption rate of the Cummins ISX-450 engine decreased with the use of biodiesel blends relative to CARB ULSD, which produced the most potent exhaust for redox activity. The reductions in oxidative potential for the biodiesel blends were all statistically significant compared to CARB ULSD. In the presence of the metal chelator, DTPA, the ULSD sample retained about 50% of the total prooxidant activity whereas the prooxidant activity of the remaining biodiesel fuel samples was completely blocked, suggesting the biodiesel fuel prooxidants are metal associated. The oxidative activities of the particle-phase components also showed a feedstock dependency, with the WCO-50 blend exhibiting higher redox activity than the other biodiesel blends, but not at a statistically significant level. Our results for the redox activity expressed by the DTT assay are in agreement with the PAH emissions results for this engine, which were generally higher for the CARB ULSD compared to the biodiesel blends. Analogous to the particle-phase components of PM, the oxidative activity of the vapor-phase components showed some marked reductions with the biodiesel blends

relative to CARB ULSD, at least for the uncontrolled Cummins ISX-450 engine. The reductions in oxidative activity for the biodiesel blends were all found to be statistically significant. The results from the uncontrolled Cummins ISX-450 engine indicate that, in terms of ROS production, biodiesel blends would have less adverse effects on human health compared to the CARB ULSD.

For the Cummins ISX-15 engine, the vapor-phase components showed a significantly lower level of prooxidants for biodiesel and CARB ULSD exhaust compared to the uncontrolled Cummins ISX-450 engine. The oxidative activity for the SME-50 and WCO-50 blends was higher than CARB ULSD, while AFME-50 blend showed lowed oxidative activity compared to the baseline diesel fuel. It should be noted that the differences between the levels of prooxidants for the test fuels were not statistically significant. The substantially lower level of prooxidants for the Cummins ISX-15 engine, suggest that the DOC/DPF system was effective in reducing the actual toxicological impact of diesel and biodiesel emissions on human exposure by efficiently trapping highly reactive volatile and semi-volatile compounds present in the vapor phase. Overall, our results for both vehicles agree with those studies showing reductions in oxidative potential with biodiesel [Gerlofs-Nijland et al., 2013; Kooter et al., 2011]. It should be noted that some other studies have also shown increases in oxidative activity with the use of biodiesel compared to diesel fuel [Cheung et al., 2009; Guarieiro et al., 2014], in contrast to these results. A recent light-duty chassis dynamometer study on biodiesel-powered passenger cars showed higher DTT-redox activity for B10, B30, and B50 blends compared to standard road ULSD [Grigoratos et al., 2014]. Though our results largely differ from this study with regards to the fuel effect, they are in agreement with regards to the aftertreatment effect, as both studies showed lower oxidative activity for the DPF-fitted vehicles, indicating that a significant amount of potentially toxic organic compounds were trapped and oxidized in the DPF.

In addition to the fuel effect on the oxidative activity of the vapor-phase samples for both vehicles, significant levels of prooxidants were also found in the vapor-phase PM samples in both vehicles. This phenomenon was somewhat unexpected, as previous studies of ambient air samples had shown the vapor-phase to contain only a small fraction of the total prooxidants in the air sample [Cho et al., 2005]. In the present samples, the vapor-phase contained equal if not

higher levels of prooxidants compared to the particle-phase PM samples. Significant levels of prooxidants were present in the vapor-phase samples of the biodiesel exhaust as well. This difference may be a temperature effect; the temperature at which the exhaust particles are collected is likely to be higher than the ambient temperatures used in field PM studies. In particular, the distribution between particle- and vapor-phase content of quinones, the highly reactive organic compounds with prooxidant and electrophilic activity, in exhaust is very sensitive to temperature [Delgado-Saborit et al., 2013].

### 4.15 Cellular Assays

To assess potential adverse health effects of samples, inflammatory and protective responses to the samples by a mouse macrophage cell line (Raw 264.7) were determined. The expression of the cytokine, tumor necrosis factor alpha (TNFα) by the cells in response to the exhaust samples was used as the inflammatory response. TNFα is a common inflammatory response and is often the most robust compared to other cytokines, so it appears to be more sensitive to proinflammatory insult [Veronesi et al., 1999]. When the vapor sample size was too small, individual samples were pooled for cell studies. The results, shown in Figure 4-43, represent the observed values less the appropriate blanks; i.e., for the Teflon (TF) samples, a clean filter, for the XAD an extract of fresh XAD resin. The cellular responses to the CARB ULSD samples were determined first because of their high prooxidant content. In previous studies conducted at UCLA, it was found that the prooxidant content of PM samples is a predictor of TNFα expression and that vapor-phase electrophile content is a predictor of cellular hemeoxygenase-1 levels. The CARB ULSD results are consistent with those trends. Some biodiesel particle-phase samples from the uncontrolled Cummins ISX-450 engine were capable of increasing TNFα compared to the activity of CARB ULSD. Of interest were the high negative values of the uncontrolled Cummins ISX-450 engine XAD or vapor samples, which could reflect suppression of the TNFα response (Figure 4-44). In micro array studies with ambient vapor samples from the LA basin, a suppression of the mRNA for TNFα in a bronchial epithelial cell line has been observed [Shinkai et al., 2013]. The negative TNFα response to the vapor phase samples may reflect the effects of the actions of the vapor components on the antioxidant-antielectrophile response element (ARE) [Li et al., 2000]. This element is associated with a protective response and micro array

studies with vapor phase samples in Riverside showed that vapor phase components [Shinkai et al., 2013] suppressed TNFα mRNA by 40%.

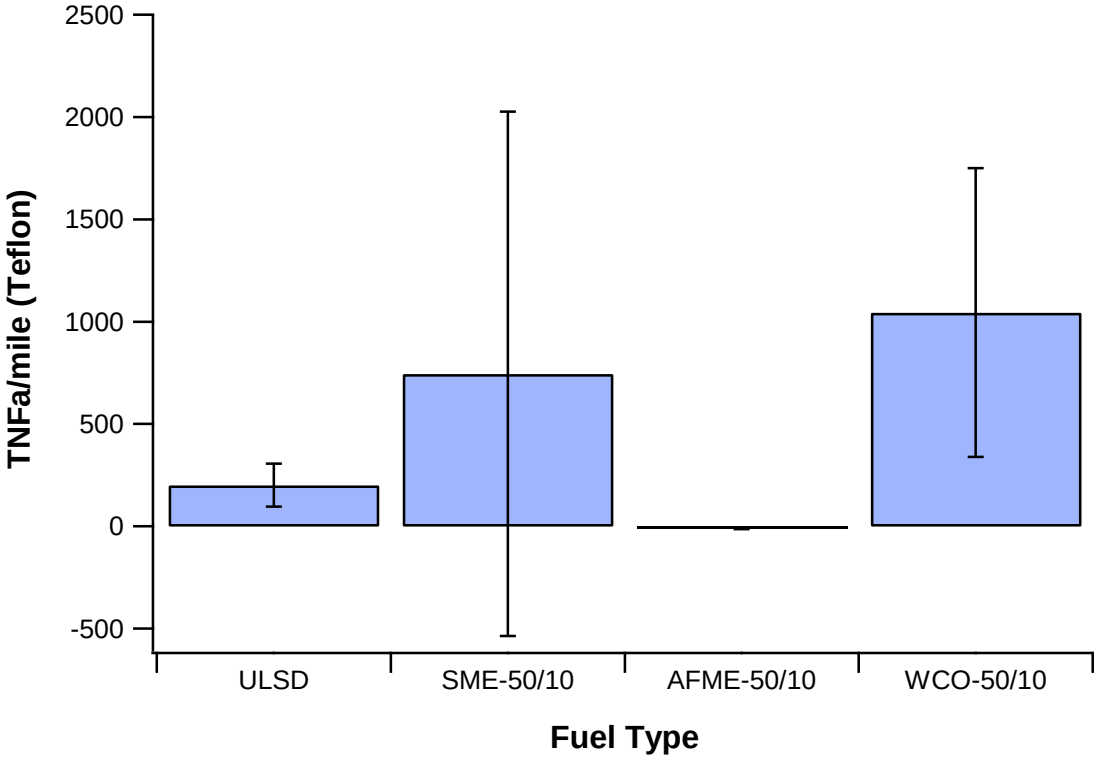


**Figure 4-43 TNFα responses of the particle-phase components of PM for both vehicles**

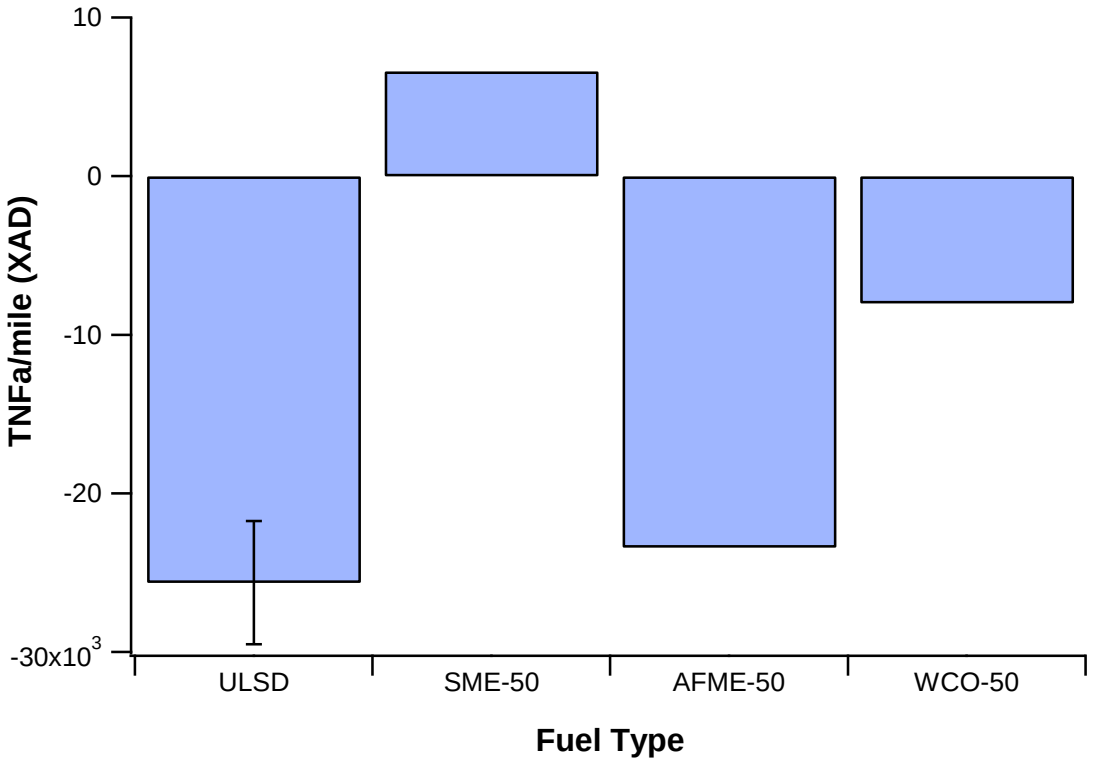


**Figure 4-44 TNFα responses of the vapor-phase components of PM for the Cummins ISX-450 engine**

The negative TNFα values obtained under the present test conditions for some samples raised a question regarding the validity of these negative values, i.e., are they simply blank or no response or does the negative value have significance. We believe the answer is a partial yes, i.e., the negative value, which means the values are lower than those for the filter blanks, reflects an action by components the particles on the TNF expression system. We have previously observed negative dose response relationships between concentration and effect when we exposed the diesel exhaust particles we use as the "standard" for our cellular and chemical assays (see Figure 4-45).

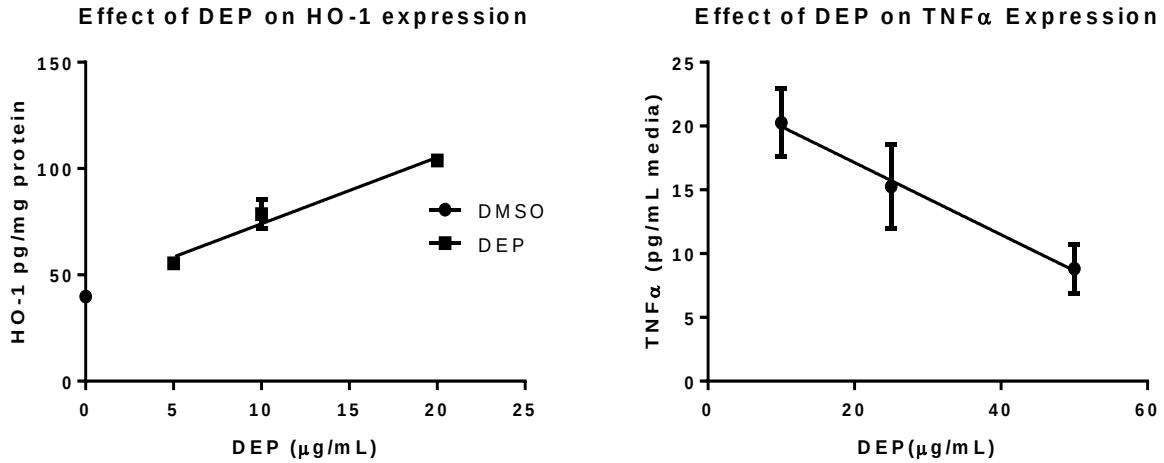


**Figure 4-45 Dose response relationships**

Figure 4-45 shows the dose response relationship between DEP concentration and cellular TNFα and HO-1 responses. Note the negative slope of the TNFα curve; this relationship indicates that the PM actually decreases the ability of cells to exhibit inflammatory responses. Such a relationship could be rationalized by the notion that DEP induce higher levels of substances that reduce the ability of the cells to increase TNFα expression, i.e., protective or adaptive agents. These agents could, for example, increase the proteins controlled by the antioxidant response element, i.e., HO-1 and phase II enzymes that inactivate reactive chemical species such as quinones and prooxidants, and electrophiles.

Ambient air samples that have been previously examined, do not respond in the same way. Figure 4-46 shows the concentration response curves of ambient air PM2.5 collected in Commerce (CM), Long Beach (LB), and San Bernardino (SB).

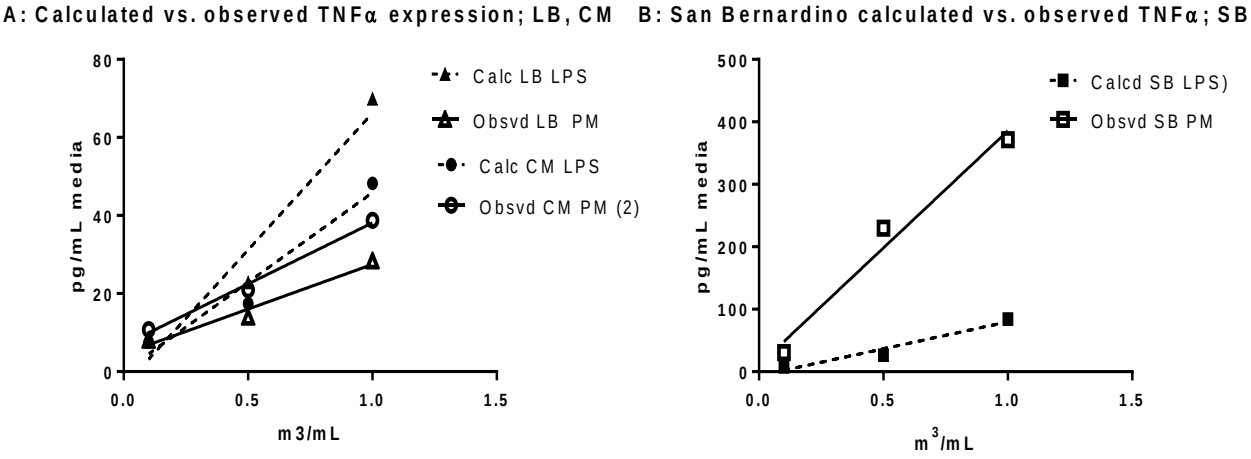


**Figure 4-46 Concentration response curves of ambient PM collected at different sites**

Figure 4-46 shows a concentration dependent increase in TNFα following exposure to ambient PM2.5. The dotted lines represent a calculated endotoxin (LPS) dose response curve for each sample, which was generated from the PM content of LPS measured in each sample. The PM2.5 concentrations vs. TNFα response curve are the solid line curves. The results indicate that only the SB samples exhibit responses significantly different from responses expected from the LPS content of the samples. It is assumed that the endotoxin LPS is not likely to be present in the vehicle samples because they were collected over a short time and immediately stored at low temperature.

Next the effects of the samples on cellular hemeoxygenase-1 (HO-1) expression were determined. HO-1 is a cellular protective enzyme, acting through the removal of heme by catalyzing its oxidation to bileverdin [Gozzelino et al., 2010]. HO-1 resolving heme is induced by various stressors, such as oxidation stress, heavy metal exposure, hypoxia, ultraviolet light, and resulted increased HO-1 mRNA expression. The results showed that the particle-phase sample for the WCO-50 blend increased the expression of HO-1 at greater levels than those exhibited by the standard, CARB ULSD fuel (Figure 4-47).

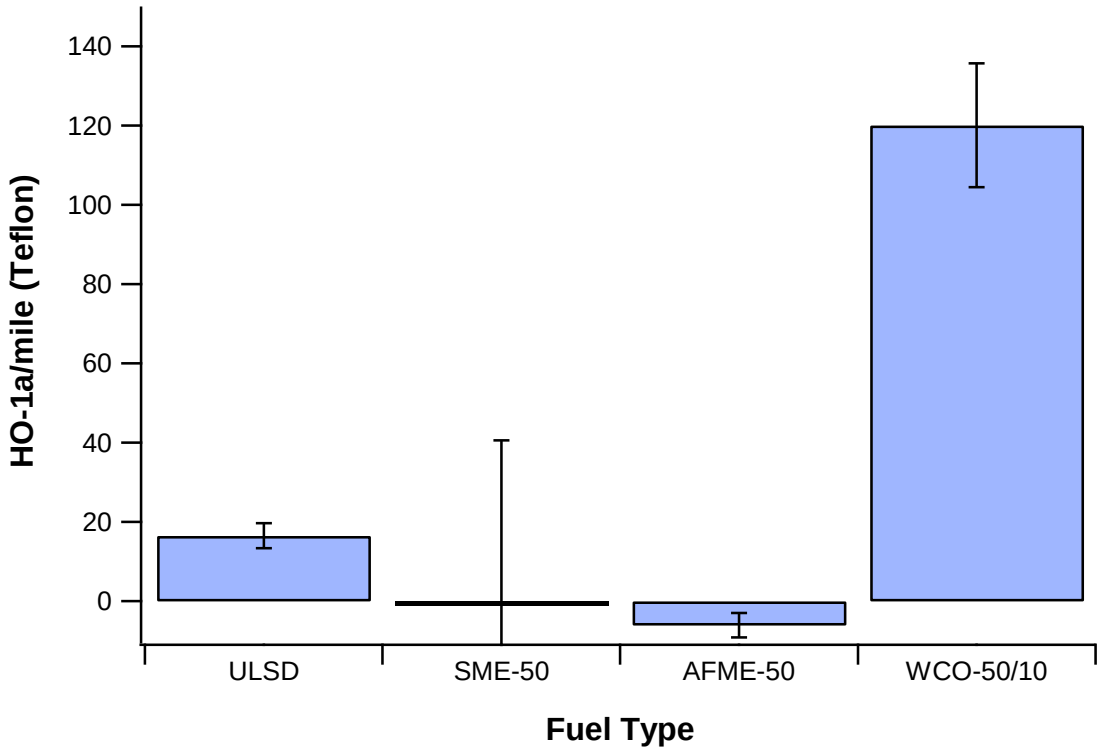


**Figure 4-47 HO-1 responses of the particle-phase components of PM for the Cummins ISX-450 engine**

For the uncontrolled Cummins ISX-450 engine, the vapor phases from the CARB ULSD caused greater expression of HO-1 than the corresponding vapor phases from the biodiesel blends (Figure 4-48), which may reflect a different distribution of the causative chemical species between the CARB ULSD and the biodiesel fuels. The chemical species responsible for increasing the HO-1 expression may be localized in the particle phase of the biodiesel fuel exhaust, whereas those chemicals may be localized in the vapor phase of the biodiesel exhaust.

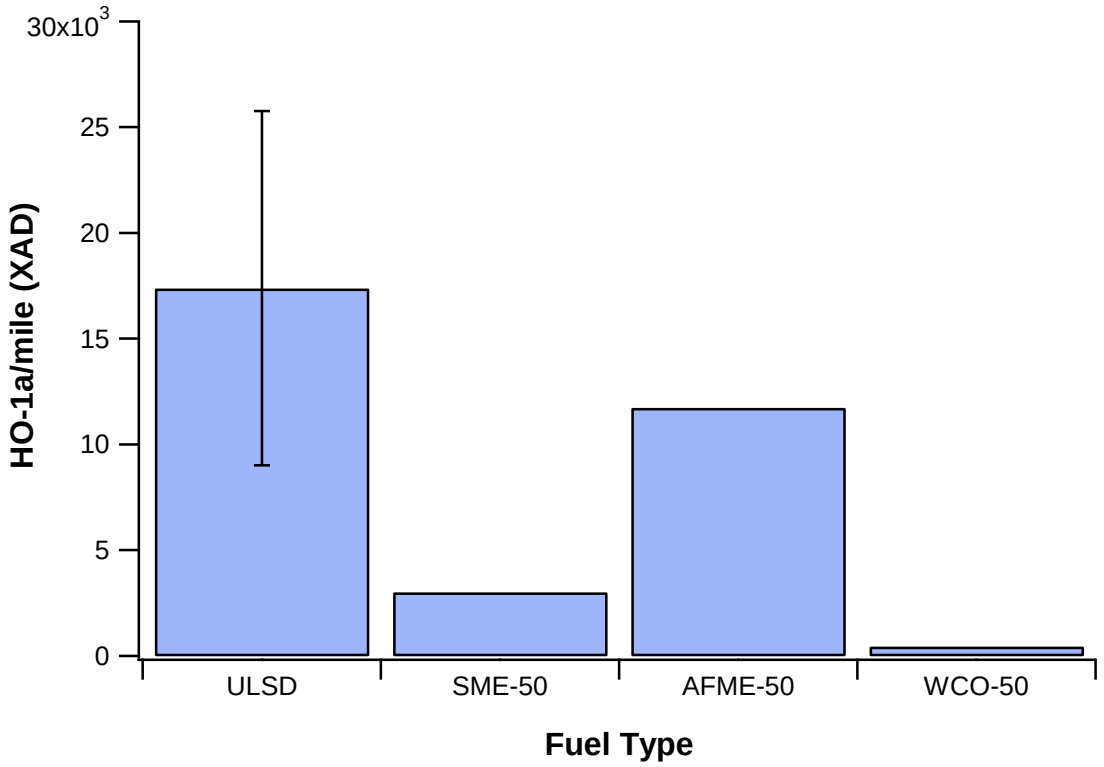


**Figure 4-48 HO-1 responses of the vapor-phase components of PM for the Cummins ISX-450 engine**

Based on the cellular data reported here, it can be hypothesized that the HO-1 responses appear to reflect the prooxidant content of the samples, as the order of expression tracks with the levels of prooxidants shown in Figures 4-40 through 4-42, suggesting that the basis for ARE activation may be prooxidant, not electrophilic activity.

### 4.16 Association Between Chemical Species and Oxidative Activity

To assess the contribution of various chemical species to the PM oxidative potential, regression analysis was conducted between the activity measured by two assays, namely the ROS macrophage assay and the DTT assay, and major chemical constituents. The results of this regression analysis are shown in Table 4-3 for the uncontrolled Cummins ISX-450 engine. Both the DTT and the macrophage ROS assay showed a reasonable correlation with an $R^2$ of 0.588. Unlike the ROS macrophage assay, the DTT assay was moderately correlated with WSOC

($R^2$=0.6849) and correlated well with n-alkanes ($R^2$=0.8451) and with hopanes and steranes ($R^2$=0.7513). Surprisingly enough, the DTT assay showed a relatively low correlation with PAHs ($R^2$=0.2952), whereas the macrophage ROS assay showed a minor correlation with $R^2$=0.19. In general, the relatively high correlations of alkanes and hopanes and steranes to DTT were unexpected, since these species are less likely to be involved in the oxidation stress mechanism due to their low ability to oxidize diesel PM. Most studies have shown a good association between the PAH content of PM and DTT [Li et al., 2003; Geller et al., 2006].

The results reported here indicate that, at least for the uncontrolled vehicle, the organic compounds contained in water-soluble components in diesel and biodiesel exhaust PM correlate well with the DTT assay. In addition, our results suggest that WSOC play a primarily role to regulate ROS generation. WSOC is a complex mixture of diverse group of species including dicarboxylic acids, polyacidic compounds, polyethers, etc. [Decesari et al., 2000]. An indirect effect of WSOC is determined by its contribution to the particle's hygroscopicity and hence the ability of aerosol particles to act as cloud condensation nuclei (CCN) [Asa-Awuku et al., 2008].

Apart from the organic-soluble fractions of PM, the DTT assay was found to significantly correlate with several water-soluble metals. Studies have shown that the constituents of water-soluble PM extracts (mainly transition metals) are more likely to induce oxidative DNA damage than the organic compounds. After inhalation and deposition of PM in the lung, alveoli are able to stimulate the formation of ROS, especially hydroxyl and superoxide anion radicals. These ROS, which can be generated by transition metals, initiate a cascade of reactions and can play an important role in oxidative damage to cellular membrane lipids, proteins-enzymes, and DNA. In addition, ROS can initiate pulmonary inflammation and, through complex mechanisms, might contribute to the impairment of excision repair mechanisms of DNA and activation of oncogenes [Valavanidis et al., 2008]. Under the present conditions, the highest correlations for DTT were observed for divalent transition metals ($R^2$=0.9943), Higher valent/hydrolyzed metals ($R^2$=0.996), redox active transition metals ($R^2$=0.9777), heavy metals ($R^2$=0.9626), rare earth ($R^2$=0.9534), and alkaline earth metals ($R^2$=0.9102). For individual water-soluble metals, the highest correlation was observed for Cu ($R^2$=0.9931), followed by Fe ($R^2$=0.979), and Cr

($R^2$=0.9035). It should be noted that none of the metal groups or the individual water-soluble metals significantly correlated with the macrophage ROS assay. While our results on water-soluble metals showed significantly high correlations with the DTT assay, they largely differ from those reported in a previous heavy-duty chassis dynamometer study of retrofitted vehicles, which showed strong correlations of redox-active metals with the macrophage ROS assay [Verma et al., 2010].

Iron, Cr, Mn, and Cu can stimulate the generation of hydroxyl radicals by Fenton-type reactions, causing extensive oxidative damage to cellular macromolecules. These metals are considered to be the most abundant redox transition metals in diesel exhaust particles [Nico et al., 2009]. Iron has two major oxidation states, Fe (II) and Fe (III). The solubility of Fe (II) is dramatically higher than that of Fe (III); equilibrium concentrations of Fe (III) or Fe (II) from ferrihydrite (am-$Fe(OH)_3$) and am-$Fe(OH)_2$ with pure water are approximately $10^{-5}$ M and $10^{-10}$ M, respectively. The main mechanism of Fe toxicity is generation of ROS, such as $H_2O_2$, OH, and $HO_2$, through Fenton-type chemistry. Similar to Fe, Cr has two major oxidation states, Cr(III) and Cr(VI). Chromium(III) compounds are generally insoluble and non-toxic, whereas Cr(VI), as chromate, is highly soluble, toxic, and potentially carcinogenic [Gad 1989]. Manganese has three readily available oxidation states: Mn(II), Mn(III), and Mn(IV). Overall uptake of Mn from pulmonary dosing measured in vivo showed absorbed Mn being significantly greater from soluble Mn(II) salts as compared with insoluble Mn(III) and Mn(IV) oxides [Dorman et al. 2001; Aschner et al. 2005]. Manganese appears to exert its toxic effects through a variety of pathways, including ROS formation, direct oxidation of biological molecules (specifically neurotransmitters) by Mn(III), disruption of cellular Ca, and alterations in Fe homeostasis [Reaney et al. 2005]. Therefore, while Mn(II) salts are more bioavailable, the cytotoxicity of Mn(III) compounds appears to be significantly greater than those of Mn(II). Our study showed that the higher water solubility of the more abundant redox-active metals makes them more bioavailable to probably participate in the reactions yielding ROS activity of diesel and biodiesel exhaust particles.

It should be noted that several water-soluble trace metals were present at high concentrations in the PM extracts (Zn, Pb sum, Cd), and effectively removed on Chelex, exhibited relatively good correlations with the DTT assay. Zinc exhibited an $R^2$ of 0.7278, the measured $R^2$ of Pb was

0.8528, while Cd correlation with DTT had an $R^2$ of 0.4587. These three metals do not have active redox cycles and their ability to induce ROS formation in vitro is typically lower than that of redox-active metals [Szivák et al., 2009]. Though Cd, Pb, and Zn may not be directly redox-active, they (particularly Cd and Pb) can induce oxidative stress via several other mechanisms including depletion of cellular antioxidant pools (e.g., GSH) and increased lipid peroxidation [Pinto et al., 2003]. Cadmium is particularly active in this regard, likely reflecting its higher affinity for thiol groups [Topperwein et al., 2007].

**Table 4-3 Correlation for DTT activity and selected chemical PM species for the Cummins ISX-450 engine**

| **Species** | **$R^2$** |
|---|---|
| ROS | 0.588 |
| WSOC | 0.6849 |
| Hopanes and Steranes | 0.7513 |
| Alkanes | 0.8451 |
| PAHs | 0.2952 |
| Redox active transition metals | 0.9777 |
| Alkaline earth metals | 0.9201 |
| Heavy metals | 0.9626 |
| Divalent transition metals | 0.9943 |
| PGE | 0.8907 |
| Rare metals | 0.9534 |
| Semi-metals | 0.2959 |
| Higher valent/hydrolyzed metals | 0.996 |
| Fe | 0.979 |
| Cu | 0.9931 |

| | |
|---|---|
| Cr | 0.9035 |
| Mn | 0.5883 |
| Co | 0.3186 |

For the Cummins ISX-15 engine, there are no correlations between the DTT assay and various chemical species of PM because this assay was not performed in the particle-phase due to the very low PM mass. Table 4-4 presents correlations between the ROS activity and some major PM constituents. The highest correlation was seen for the hopanes and steranes ($R^2$=0.4809), followed by the PGE ($R^2$=0.3078), Fe ($R^2$=0.2682), and Mn ($R^2$=0.257). It is interesting to note that the WSOC, PAHs, alkanes, and most of the transition metals did not show a significant correlation with ROS assay or were close to zero, which is not surprising, given the very low levels of these species due to the presence of the DOC/DPF system.

**Table 4-4 Correlation for macrophage ROS activity and selected chemical PM species for the Cummins ISX-15 engine**

| **Species** | **$R^2$** |
|---|---|
| Hopanes and Steranes | 0.4809 |
| Alkanes | 0.153 |
| WSOC | 0.1704 |
| Divalent transition metals | 0.161 |
| PGE | 0.3078 |
| Mn | 0.257 |
| Fe | 0.2682 |

# 5 Conclusions

This study investigated the criteria emissions, gaseous toxic pollutants, and the physicochemical and toxicological characteristics of particulate matter emitted from two heavy-duty vehicles

when operated on CARB ULSD and different biodiesel blends. Experiments were conducted on a truck equipped with a 2010 MY Cummins ISX-15 heavy-duty diesel engine with a DOC/DPF and SCR aftertreatment system and meeting EPA's current emission standards, and on a truck with a 2002 MY Cummins ISX-450 heavy-duty diesel engine without exhaust aftertreatment. The biodiesel utilized for this study included a soy-based methyl ester, an animal fat methyl ester, and a waste cooking oil methyl ester. The methyl esters were used as blends at a 50% concentration with a typical CARB ULSD. Emission measurements were performed over the EPA UDDS test cycle on heavy-duty chassis dynamometer.

The main findings of this study is that THC, NMHC, CO, and PM mass emissions for the uncontrolled Cummins ISX-450 engine showed reductions with the use of biodiesel blends compared to CARB ULSD. For the Cummins ISX-15 engine, THC and NMHC emissions were practically below the detection limits, as these species were effectively fully oxidized in the DOC/DPF system. CO and PM mass emissions were also low for the DOC/DPF equipped engine, and did not show any fuel effects. $CO_2$ emissions showed some moderate decreases with the biodiesel blends relative to CARB ULSD, which is an indication that the engine efficiency wasn't influenced by the high biodiesel blend ratio. Overall, $NO_x$ emissions exhibited increases with biodiesel for both vehicles with the differences in $NO_x$ emissions relative to CARB ULSD being statistically significant for the newer Cummins ISX-15 engine. For the Cummins ISX-15 engine, $NO_x$ emissions showed some feedstock dependency with the unsaturated SME-50 producing higher $NO_x$ than CARB ULSD and AFME-50 blend. In addition, for the SCR-fitted vehicle $NO_x$ emissions were strongly dependent by the SCR system temperature with $NO_x$ emissions being consistently lower when the SCR temperature was above 250 °C. Particle number emissions did not show any strong trends between the test fuels for the older engine, while for the newer engine particle number emissions were below the tunnel background levels. The older engine showed bimodal particle size distributions with peaks at around 55 nm and 11 nm in diameter. For the newer engine, the particle size distributions were dominated by nucleation mode particles with peaks around 11 nm in diameter.

Ammonia emissions were found to be significantly higher for the SCR-fitted vehicle compared to the uncontrolled vehicle, with the biodiesel blends producing higher $NH_3$ emissions relative

to the baseline CARB ULSD. The higher $NH_3$ emissions ($NH_3$ slip) for the biodiesel blends could be related to the higher biodiesel $NO_x$ emissions for this vehicle and it was likely a consequence of more injected urea to suppress engine-out $NO_x$ emissions.

Formaldehyde and acetaldehyde were the most abundant carbonyls in the exhaust with biodiesel generally showing lower formaldehyde and acetaldehyde emissions than CARB ULSD. There were no significant differences between the fuels for 1,3-butadiene for any of the test vehicles, while for the uncontrolled vehicle benzene emissions decreased with the use of biodiesel relative to CARB ULSD. For the Cummins ISX-450 engine, all the mono-aromatic compounds showed reductions with the biodiesel blends relative to CARB ULSD, whereas no strong fuel trends were seen for the newer engine.

Overall, the use of biodiesel resulted in PAH emission decreases compared to CARB ULSD. For the Cummins ISX-15 engine, most PAH compounds were practically undetectable due to the presence of the DOC/DPF system. For the Cummins ISX-15 engine, hopane and sterane emissions were found to be at substantially lower concentrations than those of the uncontrolled Cummins ISX-450 engine, which was due to the newness of the diesel engine and also due to the presence of the DOC/DPF configuration. For both vehicles, the dominant alkane species ranged from nonadecane to pentacosane, which could be attributed to fuel combustion. Long-chain alkanes were also present, which is an indication of lubricant oil contribution. The Cummins ISX-450 engine emitted higher levels of alkanes, while the Cummins ISX-15 engine had overall lower alkane emissions. The ionic species were found at substantially lower levels for the DOC/DPF-fitted engine than the uncontrolled Cummins ISX-450 engine, with the fuel effect not being particularly strong for either of the test vehicles.

For both vehicles, the elemental matrix was composed largely of alkaline earth metals and divalent transition metals, followed by redox active transition metals. Overall, the Cummins ISX-15 engine showed lower concentrations of water-soluble metals than the uncontrolled Cummins ISX-450 engine. The use of biodiesel generally decreased the emissions of water-soluble metals compared to CARB ULSD for both vehicles, especially the redox active transition metals.

The results for the health-related parameters, as measured in the present study by the DTT assay, suggest that high-concentration biodiesel blends in an older and a modern technology vehicle could be less harmful than petroleum diesel fuel from an oxidative stress level perspective. Our study showed that the biodiesel blend particle-phase samples had a lower prooxidant content compared to the CARB ULSD fuel samples, but the biodiesel blend vapor-phase samples contained proportionally higher levels of prooxidants. These results suggest there may be a difference in the distribution of reactive chemical species in biodiesel fuel exhaust compared to petroleum diesel.

The vapor-phase samples from the Cummins ISX-450 engine appeared to actually suppress the expression of TNFα. The change from CARB ULSD fuel to biodiesel fuels in a non-controlled engine appeared to have beneficial changes with respect to the expression of the inflammatory cytokine but the limited data precluded statistical evaluation. Of the biodiesel samples, the AFME-50 blend showed the most favorable response; HO-1 levels were positive and the TNFα response the lowest.

Further analysis supported that DTT activity was strongly associated with the water-soluble organic carbon (WSOC) and redox active transition metals, but not with the PAHs.

# 6 References

Ackland M.L., Zou L., Freestone D., van de Waasenburg S., Michalczyk A.A. Diesel exhaust particulate matter induces multinucleate cells and zinc transporter-dependent apoptosis in human airway cells. Immunol Cell Biol. 2007, 85, 617–622.

Agarwal A.K., Gupta T., Kothari A. Particulate emissions from biodiesel vs diesel fuelled compression ignition engine. Renewable and Sustainable Energy Reviews 2011, 15, 3278-3300.

Asa-Awuku, A., Sullivan A.P., Hennigan C.J., Weber R.J., Nenes A. Investigation of molar volume and surfactant characteristics of water-soluble organic compounds in biomass burning aerosol. Atmos. Chem. And Phys., 2008, 8, 799-812.

Aschner M., Erikson K.M., et al. Manganese dosimetry: Species differences and implications for neurotoxicity. Critical Reviews in Toxicology 2005, 35, 1–32.

Ayres, J.G., Borm, P., Cassee, F.R., Castranova, V., Donaldson, K., et al. Evaluating the toxicity of airborne particulate matter and nanoparticles by measuring oxidative stress potential – a workshop report and consensus statement. Inhalation Toxicology 2008, 20 (1), 75–99.

Bakeas E., Karavalakis G., Stournas S. Biodiesel emissions profile in modern diesel vehicles. Part 1: Effect of biodiesel origin on the criteria emissions. Science of the Total Environment 2011, 409, 1670-1676.

Ban-Weiss G. A., Chen J. Y., Buchholz B. A., Dibble R. W. A numerical investigation into the anomalous slight NOx increase when burning biodiesel; A new (old) theory. Fuel Processing Technology 2007, 88, 659-667.

Betha R., Balasubramanian R. Emissions of particulate-bound elements from biodiesel and ultra low sulfur diesel: size distribution and risk assessment. Chemosphere 2013, 90, 1005-1015.

Biswas S., Verma V., Schauer J.J., Cassee F.R., Cho A.K., et al. Oxidative potential of semi-volatile and non volatile particulate matter (PM) from heavy-duty vehicles retrofitted with emission control technologies. Environ Sci Technol 2009, 43, 3905-3912.

Bittle J.A., Knight B.M., Jacobs T.J. Interesting behavior of biodiesel ignition delay and combustion duration. Energy and Fuels 2010, 24, 4166-4177.

Bowler R.P., Crapo J.D. Oxidative stress in allergic respiratory diseases. The Journal of Allergy and Clinical Immunology. 2002, 110, 349–356.

Brito J.M., Belotti L., Toledo A.C., Antonangelo L., Silva F.S., et al., Acute Cardiovascular and Inflammatory Toxicity Induced by Inhalation of Diesel and Biodiesel Exhaust Particles. Toxicological Sciences 2010, 116, 67-78.

Cahill T.M. Okamoto R.A. Emissions of acrolein and other aldehydes from biodiesel-fueled heavy-duty vehicles. Environ Sci Technol 2012, 46, 8382-8388.

Cheng A., Upatnieks A. Mueller C. Investigation of the impact of biodiesel fuelling on NOx emissions using an optical direct injection diesel engine. International Journal of Engine Research 2006, 7, 297-318.

Cheung K.L., Polidori A., Ntziachristos L., Tzamkiozis T., Samaras Z., et al. Chemical Characteristics and Oxidative Potential of Particulate Matter Emissions from Gasoline, Diesel, and Biodiesel Cars. Environ Sci Technol 2009, 43, 6334-6340.

Cho A.K., Sioutas C., Miguel A.H., Kumagai Y., et al. Redox activity of airborne particulate matter at different sites in the Los Angeles Basin. Environ Res, 2005, 99, 40-47.

Cocker D.R., Shah S., Johnson K., Miller J.W., Norbeck J. Development and Application of a Mobile Laboratory for Measuring Emissions from Diesel Engines. I Regulated Gaseous Emissions. Environ Sci Technology 2004a, 38, 2182-2189.

Cocker D.R., Shah S.D., Johnson K.J., Zhu X., et al. Development and Application of a Mobile Laboratory for Measuring Emissions from Diesel Engines. 2. Sampling for Toxics and Particulate Matter, Environ Sci Technology 2004b, 38, 6809-6816

Correa, S.M., Arbilla, G. Aromatic hydrocarbons emissions in diesel and biodiesel exhaust," Atmospheric Environment 2006, 40, 6821-6826.

Correa S.M., Arbilla G. Carbonyl emissions in diesel and biodiesel exhaust. Atmospheric Environment 2008, 42, 769-775.

Decesari S., Facchini M.C., Fuzzi S., Tagliavini E. Characterization of water-soluble organic compounds in atmospheric aerosol: A new approach. Journal of Geophysical Research-Atmospheres 2000, 105 (D1), 1481-1489.

Delgado-Saborit J.M., Alam M.S., Godri Pollitt K.J., Christopher Stark C., Harrison R. M. Analysis of atmospheric concentrations of quinones and polycyclic aromatic hydrocarbons in vapour and particulate phases. Atmospheric Environment, 2013, 77, 974-982.

Dorman D.C., Struve M.F., et al. Influence of particle solubility on the delivery of inhaled manganese to the rat brain: Manganese sulfate and manganese tetroxide pharmacokinetics following repeated (14-day) exposure. Toxicology and Applied Pharmacology 2001, 170, 79–87.

Durbin T.D., Collins J.R., Norbeck J.M., Smith M.R. Effects of biodiesel, biodiesel blends, and a synthetic diesel on emissions from light heavy-duty diesel vehicles. Environ Sci Technol 2000, 34, 349-355.

Durbin T.D., Miller J.W., Johnson K., Hajbabaei M., et al. CARB Assessment of the Emissions from the Use of Biodiesel as a Motor Vehicle Fuel in California "Biodiesel Characterization and NOx Mitigation Study". CARB Final Report, October 2011, http://www.arb.ca.gov/fuels/diesel/altdiesel/20111013_CARB%20Final%20Biodiesel%20Report.pdf

Eckerle W.A., Lyford-Pike E.J., Stanton D.W., LaPointe L.A., Whitacre S.D., et al. Effects of methyl ester biodiesel blends on NOx emissions SAE Technical Paper 2008-01-0078, 2008.

Eiguren-Fernandez A., Shinyashiki M., Schmitz D.A., DiStefano E., et al., Redox and electrophilic properties of vapor- and particle-phase components of ambient aerosols. Environmental Research 2010, 110, 207-212.

Fontaras G., Karavalakis G., Kousoulidou M., Tzamkiozis T., Ntziachristos L., Bakeas E., Stournas S., Samaras Z. Effects of biodiesel on passenger car fuel consumption, regulated and non-regulated pollutant emissions over legislated and real world driving cycles. Fuel 2009, 88, 1608-1617.

Fontaras G., Kousoulidou M., Karavalakis G., Tzamkiozis T., Pistikopoulos P., Ntziachristos L., Bakeas E., Stournas S., and Samaras Z. Effects of low concentration biodiesel blends application on modern passenger cars. Part 1: Feedstock impact on regulated pollutants, fuel consumption and particle emissions. Environmental Pollution 2010a, 158, 1451-1460.

Fontaras G., Karavalakis G., Kousoulidou M., Ntziachristos L., Bakeas E., Stournas S., Samaras Z. Effects of low concentration biodiesel blend application on modern passenger cars. Part 2: Impact on carbonyl compound emissions. Environmental Pollution 2010b, 158, 2496-2503.

Gad S.C. Acute and Chronic Systemic Chromium Toxicity. Science of the Total Environment 1989, 86, 149–157.

Geller M.D., Ntziachristos L., Mamakos A., Samaras Z., Schmitz D.A., et al., Physicochemical and redox characteristics of particulate matter (PM) emitted from gasoline and diesel passenger cars. Atmospheric Environment 2006, 40, 6988-7004.

Gerlofs-Nijland M., Totlandsdal A.I., Tzamkiozis T., Leseman D.L.A.C., Samaras Z., et al. Cell toxicity and oxidative potential of engine exhaust particles: Impact of using particulate filter or biodiesel fuel blend. Environ Sci Technol 2013, 47, 5931-5938.

Giakoumis E.G., Rakopoulos C.D., Dimaratos A.M., Rakopoulos D.C. Exhaust emissions of diesel engines operating under transient conditions with biodiesel fuel blends. Progress in Energy and Combustion Science 2012, 38, 691-715.

Gozzelino R., Jeney V., Soares M.P. Mechanisms of cell protection by heme oxygenase-1. Annu Rev Pharmacol Toxicol 2010, 50, 323-354.

Grigoratos T., Fontaras G., Kalogirou M., Samara C., et al. Effect of rapeseed methylester blending on diesel passenger car emissions-Part 2: Unregulated emissions and oxidation activity. Fuel 2014, 128, 260-267.

Grosjean D., Grosjean E., Gertler A.W. On-road emissions of carbonyls from light-duty and heavy-duty vehicles. Environ Sci Technol 2001, 35, 45-53.

Guarieiro A.L.N., da S. Santos J.V., Eiguren-Fernandez A., Torres E.A., et al. Redox activity and PAH content in size-classified nanoparticles emitted by a diesel engine fuelled with biodiesel and diesel blends. Fuel 2014, 116, 490-497.

Hajbabaei M., Johnson K.C., Okamoto R.A., Mitchell A., et al. Evaluation of the impacts of biodiesel and second generation biofuels on NOx emissions for CARB diesel fuels. Environ. Sci. Technol. 2012, 46, 9163-9173.

He C., Ge Y., Tan J., You K., Han X., Wang J., You Q, Shah A.N. Comparison of carbonyl compounds emissions from diesel engine fueled with biodiesel and diesel, Atmospheric Environment 2009, 43, 3657–3661.

Heikkila J., Virtanen A., Ronkko T., keskinen J., et al. Nanoparticle emissions from a heavy-duty engine running on alternative diesel fuels. Environ Sci Technol 2009, 43, 9501-9506.

Hoekman S.K., Robbins C. Review of the effects of biodiesel on NOx emissions. Fuel Processing Technology 2012, 96, 237-249.

Karavalakis G., Bakeas E., Stournas S. Influence of oxidized biodiesel blends on regulated and unregulated emissions from a diesel passenger car. Environ. Sci. Technol. 2010a, 44, 5306-5312.

Karavalakis G., Fontaras G., Ampatzoglou D., Kousoulidou M., Stournas S., Samaras Z., Bakeas E. Effects of low concentration biodiesel blends application on modern passenger cars. Part 3: Impact on PAH, nitro-PAH, and oxy-PAH emissions. Environmental Pollution 2010b, 158, 1584-1594.

Karavalakis G., Boutsika V., Stournas S., Bakeas E. Biodiesel emissions profile in modern diesel vehicles. Part 2: Effect of biodiesel origin on carbonyl, PAH, nitro-PAH and oxy-PAH emissions. Science of the Total Environment 2011, 409(4), 738-747.

Kawano D., Mizushima N., Ishii H., Goto Y., Iwasa K. Exhaust emission characteristics of commercial vehicles fuelled with biodiesel. SAE Technical Paper 2010-01-2276, 2010.

Knothe G., Sharp C.A., Ryan T.W. Exhaust emissions of biodiesel, petrodiesel, neat methyl esters, and alkanes in a new technology engine. Energy and Fuels 2006, 20, 403-408.

Kooter I.M., van Vugt M.A.T.M., Jedynska A.D., Tromp P.C., Houtzager M.M.G., et al. Toxicological characterization of diesel engine emissions using biodiesel and a closed soot filter. Atmospheric Environment 2011, 45, 1574-1580.

Kousoulidou M., Fontaras G., Ntziachristos L., Samaras Z. Biodiesel blend effects on common-rail diesel combustion and emissions. Fuel 2010, 89, 3442-3449.

Lammert M.P., McCormick R.L., Sindler P., Williams A. Effect of B20 and low aromatic diesel on transit bus NOx emissions over driving cycles with a range of kinetic intensity. SAE Technical Paper 2012-01-1984, 2012.

Landreman A.P., Shafer M.M. Hemming J.C. Hannigan M.P., Schauer J.J. A macrophage-based method for the assessment of the reactive oxygen species (ROS) activity of atmospheric

particulate matter (PM) and application to routine (daily-24 h) aerosol monitoring studies. Aerosol Science and Technology 2008, 42, 946-957.

Lapuerta M., Armas O., Fernandez J.R. Effect of biodiesel fuels on diesel engine emissions. Progress in Energy and Combustion Science 2008, 34, 198-223.

Lea-Langton A., Li H., Andrews G.E. Comparison of particulate PAH emissions for diesel, biodiesel and cooking oil using a heavy duty DI diesel engine. SAE Technical Paper Series 2008-01-1811, 2008.

Li N., Venkatesan M.I., Miguel A., Kaplan R., Gujuluva C., et al. Induction of heme oxygenase-1 expression in macrophages by diesel exhaust particle chemicals and quinones via the antioxidant-responsive element. J Immunol 2000, 165, 3393-401.

Li N., Kim S., Wang M., Froines J., Sioutas C., Nel A. Use of a stratified oxidative stress model to study the biological effects of ambient concentrated and diesel exhaust particulate matter. Inhalation Toxicology. 2002a, 14, 459–486.

Li N., Wang M., Oberley T.D., Sempf J.M., Nel A.E. Comparison of the pro-oxidative and proinflammatory effects of organic diesel exhaust particle chemicals in bronchial epithelial cells and macrophages. Journal of immunology. 2002b, 169, 4531–4541.

Li N., Sioutas C., Cho A., Schmitz D., Misra C., et al. Ultrafine Particulate Pollutants Induce Oxidative Stress and Mitochondrial Damage. Environ. Health. Persp. 2003, 111, 455–460.

Lim McKenzie C.H., Ayoko G.A., Morawska L., Ristovski Z.D., Jayaratne E.R. Influence of fuel composition on polycyclic aromatic hydrocarbon emissions from a fleet of in-service passenger cars. Atmospheric Environment 2007, 41, 150-160.

Lin Y.C., Wu T.Y., Ou-Yang W.C., Chen C.B. Reducing emissions of carbonyl compounds and regulated harmful matters from a heavy-duty diesel engine fueled with paraffinic/biodiesel blends at one low steady-state condition. Atmospheric Environment 2009, 43, 2642-2647.

Lough G.C., Schauer J.J., Park J-S, Shafer M.M., et al., Emissions of metals associated with motor vehicle roadways. Environ Sci Technol 2005, 39, 826-836.

Macor A., Avella F., Faedo D. Effects of 30% v/v biodiesel/diesel fuel blend on regulated and unregulated pollutant emissions from diesel engines. Applied Energy 2011, 88, 4989-5001.

Martini G., Astorga C., Farfaletti A. Effect of biodiesel fuels on pollutant emissions from EURO 3 LD diesel vehicles. Transport and Air Quality Unit; Institute for Environment and Sustainability, EC-Joint Research Centre, 2007.

McCormick R.L., Graboski M.S., Alleman T.L., Herring A.M., Tyson K.S. Impact of biodiesel source material and chemical structure on emissions of criteria pollutants from a heavy-duty engine. Environ. Sci. Techol. 2001, 35, 1742-1747.

McWilliam L., Zimmermann, A. Emissions and performance implications of biodiesel use in an SCR-equipped Caterpillar C6.6. SAE Technical Paper 2010-01-2157, 2010.

Mizushima N., Murata Y., Suzuki H., Ishii H., Goto Y., Kawano D. Effect of biodiesel on NOx reduction performance of urea-SCR system. SAE Technical Paper 2010-01-2278, 2010.

Mueller C.J., Pitz W.J., Pickett L.M., Martin G.C., Siebers D.L., Westbrook C.K. Effects of Oxygenates on Soot Processes in DI Diesel Engines: Experiments and Numerical Simulations. SAE Technical Paper 2003-01-1791, 2003.

Mueller C., Boehman A., Martin G. An experimental investigation of the origin of increased NOx emissions when fueling a heavy-duty compression-ignition engine with soy biodiesel. SAE International Journal of Fuels and Lubricants 2009, 2, 789-816.

Muncrief R.L., Rooks C.W., Cruz M., Harold M.P. Combining biodiesel and exhaust gas recirculation for reduction in NOx and particulate emissions. Energy Fuels 2008, 22, 1285−96.

Nikanjam M., Rutherford J., Morgan P. Performance and emissions of diesel and alternative diesel fuels in modern light-duty diesel vehicles. SAE Technical Paper 2011-01-0198, 2011.

Nico P.S., Kumfer B.M., Kennedy I.M., Anastasio C. Redox dynamics of mixed metal (Mn, Cr, and Fe) ultrafine particles. Aerosol Science and Technology 2009, 43, 60-70.

Oberdorster G., Oberdorster E., Oberdorster J. Nanotoxicalogy: An emerging discipline evolving from studies of ultrafine particles. Environmental Health Perspectives 2005, 113, 823-839.

O'Brien, P.I. Molecular mechanisms of quinone cytotoxicity. Chem Biol Interact 1991, 80, 1-41, 1991.

Pinto E., Sigaud-Kutner T. C. S., Leitao M. A. S., Okamoto O. K., Morse D., Colepicolo P. Heavy metal-induced oxidative stress in algae. J. Phycol., 2003, 39, 1008–1018.

Ratcliff M.A., Dane A.J., Williams A., Ireland J., Luecke J., McCormick R.L. et al. Diesel particle filter and fuel effects on heavy-duty diesel engine emissions. Environ Sci Technol 2010, 44, 8343-8349.

Reaney S.H., Smith D.R. Manganese oxidation state mediates toxicity in PC12 cells. Toxicology and Applied Pharmacology 2005, 205, 271–281.

Schönborn A., Ladommatos N., Williams J., Allan R., Rogerson J. The influence of molecular structure of fatty acid monoalkyl esters on diesel combustion. Combustion and Flame 2009, 156, 1396-1412.

Shinkai Y., Nakajima S., Eiguren-Fernandez A., Di Stefano E., Schmitz D.A., et al. Ambient vapor samples activate the Nrf2-ARE pathway in human bronchial epithelial BEAS-2B cells. Environ Toxicol 2013, 25, 1222-30.

Shinyashiki M., Eiguren-Fernandez A., Schmitz D.A., Di Stefano E., Li N., et al. Electrophilic and redox properties of diesel exhaust particles. Environmental Research 2009, 109, 239-244.

Sun J., Caton J.A., Jacobs T.J. Oxides of nitrogen emissions from biodiesel-fuelled diesel engines. Progress in Energy and Combustion Science 2010, 36, 677-695.

Surawski N.C., Miljevic B., Ayoko G.A., Elbagir S., Stevanovic S., Fairfull-Smith K.E., et al. Physicochemical characterization of particulate emissions from a compression ignition engine: the influence of biodiesel feedstock. Environ Sci Technol 2011, 45, 10337-10343.

Szivák I., Bhera R. Sigg L. Metal-induced reactive oxygen species production in chlamydomonas reinhardtii (Chlorophyceae). J. Phycol., 2009, 45, 427–435.

Szybist J.P., Boehman A.L., Haworth D.C., Koga H. Premixed ignition behavior of alternative diesel fuel-relevant compounds in a motored engine experiment. Combustion and Flame 2007, 149, 112-128.

Takizawa H., Ohtoshi T., Kawasaki S., Kohyama T., Desaki M., et al. Diesel exhaust particles induce NF-kappa B activation in human bronchial epithelial cells in vitro: importance in cytokine transcription. Journal of Immunology. 1999, 162, 4705–4711.

Tinsdale M., Price P., Chen R. The impact of biodiesel on particle number, size and mass emissions from a Euro 4 diesel vehicle. SAE Technical Paper, 2010-01-0796, 2010.

Topperwein S., Behra R., Sigg L. Competition among zinc, manganese, and cadmium uptake in the freshwater alga *Scenedesmus vacuolatus.* Environ. Toxicol. Chem. 2007, 26, 483–490.

Turrio-Baldassarri L., Battistelli C.L., Conti L., Crebelli R., De Berardis B., et al. Emission comparison of urban bus engine fueled with diesel oil and 'biodiesel' blend. Science of the Total Environment 2004, 327, 147-162.

Tzamkiozis T., Ntziachristos L., Mamakos A., Fontaras G., Samaras Z. Aerodynamic and mobility size distribution measurements to reveal biodiesel effects on diesel exhaust aerosol. Aerosol Science and Technology 2011, 45, 587-595.

Valavanidis A., Fiotakis K., Vlachogianni T. Airborne Particulate Matter and Human Health: Toxicological Assessment and Importance of Size and Composition of Particles for Oxidative Damage and Carcinogenic Mechanisms. Journal of Environmental Science and Health, Part C: Environmental Carcinogenesis and Ecotoxicology Reviews 2008, 26, 339-362.

Verma V., Shafer M.M., Schauer J.J., Sioutas C. Contribution of transition metals in the reactive oxygen species activity of PM emissions from retrofitted heavy-duty vehicles. Atmospheric Environment 2010, 44, 5165-5173.

Veronesi B., Oortgiesen M., Carter J.D., Devlin R.B. Particulate matter initiates inflammatory cytokine release by activation of capsaicin and acid receptors in a human bronchial epithelial cell line. Toxicol Appl Pharmacol 1999, 154, 106-15.

Walkowicz K., Na K., Robertson W., Sahay K., Bogdanoff M., Weaver C., Carlson R. On-Road and In-Laboratory Testing to Demonstrate Effects of ULSD, B20, and B99 on a Retrofit Urea-SCR Aftertreatment System. SAE Technical Paper 2009-01-2733, 2009.

Wang W.G., Lyons D.W., Clark N.N., Gautam M., Norton P.M. Emissions from nine heavy trucks fueled by diesel and biodiesel blend without engine modification. Environ Sci Technol 2000, 34, 933-939.

Westphal G.A., Krahl J., Munack A., Rosenkranz N., Schroder O. Combustion of hydrotreated vegetable oil and jatropha methyl ester in a heavy duty engine: emissions and bacterial mutagenicity. Environ Sci Technol 2013, 47, 6038-6046.

Xue J., Grift T.E., Hansen A.C. Effect of biodiesel on engine performances and emissions. Renewable and Sustainable Energy Reviews 2011, 15, 1098-1116.

Yanamala N., Hatfield M.K., Farcas M.T., Schwegler-Berry D., Hummer J.A., et al. Biodiesel versus diesel exposure: Enhanced pulmonary inflammation, oxidative stress, and differential morphological changes in the mouse lung. Toxicology and Applied Pharmacology 2013, 272, 373-383.

Yang H.H., Chien S.M., Lo M.Y., Lan J.C.W., Lu W.C., et al. Effects of biodiesel on emissions of regulated air pollutants and polycyclic aromatic hydrocarbons under engine durability testing. Atmospheric Environment 2007, 41, 7232-7240.

Young L.H., Liou Y.J., Cheng M.T., Lu J.H., Yang H.H., et al. Effects of biodiesel, engine load and diesel particulate filter on nonvolatile particle number size distributions in heavy-duty diesel engine exhaust. Journal of Hazardous Materials 2012, 199-200, 282-289.

Zhang Y., Boehman A.L. Impact of biodiesel on NOx emissions in a common rail direct injection diesel engine. Energy and Fuels 2007, 21, 2003-2012.